

Republic of Iraq  
Ministry of Higher Education  
And Scientific Research  
University of Babylon

**DEVELOPING TURBULENT FLOW AND HEAT TRANSFER  
THROUGH DUCTS OF RECTANGULAR AND  
CIRCULAR CROSS SECTION**

A thesis

Submitted to the College of Engineering

University of Babylon in Partial Fulfillment of the Requirements for The  
degree of Master of Science in Mechanical Engineering

By

**ALI NU'MAN IBRAHIM**  
**(B. Sc)**

١٤٢٦ HIJRI

٢٠٠٥ AC

## Abstract

In the present work, developing turbulent flow and heat transfer through rectangular and circular duct have been studied numerically. The study includes the numerical solution of the continuity, momentum, and energy equations (which govern the working fluid) together with the two equations of the (k-ε) turbulence model. The clustering of the grid in the radial direction near walls for each duct was used in the numerical solution. A computer program in FORTRAN 90 was built to perform the numerical solution for each duct.

The air at (30 °C) was used as the working fluid to flow once through rectangular duct of dimensions ( $L=3D_h$  and  $(0.016m * 0.01m)$  cross section and again through circular duct of diameter ( $D=0.01m$ ) and length ( $L=3D$ ). The study was made for two values of Reynolds number ( $Re=1000$  and  $Re=12000$ ) for each duct. Two cases of thermal boundary conditions were studied: Constant Wall Temperature and Constant Heat Flux respectively, but there were no satisfactory results obtained for constant heat flux case of circular duct. For all studies cases, the hydrodynamic and thermal boundary layers are simultaneously growing in the process of developing.

The computational algorithm is able to calculate all the hydrodynamic properties such as velocities, friction factor, and turbulence structure (which include the Reynolds stress, the turbulent kinetic energy and eddy viscosity). Also the computational algorithm is able to predict all the thermal properties such as the temperature, Nusselt number and the turbulent heat fluxes.

The results showed that, Thermal Entry Length lies between,  $x/D$  (1.5-1.6) for the two ducts which means that the developing of thermal boundary layer is so fast because the very high heat transfer coefficients

which result from very high velocities near walls and the very small selected dimensions of each duct. The very high velocities near walls may result from the using of wall function with very small size of spacing between the clustered nodal points especially near walls. The present work shows that there is a possibility to check the constant heat flux solution from that of the constant wall temperature. The validity of thermal results for constant wall temperature is verified and shows that there is a good agreement between the results of present numerical solution and the correlation related to it.

جمهورية العراق  
وزارة التعليم العالي والبحث العلمي  
جامعة بابل

# الإنسياب الإضطرابي المتطوّر وانتقال الحرارة خلال مجاري مستطيلة و دائرية المقطع

رسالة مقدمة إلى كلية الهندسة في جامعة بابل وهي جزء من متطلبات نيل درجة الماجستير  
علوم في الهندسة الميكانيكية

من قبل المهندس  
علي نعمان إبراهيم

٢٠٠٥ م

١٤٢٦ هـ

## الخلاصة

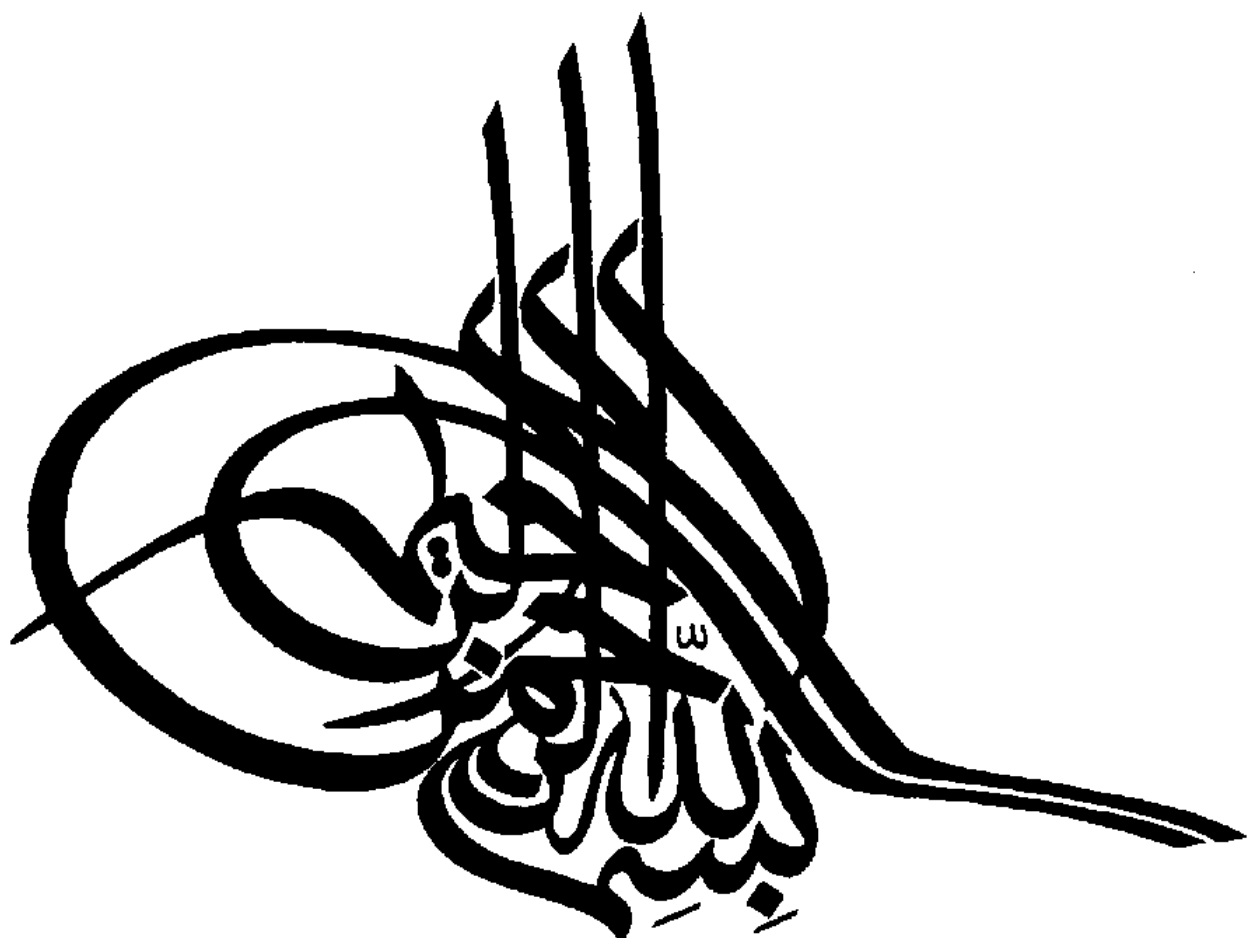
يتضمن البحث الحالي دراسة نظرية عددية للجريان المضطرب غير تام التطور وانتقال الحرارة خلال مجرى مستطيل وآخر دائري. حيث تضمنت الدراسة إعداد نموذج رياضي لإجراء الحل العددي لمعادلات الكتلة والزخم والطاقة ومعادلتى نموذج (k-ε) للإضطراب باستخدام طريقة الفروقات المحددة (FDM). تضمن الحل العددي استخدام التنعيم للشبكة العقدية بالإتجاه القطري قرب الجدران لكل مجرى. تم بناء برنامج باستخدام لغة (FORTRAN ٩٠) لإنجاز الحل العددي لكل مجرى.

أستُخدم الهواء بدرجة حرارة ٢٠ °م كمائع شغل ليمر خلال مجرى مستطيل ذي طول (L=٣٥D<sub>h</sub>) و مقطع عرضي (٠.٠٠٥m \* ٠.٧٦٢m) وكذلك يمر خلال مجرى دائري بقطر (D=٠.٢٠١m) و طول (L=٣٥D). أُجريت الدراسة لقيمتين من أرقام رينولدز Re=٦٠٠٠٠ و Re=١٢٠٠٠٠ لكل مجرى و لحالتين من الشروط الحدودية الحرارية: حالة بثبوت درجة حرارة الجدار والأخرى بثبوت الفيض الحراري ولكن لم تكن نتائج حالة بثبوت الفيض الحراري للمجرى الدائري مرضية. لجميع حالات الدراسة تم اعتبار عملية التطور تحدث آنياً للطبقتين المتاخمتين الهيدروديناميكية والحرارية.

إمكانية الحل العددي تتضمن حساب جميع الصفات الهيدروديناميكية مثل مركبات منحنيات السرعة , معامل الإحتكاك و هيكل الإضطراب (الذي يتضمن إجهادات رينولدز , الطاقة الحركية للإضطراب و اللزوجة الدوامية). و كذلك تتضمن إمكانية الحل العددي القدرة على تنبؤ جميع الصفات الحرارية مثل توزيع درجات الحرارة , رقم نسلت و الفيض الحراري المضطرب لمنطقة الحساب.

بيّنت النتائج بأن طول الدخول الحراري, X/D يتراوح ما بين (١.٤ إلى ١.٦) لكلا المجرين والذي يعني بأن تطور الطبقة المتاخمة الحرارية هو سريع جداً بسبب إنتقال الحرارة العالي جداً والذي يرجع إلى السرعة العالية قرب الجدران والأبعاد الصغيرة التي أُختيرت لكل مجرى. السرعة العالية قرب الجدران ربما نشأت من إستخدام دالة الجدار مع

التزحيف للنقاط العقدية بأبعاد صغيرة جداً خاصةً قرب الجدران. ومن نتائج العمل الحالي يتبيّن بأن هنالك إمكانية لفحص الحل العددي لحالة التسخين بثبوت الفيض الحراري من الحل العددي لحالة التسخين بثبوت درجة حرارة الجدار. تم التأكد من صحّة النتائج الحرارية لحالة التسخين بثبوت درجة حرارة الجدار حيث كان هنالك توافق جيد بين الحل العددي الحالي والعلاقات التجريبية المتعلقة به لباحثين سابقين.



## APPENDIX A

### **Derivation of the Governing Equations for Turbulent flows in terms of Cartesian Coordinates**

The fundamental difference between laminar and turbulent flow lies in the chaotic, random behavior of the various fluid parameters. Such flows can be described in terms of their mean values (denoted with an over bar) on which are superimposed the fluctuations (denoted with a prime) [ $\gamma$ ]. Thus, in the turbulent flow the main dependent variables are replaced by the sum of the time mean and instantaneous fluctuation. Then the resulting equations are time averaged. The velocities, pressures, and temperature in the governing equations should be replaced by the following equations:-

$$\left. \begin{aligned} u &= \bar{u} + u' \\ v &= \bar{v} + v' \\ w &= \bar{w} + w' \\ p &= \bar{p} + p' \\ T &= \bar{T} + T' \end{aligned} \right\} \dots (A.1)$$

In the study of turbulence one often has to carry out an averaging procedure not only on single quantities but also on products of quantities. Here the overscores have the following properties.

Let  $A = \bar{A} + a$  and  $B = \bar{B} + b$ . In any further averaging procedure  $\bar{A}$  and  $\bar{B}$  may be treated as constants. Thus

$$\overline{\bar{A} + a} = \bar{\bar{A} + a} = \bar{A} + \bar{a} = A + \bar{a} \text{ whence } \bar{a} = 0$$

$$\overline{\bar{A}\bar{B}} = \bar{\bar{A}\bar{B}} = \bar{A}\bar{B} = AB$$

$$\overline{\bar{A}b} = \bar{\bar{A}b} = \bar{A}\bar{b} = 0 \text{ since } \bar{b} = 0$$

Similarly

$$\overline{\bar{B}a} = \bar{\bar{B}a} = \bar{B}\bar{a} = 0 \text{ since } \bar{a} = 0$$

$$\overline{AB} = \overline{(\bar{A} + a)(\bar{B} + b)} = \overline{\bar{A}\bar{B}} + \overline{\bar{A}b} + \overline{\bar{B}a} + \overline{ab} = AB + \overline{ab} \text{ [Hinze, 1909]}$$

The governing equations for laminar, incompressible, steady flow in rectangular or square duct without External forces are:-

1. Continuity equation:

$$\frac{\partial u}{\partial x} + \frac{\partial v}{\partial y} + \frac{\partial w}{\partial z} = 0 \quad \dots (A.1)$$

2. Momentum Equation:

X-direction

$$u \frac{\partial u}{\partial x} + v \frac{\partial u}{\partial y} + w \frac{\partial u}{\partial z} = \frac{-1}{\rho} \frac{\partial p}{\partial x} + \nu \left( \frac{\partial^2 u}{\partial x^2} + \frac{\partial^2 u}{\partial y^2} + \frac{\partial^2 u}{\partial z^2} \right) \quad \dots (A.2)$$

Y-direction

$$u \frac{\partial v}{\partial x} + v \frac{\partial v}{\partial y} + w \frac{\partial v}{\partial z} = \frac{-1}{\rho} \frac{\partial p}{\partial y} + \nu \left( \frac{\partial^2 v}{\partial x^2} + \frac{\partial^2 v}{\partial y^2} + \frac{\partial^2 v}{\partial z^2} \right) \quad \dots (A.3)$$

Z-direction

$$u \frac{\partial w}{\partial x} + v \frac{\partial w}{\partial y} + w \frac{\partial w}{\partial z} = \frac{-1}{\rho} \frac{\partial p}{\partial z} + \nu \left( \frac{\partial^2 w}{\partial x^2} + \frac{\partial^2 w}{\partial y^2} + \frac{\partial^2 w}{\partial z^2} \right) \quad \dots (A.4)$$

3. Energy Equation:

$$u \frac{\partial T}{\partial x} + v \frac{\partial T}{\partial y} + w \frac{\partial T}{\partial z} = \frac{\nu}{Pr} \left( \frac{\partial^2 T}{\partial x^2} + \frac{\partial^2 T}{\partial y^2} + \frac{\partial^2 T}{\partial z^2} \right) \quad \dots (A.5)$$

To make all the above equations valid for turbulent flows, the dependent variables (u, v, w, p, and T) should be expressed in terms of its mean and fluctuated components. This will be done for continuity equation by substituting the important relations for variables u, v and w from equation (A.1) into (A.1) to get

$$\frac{\partial(\bar{u} + u')}{\partial x} + \frac{\partial(\bar{v} + v')}{\partial y} + \frac{\partial(\bar{w} + w')}{\partial z} = 0$$

$$\frac{\partial \bar{u}}{\partial x} + \frac{\partial u'}{\partial x} + \frac{\partial \bar{v}}{\partial y} + \frac{\partial v'}{\partial y} + \frac{\partial \bar{w}}{\partial z} + \frac{\partial w'}{\partial z} = 0$$

$$\frac{\partial u}{\partial x} + \frac{\partial v}{\partial y} + \frac{\partial w}{\partial z} = 0 \quad \dots (A.7)$$

For momentum equation:-

If equation (A.7) is multiplied by  $u$ , will become

$$u \left( \frac{\partial u}{\partial x} + \frac{\partial v}{\partial y} + \frac{\partial w}{\partial z} \right) = 0 \quad \dots (A.8)$$

To achieve the averaging processes for all variables the convective terms (like  $u \frac{\partial u}{\partial x}$ ) should be converted to a simple form by adding (A.7) and (A.8)

to get:-

$$\frac{\partial(u^2)}{\partial x} + \frac{\partial(uv)}{\partial y} + \frac{\partial(uw)}{\partial z} = \frac{-1}{\rho} \frac{\partial p}{\partial x} + \nu \left( \frac{\partial^2 u}{\partial x^2} + \frac{\partial^2 u}{\partial y^2} + \frac{\partial^2 u}{\partial z^2} \right) \quad \dots (A.9)$$

Substitute from relations of equation (A.1) into equation (A.9) to get

$$\frac{\partial(\bar{u} + u')(\bar{u} + u')}{\partial x} + \frac{\partial((\bar{u} + u')(\bar{v} + v'))}{\partial y} + \frac{\partial((\bar{u} + u')(\bar{w} + w'))}{\partial z} = \frac{-1}{\rho} \frac{\partial(\bar{p} + p')}{\partial x} + \nu \left( \frac{\partial^2(\bar{u} + u')}{\partial x^2} + \frac{\partial^2(\bar{u} + u')}{\partial y^2} + \frac{\partial^2(\bar{u} + u')}{\partial z^2} \right)$$

Resolve the terms in brackets of the above equation and then time average the result to get

$$\frac{1}{2} \frac{\partial(\bar{u}^2 + 2\bar{u}u' + u'^2)}{\partial x} + \frac{\partial((\bar{u}\bar{v} + \bar{u}v' + \bar{v}u' + u'v'))}{\partial y} + \frac{\partial((\bar{u}\bar{w} + \bar{u}w' + \bar{w}u' + w'u'))}{\partial z} = \frac{-1}{\rho} \frac{\partial(\bar{p} + p')}{\partial x} + \nu \left( \frac{\partial^2(\bar{u} + u')}{\partial x^2} + \frac{\partial^2(\bar{u} + u')}{\partial y^2} + \frac{\partial^2(\bar{u} + u')}{\partial z^2} \right)$$

$$\frac{\partial \bar{u}^2}{\partial x} + \frac{\partial \bar{u}'^2}{\partial x} + \frac{\partial \bar{u}v}{\partial y} + \frac{\partial \bar{u}'v'}{\partial y} + \frac{\partial \bar{u}w}{\partial z} + \frac{\partial \bar{u}'w'}{\partial z} = \frac{-1}{\rho} \frac{\partial p}{\partial x} + \nu \left( \frac{\partial^2 \bar{u}}{\partial x^2} + \frac{\partial^2 \bar{u}}{\partial y^2} + \frac{\partial^2 \bar{u}}{\partial z^2} \right) \quad \dots (A.10)$$

Resolve the terms which contains a multiplied mean velocities in (A.10), get

$$u \frac{\partial u}{\partial x} + u \frac{\partial u}{\partial x} + \frac{\partial \bar{u}'^2}{\partial x} + u \frac{\partial v}{\partial y} + v \frac{\partial u}{\partial y} + \frac{\partial \bar{u}'v'}{\partial y} + u \frac{\partial w}{\partial z} + w \frac{\partial u}{\partial z} + \frac{\partial \bar{u}'w'}{\partial z} = \frac{-1}{\rho} \frac{\partial p}{\partial x}$$

$$+ v \left( \frac{\partial^2 u}{\partial x^2} + \frac{\partial^2 u}{\partial y^2} + \frac{\partial^2 u}{\partial z^2} \right)$$

$$u \frac{\partial u}{\partial x} + \frac{\partial \bar{u}'^2}{\partial x} + v \frac{\partial u}{\partial y} + \frac{\partial \bar{u}'v'}{\partial y} + w \frac{\partial u}{\partial z} + \frac{\partial \bar{u}'w'}{\partial z} + \left( u \frac{\partial u}{\partial x} + u \frac{\partial v}{\partial y} + u \frac{\partial w}{\partial z} \right) = \frac{-1}{\rho} \frac{\partial p}{\partial x}$$

$$+ v \left( \frac{\partial^2 u}{\partial x^2} + \frac{\partial^2 u}{\partial y^2} + \frac{\partial^2 u}{\partial z^2} \right)$$

from (A.8)

Rearrange the above equation to get

$$u \frac{\partial u}{\partial x} + v \frac{\partial u}{\partial y} + w \frac{\partial u}{\partial z} = \frac{-1}{\rho} \frac{\partial p}{\partial x} + v \left( \frac{\partial^2 u}{\partial x^2} + \frac{\partial^2 u}{\partial y^2} + \frac{\partial^2 u}{\partial z^2} \right) + \frac{\partial(-\bar{u}'^2)}{\partial x} + \frac{\partial(-\bar{u}'v')}{\partial y} + \frac{\partial(-\bar{u}'w')}{\partial z}$$

... (A.11)

Repeat for Y and Z-directions the same procedure which achieved to X-direction for getting equation (A.11), to get:-

For Y-directions

$$u \frac{\partial v}{\partial x} + v \frac{\partial v}{\partial y} + w \frac{\partial v}{\partial z} = \frac{-1}{\rho} \frac{\partial p}{\partial y} + v \left( \frac{\partial^2 v}{\partial x^2} + \frac{\partial^2 v}{\partial y^2} + \frac{\partial^2 v}{\partial z^2} \right) + \frac{\partial(-\bar{u}'v')}{\partial x} + \frac{\partial(-\bar{v}'^2)}{\partial y} + \frac{\partial(-\bar{v}'w')}{\partial z}$$

... (A.12)

For Z-directions

$$u \frac{\partial w}{\partial x} + v \frac{\partial w}{\partial y} + w \frac{\partial w}{\partial z} = \frac{-1}{\rho} \frac{\partial p}{\partial z} + v \left( \frac{\partial^2 w}{\partial x^2} + \frac{\partial^2 w}{\partial y^2} + \frac{\partial^2 w}{\partial z^2} \right) + \frac{\partial(-\bar{u}'w')}{\partial x} + \frac{\partial(-\bar{v}'w')}{\partial y} + \frac{\partial(-\bar{w}'^2)}{\partial z}$$

... (A.13)

Multiply equations (A.11), (A.12), and (A.13) by the density,  $\rho$  to get:-

$$\rho u \frac{\partial u}{\partial x} + \rho v \frac{\partial u}{\partial y} + \rho w \frac{\partial u}{\partial z} = -\frac{\partial p}{\partial x} + \mu \left( \frac{\partial^2 u}{\partial x^2} + \frac{\partial^2 u}{\partial y^2} + \frac{\partial^2 u}{\partial z^2} \right) + \frac{\partial(-\rho \bar{u}'^2)}{\partial x} + \frac{\partial(-\rho \bar{u}'v')}{\partial y} + \frac{\partial(-\rho \bar{u}'w')}{\partial z}$$

... (A.14)

$$\rho u \frac{\partial v}{\partial x} + \rho v \frac{\partial v}{\partial y} + \rho w \frac{\partial v}{\partial z} = -\frac{\partial p}{\partial y} + \mu \left( \frac{\partial^2 v}{\partial x^2} + \frac{\partial^2 v}{\partial y^2} + \frac{\partial^2 v}{\partial z^2} \right) + \frac{\partial(-\rho \bar{u}'v')}{\partial x} + \frac{\partial(-\rho \bar{v}'^2)}{\partial y} + \frac{\partial(-\rho \bar{v}'w')}{\partial z}$$

... (A.15)

$$\rho u \frac{\partial w}{\partial x} + \rho v \frac{\partial w}{\partial y} + \rho w \frac{\partial w}{\partial z} = -\frac{\partial p}{\partial z} + \mu \left( \frac{\partial^2 w}{\partial x^2} + \frac{\partial^2 w}{\partial y^2} + \frac{\partial^2 w}{\partial z^2} \right) + \frac{\partial(-\rho \bar{u}'w')}{\partial x} + \frac{\partial(-\rho \bar{v}'w')}{\partial y} + \frac{\partial(-\rho \bar{w}'^2)}{\partial z}$$

... (A.16)

The terms  $-\overline{\rho u'^2}, -\overline{\rho v'^2}, -\overline{\rho w'^2}, -\overline{\rho u'v'}, -\overline{\rho u'w'}$  and  $-\overline{\rho v'w'}$  in equations (A.14), (A.15), and (A.16) are called *Reynolds stresses* for turbulent flow.

For energy equation:-

Convert the convective terms in equation (A.1) to the following forms:-

$$\left. \begin{aligned} u \frac{\partial T}{\partial x} &= \frac{\partial uT}{\partial x} - T \frac{\partial u}{\partial x} \\ v \frac{\partial T}{\partial y} &= \frac{\partial vT}{\partial y} - T \frac{\partial v}{\partial y} \\ w \frac{\partial T}{\partial z} &= \frac{\partial wT}{\partial z} - T \frac{\partial w}{\partial z} \end{aligned} \right\} \dots (A.14)$$

Substitute equation (A.14) into equation (A.1) to get

$$\frac{\partial uT}{\partial x} - T \frac{\partial u}{\partial x} + \frac{\partial vT}{\partial y} - T \frac{\partial v}{\partial y} + \frac{\partial wT}{\partial z} - T \frac{\partial w}{\partial z} = \frac{\nu}{Pr} \left( \frac{\partial^2 T}{\partial x^2} + \frac{\partial^2 T}{\partial y^2} + \frac{\partial^2 T}{\partial z^2} \right) \dots (A.15)$$

Now, Substitute from equation (A.1) into equation (A.15) to get

$$\begin{aligned} &\frac{\partial(\bar{u} + u')(\bar{T} + T')}{\partial x} - (\bar{T} + T') \frac{\partial(\bar{u} + u')}{\partial x} + \frac{\partial(\bar{v} + v')(\bar{T} + T')}{\partial y} - (\bar{T} + T') \frac{\partial(\bar{v} + v')}{\partial y} + \\ &\frac{\partial(\bar{w} + w')(\bar{T} + T')}{\partial z} - (\bar{T} + T') \frac{\partial(\bar{w} + w')}{\partial z} = \frac{\nu}{Pr} \left( \frac{\partial^2(\bar{T} + T')}{\partial x^2} + \frac{\partial^2(\bar{T} + T')}{\partial y^2} + \frac{\partial^2(\bar{T} + T')}{\partial z^2} \right) \end{aligned} \dots (A.16)$$

If equation (A.16) is time averaged, the result will be:-

$$\begin{aligned} &\frac{\partial(\bar{u}\bar{T} + \overline{u'T'})}{\partial x} - (\bar{T} + \overline{T'}) \frac{\partial(\bar{u} + \overline{u'})}{\partial x} + \frac{\partial(\bar{v}\bar{T} + \overline{v'T'})}{\partial y} - (\bar{T} + \overline{T'}) \frac{\partial(\bar{v} + \overline{v'})}{\partial y} + \\ &\frac{\partial(\bar{w}\bar{T} + \overline{w'T'})}{\partial z} - (\bar{T} + \overline{T'}) \frac{\partial(\bar{w} + \overline{w'})}{\partial z} = \frac{\nu}{Pr} \left( \frac{\partial^2(\bar{T} + \overline{T'})}{\partial x^2} + \frac{\partial^2(\bar{T} + \overline{T'})}{\partial y^2} + \frac{\partial^2(\bar{T} + \overline{T'})}{\partial z^2} \right) \\ &\frac{\partial uT}{\partial x} + \frac{\partial \overline{u'T'}}{\partial x} - T \frac{\partial u}{\partial x} + \frac{\partial vT}{\partial y} + \frac{\partial \overline{v'T'}}{\partial y} - T \frac{\partial v}{\partial y} + \frac{\partial wT}{\partial z} + \frac{\partial \overline{w'T'}}{\partial z} - T \frac{\partial w}{\partial z} = \frac{\nu}{Pr} \left( \frac{\partial^2 T}{\partial x^2} + \frac{\partial^2 T}{\partial y^2} + \frac{\partial^2 T}{\partial z^2} \right) \end{aligned} \dots (A.17)$$

Substitute from equation (A.14) into equation (A.13) to get

$$u \frac{\partial T}{\partial x} + T \frac{\partial u}{\partial x} + \frac{\partial \overline{u'T'}}{\partial x} - T \frac{\partial u}{\partial x} + v \frac{\partial T}{\partial y} + T \frac{\partial v}{\partial y} + \frac{\partial \overline{v'T'}}{\partial y} - T \frac{\partial v}{\partial y} + w \frac{\partial T}{\partial z} + T \frac{\partial w}{\partial z} + \frac{\partial \overline{w'T'}}{\partial z} - T \frac{\partial w}{\partial z}$$

$$= \frac{\nu}{Pr} \left( \frac{\partial^2 T}{\partial x^2} + \frac{\partial^2 T}{\partial y^2} + \frac{\partial^2 T}{\partial z^2} \right)$$

Rearrange the above equation to get

$$u \frac{\partial T}{\partial x} + v \frac{\partial T}{\partial y} + w \frac{\partial T}{\partial z} = \frac{\nu}{Pr} \left( \frac{\partial^2 T}{\partial x^2} + \frac{\partial^2 T}{\partial y^2} + \frac{\partial^2 T}{\partial z^2} \right) + \frac{\partial(-\overline{u'T'})}{\partial x} + \frac{\partial(-\overline{v'T'})}{\partial y} + \frac{\partial(-\overline{w'T'})}{\partial z}$$

... (A.18)

Multiply equations (A.18) by the density,  $\rho$  to get

$$\rho u \frac{\partial T}{\partial x} + \rho v \frac{\partial T}{\partial y} + \rho w \frac{\partial T}{\partial z} = \frac{\mu}{Pr} \left( \frac{\partial^2 T}{\partial x^2} + \frac{\partial^2 T}{\partial y^2} + \frac{\partial^2 T}{\partial z^2} \right) + \frac{\partial(-\rho \overline{u'T'})}{\partial x} + \frac{\partial(-\rho \overline{v'T'})}{\partial y} + \frac{\partial(-\rho \overline{w'T'})}{\partial z}$$

... (A.19)

The terms  $-\rho \overline{u'T'}$ ,  $-\rho \overline{v'T'}$  and  $-\rho \overline{w'T'}$  in equation (A.19) are called *turbulent heat fluxes* for turbulent flow.

If an isotropic turbulence is assumed, the Reynolds stresses and turbulent heat fluxes can be represented by the following expressions:

$$\left. \begin{aligned} -\rho \overline{u'^2} &= 2\mu_t \frac{\partial u}{\partial x}, -\rho \overline{v'^2} = 2\mu_t \frac{\partial v}{\partial y}, -\rho \overline{w'^2} = 2\mu_t \frac{\partial w}{\partial z} \\ -\rho \overline{u'v'} &= \mu_t \left( \frac{\partial u}{\partial y} + \frac{\partial v}{\partial x} \right), -\rho \overline{u'w'} = \mu_t \left( \frac{\partial u}{\partial z} + \frac{\partial w}{\partial x} \right), -\rho \overline{v'w'} = \mu_t \left( \frac{\partial v}{\partial z} + \frac{\partial w}{\partial y} \right) \\ -\rho \overline{u'T'} &= \frac{\mu_t}{Pr_t} \frac{\partial T}{\partial x}, -\rho \overline{v'T'} = \frac{\mu_t}{Pr_t} \frac{\partial T}{\partial y}, -\rho \overline{w'T'} = \frac{\mu_t}{Pr_t} \frac{\partial T}{\partial z} \end{aligned} \right\}$$

... (A.20)

Momentum Equation:-

For X-direction

After substituting the Reynolds stresses from equation (A.20) into the X-direction of momentum equations for turbulent flows, the result will be:-

$$\begin{aligned} \rho u \frac{\partial u}{\partial x} + \rho v \frac{\partial u}{\partial y} + \rho w \frac{\partial u}{\partial z} &= -\frac{\partial p}{\partial x} + \frac{\partial}{\partial x} \left( \mu \frac{\partial u}{\partial x} \right) + \frac{\partial}{\partial y} \left( \mu \frac{\partial u}{\partial y} \right) + \frac{\partial}{\partial z} \left( \mu \frac{\partial u}{\partial z} \right) \\ &+ 2 \frac{\partial}{\partial x} \left( \mu_t \frac{\partial u}{\partial x} \right) + \frac{\partial}{\partial y} \left( \mu_t \left( \frac{\partial u}{\partial y} \right) \right) + \frac{\partial}{\partial y} \left( \mu_t \left( \frac{\partial v}{\partial x} \right) \right) + \frac{\partial}{\partial z} \left( \mu_t \left( \frac{\partial u}{\partial z} \right) \right) + \frac{\partial}{\partial z} \left( \mu_t \left( \frac{\partial w}{\partial x} \right) \right) \end{aligned}$$

Now, the turbulent stresses are added to laminar by using the concept of mean effective viscosity,  $\mu_{eff}$  ( $\mu_{eff} = \mu + \mu_t$ ) as follows:

$$\begin{aligned} \rho u \frac{\partial u}{\partial x} + \rho v \frac{\partial u}{\partial y} + \rho w \frac{\partial u}{\partial z} &= -\frac{\partial p}{\partial x} + \frac{\partial}{\partial x} \left( \mu_{eff} \frac{\partial u}{\partial x} \right) + \frac{\partial}{\partial y} \left( \mu_{eff} \frac{\partial u}{\partial y} \right) + \frac{\partial}{\partial z} \left( \mu_{eff} \frac{\partial u}{\partial z} \right) + \frac{\partial}{\partial x} \left( \mu_t \frac{\partial u}{\partial x} \right) \\ &+ \frac{\partial}{\partial y} \left( \mu_t \left( \frac{\partial v}{\partial x} \right) \right) + \frac{\partial}{\partial z} \left( \mu_t \left( \frac{\partial w}{\partial x} \right) \right) \end{aligned} \quad \dots \text{(A.21)}$$

By the same way, the Y and Z directions respectively will be:-

Y-direction

$$\begin{aligned} \rho u \frac{\partial v}{\partial x} + \rho v \frac{\partial v}{\partial y} + \rho w \frac{\partial v}{\partial z} &= -\frac{\partial p}{\partial y} + \frac{\partial}{\partial x} \left( \mu_{eff} \frac{\partial v}{\partial x} \right) + \frac{\partial}{\partial y} \left( \mu_{eff} \frac{\partial v}{\partial y} \right) + \frac{\partial}{\partial z} \left( \mu_{eff} \frac{\partial v}{\partial z} \right) + \frac{\partial}{\partial x} \left( \mu_t \frac{\partial u}{\partial y} \right) \\ &+ \frac{\partial}{\partial y} \left( \mu_t \left( \frac{\partial v}{\partial y} \right) \right) + \frac{\partial}{\partial z} \left( \mu_t \left( \frac{\partial w}{\partial y} \right) \right) \end{aligned} \quad \dots \text{(A.22)}$$

Z-direction

$$\begin{aligned} \rho u \frac{\partial w}{\partial x} + \rho v \frac{\partial w}{\partial y} + \rho w \frac{\partial w}{\partial z} &= -\frac{\partial p}{\partial z} + \frac{\partial}{\partial x} \left( \mu_{eff} \frac{\partial w}{\partial x} \right) + \frac{\partial}{\partial y} \left( \mu_{eff} \frac{\partial w}{\partial y} \right) + \frac{\partial}{\partial z} \left( \mu_{eff} \frac{\partial w}{\partial z} \right) + \frac{\partial}{\partial x} \left( \mu_t \frac{\partial u}{\partial z} \right) \\ &+ \frac{\partial}{\partial y} \left( \mu_t \left( \frac{\partial v}{\partial z} \right) \right) + \frac{\partial}{\partial z} \left( \mu_t \left( \frac{\partial w}{\partial z} \right) \right) \end{aligned} \quad \dots \text{(A.23)}$$

Energy Equation:

Substitute the relations of turbulent heat fluxes of (A.20) into (A.19) to get

$$\begin{aligned} \rho u \frac{\partial T}{\partial x} + \rho v \frac{\partial T}{\partial y} + \rho w \frac{\partial T}{\partial z} &= \frac{\partial}{\partial x} \left( \frac{\mu}{Pr} \frac{\partial T}{\partial x} \right) + \frac{\partial}{\partial y} \left( \frac{\mu}{Pr} \frac{\partial T}{\partial y} \right) + \frac{\partial}{\partial z} \left( \frac{\mu}{Pr} \frac{\partial T}{\partial z} \right) + \frac{\partial}{\partial x} \left( \frac{\mu_t}{Pr_t} \frac{\partial T}{\partial x} \right) \\ &+ \frac{\partial}{\partial y} \left( \frac{\mu_t}{Pr_t} \frac{\partial T}{\partial y} \right) + \frac{\partial}{\partial z} \left( \frac{\mu_t}{Pr_t} \frac{\partial T}{\partial z} \right) \end{aligned} \quad \dots \text{(A.24)}$$

By using the concept of effective diffusion coefficient  $\frac{\mu_{eff}}{Pr_{eff}}$

( $\frac{\mu_{eff}}{Pr_{eff}} = \frac{\mu}{Pr} + \frac{\mu_t}{Pr_t}$ ), (A.74) will become

$$\rho u \frac{\partial T}{\partial x} + \rho v \frac{\partial T}{\partial y} + \rho w \frac{\partial T}{\partial z} = \frac{\partial}{\partial x} \left( \frac{\mu_{eff}}{Pr_{eff}} \frac{\partial T}{\partial x} \right) + \frac{\partial}{\partial y} \left( \frac{\mu_{eff}}{Pr_{eff}} \frac{\partial T}{\partial y} \right) + \frac{\partial}{\partial z} \left( \frac{\mu_{eff}}{Pr_{eff}} \frac{\partial T}{\partial z} \right) \quad \dots (A.75)$$

## APPENDIX B

### **Derivation of Finite Difference Equation for First Derivative of Dependent Variable $\Psi$ with Clustering**

For finding the finite difference form of first derivative for all dependent variables in r-direction in circular duct or y-direction in rectangular duct which is affected by four clustered nodal points as shown in figure (B-1), the following derivation will be done for rectangular duct to be also applied for circular duct:-

Before beginning the derivation, there is an important factor which should be explained with some details. This factor is the expansion factor,  $E$  which expresses the value of increment in the radial direction,  $\Delta y$  of the next node with respect to the previous node when  $\Delta y$  starts from the lower wall (see figure (B.1)). When the fine grid is required near the walls the value of  $E$  should be selected to be less than 1. In the present work the appropriate value of  $E$  is 0.5.

Let  $\Psi$  varies as fourth degree polynomial function as follows:-

$$\Psi = a + by + cy^2 + dy^3 + ey^4 \quad \dots (B-1)$$

Derive (B-1) with respect to y at (y=0), to get:

$$\left. \frac{\partial \Psi}{\partial y} \right|_{y=0} = b \quad \dots (B-2)$$

Apply equation (B-1) at each node of the nodes shown in figure (B-1), as follows:

$$\Psi_{i,j} \Big|_{y=0} = a \quad \dots (B-3)$$

$$\Psi_{i,j+1} \Big|_{y=\Delta y} = a + b\Delta y + c\Delta y^2 + d\Delta y^3 + e\Delta y^4 \quad \dots (B-4)$$

$$\text{Let } \eta = \frac{1}{E}$$

$$\Psi_{i,j+2} \Big|_{y=2\Delta y} = a + b(1 + \eta)\Delta y + c(1 + \eta)^2 \Delta y^2 + d(1 + \eta)^3 \Delta y^3 + e(1 + \eta)^4 \Delta y^4 \quad \dots \text{(B-}\circ\text{)}$$

$$\begin{aligned} \Psi_{i,j+3} \Big|_{y=3\Delta y} &= a + b(1 + \eta + \eta^2)\Delta y + c(1 + \eta + \eta^2)^2 \Delta y^2 + d(1 + \eta + \eta^2)^3 \Delta y^3 \\ &+ e(1 + \eta + \eta^2)^4 \Delta y^4 \quad \dots \text{(B-}\grave{\text{v}}\text{)} \end{aligned}$$

$$\begin{aligned} \Psi_{i,j+4} \Big|_{y=4\Delta y} &= a + b(1 + \eta + \eta^2 + \eta^3)\Delta y + c(1 + \eta + \eta^2 + \eta^3)^2 \Delta y^2 \\ &+ d(1 + \eta + \eta^2 + \eta^3)^3 \Delta y^3 + e(1 + \eta + \eta^2 + \eta^3)^4 \Delta y^4 \quad \dots \text{(B-}\vee\text{)} \end{aligned}$$

Subtract equation (B.ϣ) from equations (B.ξ), (B.∘), (B.ϖ), and (B.∨)

respectively to get:

$$\Psi_{i,j+1} - \Psi_{i,j} = b\Delta y + c\Delta y^2 + d\Delta y^3 + e\Delta y^4 = h_1 \quad \dots \text{(B-}\wedge\text{)}$$

$$\begin{aligned} \Psi_{i,j+2} - \Psi_{i,j+1} &= b(1 + \eta)\Delta y + c(1 + \eta)^2 \Delta y^2 + d(1 + \eta)^3 \Delta y^3 + e(1 + \eta)^4 \Delta y^4 = h_2 \\ &\dots \text{(B-}\grave{\text{a}}\text{)} \end{aligned}$$

$$\begin{aligned} \Psi_{i,j+3} - \Psi_{i,j+2} &= b(1 + \eta + \eta^2)\Delta y + c(1 + \eta + \eta^2)^2 \Delta y^2 + d(1 + \eta + \eta^2)^3 \Delta y^3 \\ &+ e(1 + \eta + \eta^2)^4 \Delta y^4 = h_3 \quad \dots \text{(B-}\grave{\text{b}}\text{)} \end{aligned}$$

$$\begin{aligned} \Psi_{i,j+4} - \Psi_{i,j+3} &= a + b(1 + \eta + \eta^2 + \eta^3)\Delta y + c(1 + \eta + \eta^2 + \eta^3)^2 \Delta y^2 \\ &+ d(1 + \eta + \eta^2 + \eta^3)^3 \Delta y^3 + e(1 + \eta + \eta^2 + \eta^3)^4 \Delta y^4 = h_4 \quad \dots \text{(B-}\grave{\text{c}}\text{)} \end{aligned}$$

By rearranging equations (B-∧), (B-ḁ), (B-ḃ), (B-ḅ), and (B-ḇ) in the form of square matrix and solving them by the Gauss elimination method for finding the constants a, b, c, and d in terms of  $h_1$ ,  $h_2$ ,  $h_3$ , and  $h_4$  as follows:

$$\begin{bmatrix} \Delta y & \Delta y^2 & \Delta y^3 & \Delta y^4 \\ (1 + \eta)\Delta y & (1 + \eta)^2 \Delta y^2 & (1 + \eta)^3 \Delta y^3 & (1 + \eta)^4 \Delta y^4 \\ (1 + \eta + \eta^2)\Delta y & (1 + \eta + \eta^2)^2 \Delta y^2 & (1 + \eta + \eta^2)^3 \Delta y^3 & (1 + \eta + \eta^2)^4 \Delta y^4 \\ (1 + \eta + \eta^2 + \eta^3)\Delta y & (1 + \eta + \eta^2 + \eta^3)^2 \Delta y^2 & (1 + \eta + \eta^2 + \eta^3)^3 \Delta y^3 & (1 + \eta + \eta^2 + \eta^3)^4 \Delta y^4 \end{bmatrix} \begin{bmatrix} b \\ c \\ d \\ e \end{bmatrix} = \begin{bmatrix} h_1 \\ h_2 \\ h_3 \\ h_4 \end{bmatrix}$$



$$C_1 = h_3 - (1 + \eta + \eta^2)h_1 - \frac{B_2}{B_1}(h_2 - (1 + \eta)h_1)$$

$$C_2 = h_4 - (1 + \eta + \eta^2 + \eta^3)h_1 - \frac{A_1}{B_1}(h_2 - (1 + \eta)h_1)$$

$$\begin{bmatrix} \Delta y & \Delta y^2 & \Delta y^3 & \Delta y^4 & h_1 \\ 0 & B_1 \Delta y^2 & B_4 \Delta y^3 & B_5 \Delta y^4 & h_2 - (1 + \eta)h_1 \\ 0 & 0 & D_1 \Delta y^3 & D_3 \Delta y^4 & C_1 \\ 0 & 0 & D_2 \Delta y^3 & D_4 \Delta y^4 & C_2 \end{bmatrix}$$

$$\begin{bmatrix} \Delta y & \Delta y^2 & \Delta y^3 & \Delta y^4 & h_1 \\ 0 & B_1 \Delta y^2 & B_4 \Delta y^3 & B_5 \Delta y^4 & h_2 - (1 + \eta)h_1 \\ 0 & 0 & D_1 \Delta y^3 & D_3 \Delta y^4 & C_1 \\ 0 & 0 & 0 & \left( D_4 - \frac{D_2}{D_1} D_3 \right) \Delta y^4 & \left( C_2 - \frac{D_2}{D_1} C_1 \right) \end{bmatrix}$$

By back substitution:-

$$\left. \begin{aligned} e &= \frac{\left( C_2 - \frac{D_2}{D_1} C_1 \right)}{\left( D_4 - \frac{D_2}{D_1} D_3 \right) \Delta y^4} \\ d &= \frac{C_1 - e D_3 \Delta y^4}{D_1 \Delta y^3} \\ c &= \frac{h_2 - (1 + \eta)h_1 - e B_5 \Delta y^4 - d B_4 \Delta y^3}{B_1 \Delta y^2} \\ b &= \frac{h_1 - e \Delta y^4 - d \Delta y^3 - c \Delta y^2}{\Delta y} \end{aligned} \right\} \dots \text{(B-13)}$$

Substitute  $\eta = 1.25$  in equation (B-13) to get:

$$b = \frac{2.69179h_1 - 1.422789h_2 + 0.396439h_3 - 0.0454402h_4}{\Delta y} \quad \dots (B-1 \xi)$$

Substitute equations (B-1), (B-2), (B-3), (B-4), and (B-5) into (B-6) to get:-

$$\frac{\partial \Psi}{\partial y} \Big|_{i,j} = \frac{-1.619999\Psi_{i,j} + 2.69179\Psi_{i,j+1} - 1.4227896\Psi_{i,j+2} + 0.3964391\Psi_{i,j+3} - 0.0454402\Psi_{i,j+4}}{\Delta y} \quad \dots (B-7)$$

Equation (B-7) is a general first derivative valid for all dependent variables  $\Psi$  in the radial direction which is affected by four clustered forward nodal points as shown in figure (B-1). Where  $\Delta y$  represents the smallest grid size in the radial direction close to the wall.

By the same way, the first derivative for all dependent variables in the radial direction which is affected by four clustered backward nodal points as shown in figure (B-2) will be:

$$\frac{\partial \Psi}{\partial y} \Big|_{i,N} = \frac{1.619999\Psi_{i,N} - 2.69179\Psi_{i,N-1} + 1.4227896\Psi_{i,N-2} - 0.3964391\Psi_{i,N-3} + 0.0454402\Psi_{i,N-4}}{\Delta y} \quad \dots (B-8)$$

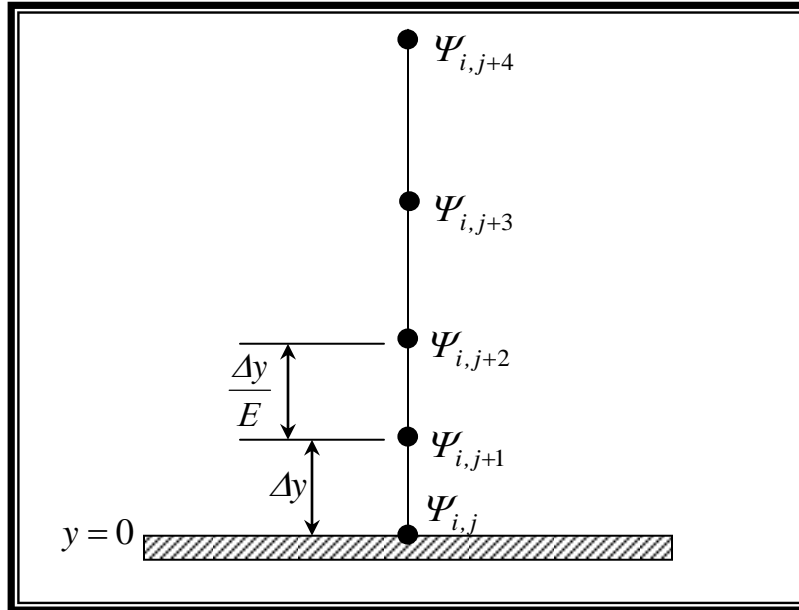


Figure (B.1) Finite Difference Clustered Grid Close to the Lower Wall

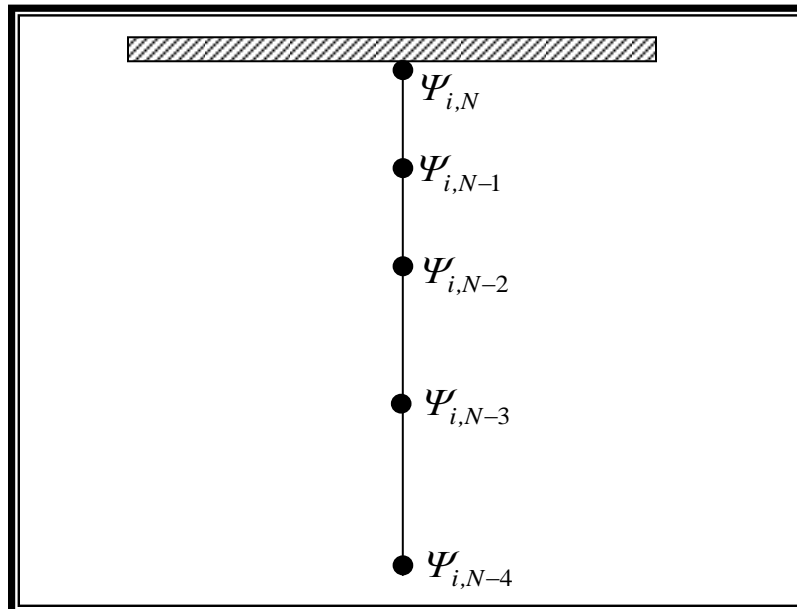
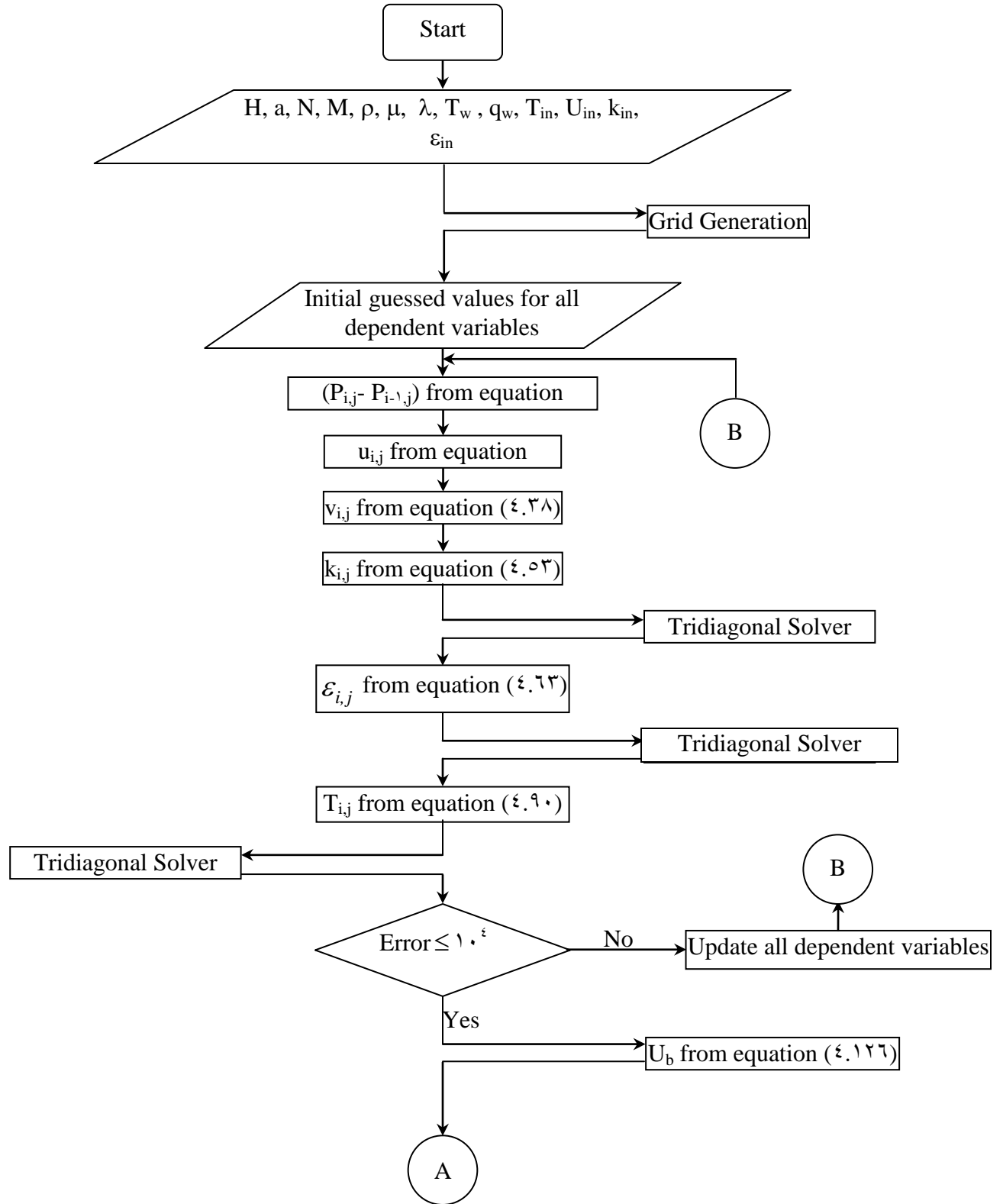


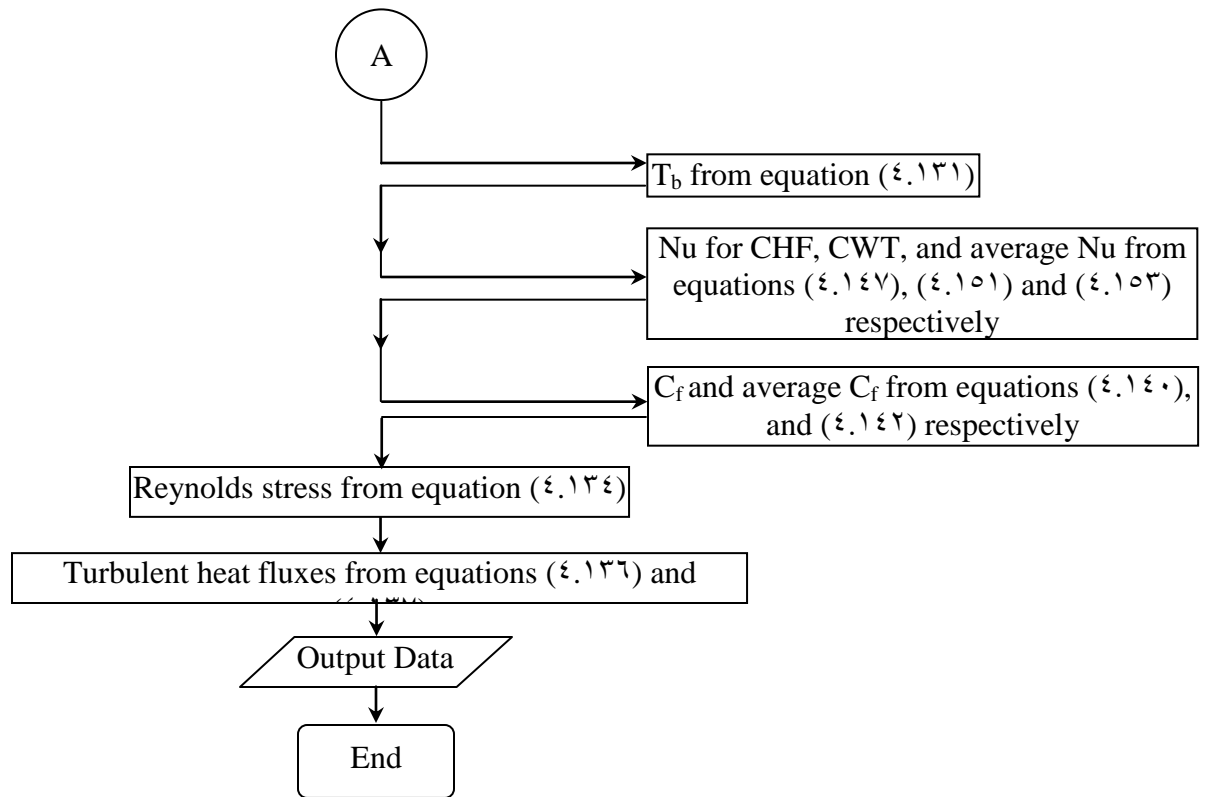
Figure (B.2) Finite Difference Clustered Grid Close to the Upper Wall

## APPENDIX C

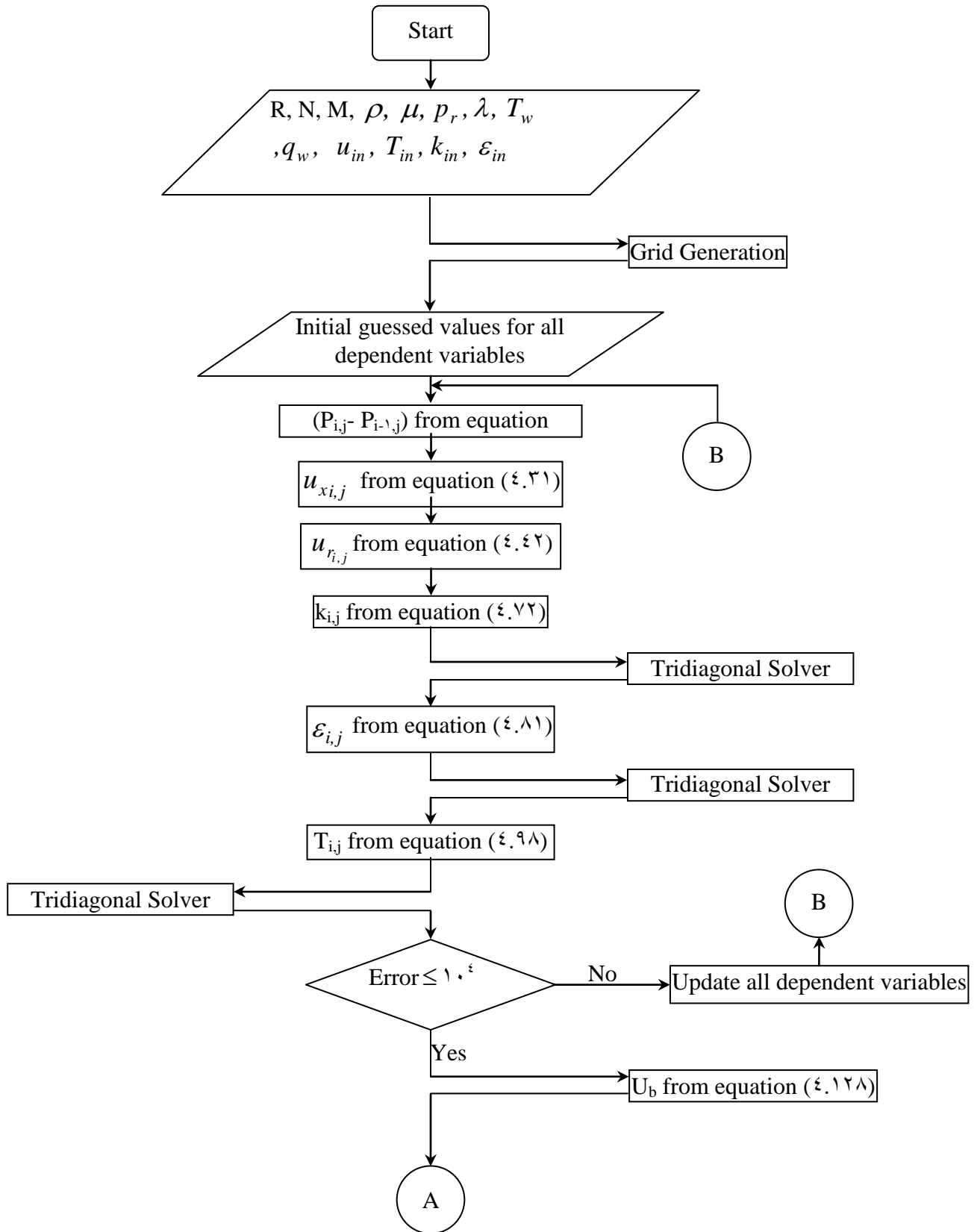
### Flowcharts of Computer Programs for Rectangular and Circular Duct

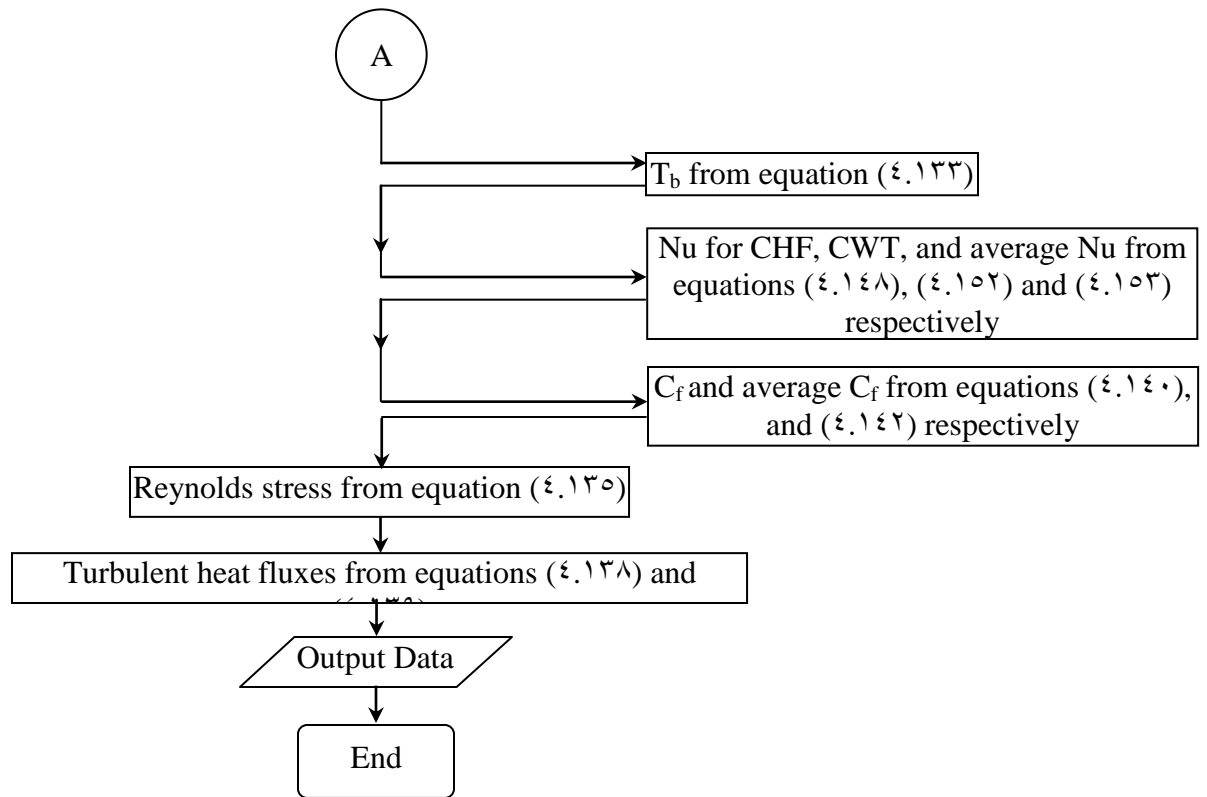
#### C.1 Rectangular Duct Flowchart:





**C.3 Circular Duct Flowchart:**





# THE COMMITTEE CERTIFICATE

We certify that we have read this thesis, entitled “**Developing Turbulent Flow and Heat Transfer through Ducts of Rectangular and Circular Cross Section**”, and as examining committee, examined the student “**Ali Nu'man Ibrahim**” in its contents and in what is connected with it, and that in our opinion it meets the standard of a thesis for the degree of Master of Science in Mechanical Engineering.

Signature:

Name: Asst. Prof.  
**Dr. Adil A. Al- moosway**  
(Member)

Date: / / ٢٠٠٥

Signature:

Name: Asst. Prof.  
**Dr. Tahseen A. Al- Hattab**  
(Member)

Date: / / ٢٠٠٥

Signature:

Name: Prof.  
**Dr. Jalal Mohammed Jalil**  
(Chairman)

Date: / / ٢٠٠٥

Signature:

Name: Asst. Pro.  
**Dr. Ihsan Y. Hussain**  
(Supervisor)

Date: / / ٢٠٠٥

Signature:

Name: Asst. Prof.  
**Dr. Emad S. Ali**  
(Supervisor)

Date: / / ٢٠٠٥

Approval of the Mechanical Engineering  
Department.

Head of the Mechanical Engineering  
Department Signature:

Name: Asst. Prof.

**Dr. Alaa M. Hussain**

Approval of the Deanery of the College  
of Engineering.

Dean of the College of Engineering

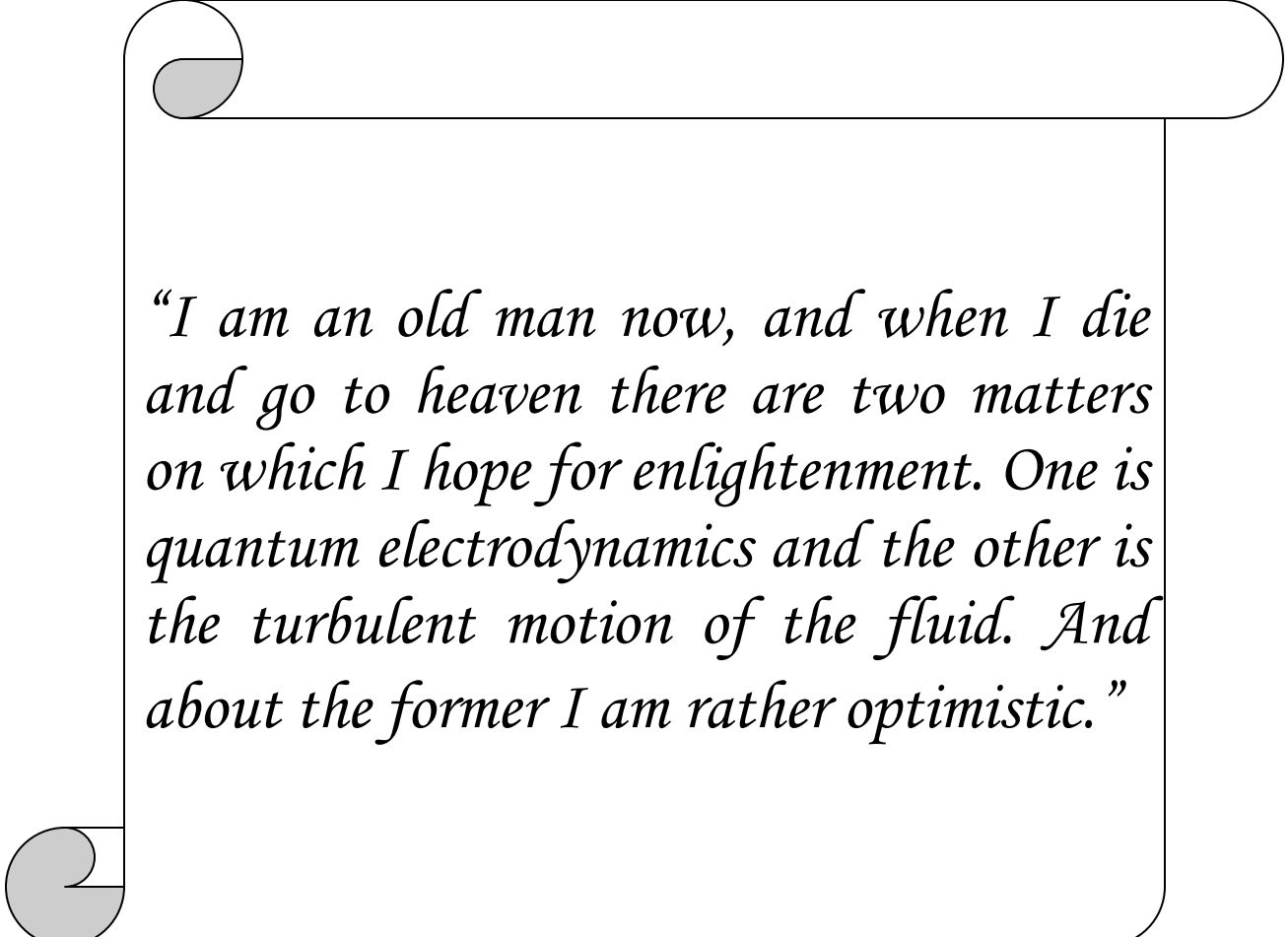
Signature:

Name: Asst. Prof.

**Dr. Haroun A. K. Shahad**

Date: / / ٢٠٠٥

Date: / / ٢٠٠٥



*“I am an old man now, and when I die and go to heaven there are two matters on which I hope for enlightenment. One is quantum electrodynamics and the other is the turbulent motion of the fluid. And about the former I am rather optimistic.”*

*Sir Horace Lamb in 1932 [1].*

# Contents

Page	Subjects
i	Contents
iii	List of Symbols
1	Chapter One : Introduction
1	1.1 General
4	1.2 Objectives
5	Chapter Two : Literature Survey
11	Scope of the present work
12	Chapter Three :Mathematical Model
12	3.1 Introduction
12	3.2 Geometrical shapes and system Coordinates
12	3.3 Assumptions and Governing Equations of Rectangular Duct
13	3.4 Assumptions and Governing Equations of Circular Duct
14	3.5 Turbulence Model
14	3.5.1 k-ε Model for Rectangular Duct
15	3.5.2 k-ε Model for Cylindrical Coordinates
16	3.6 Boundary Conditions
16	3.6.1 Boundary Conditions for Rectangular Duct
17	3.6.1 Boundary Conditions for Circular Duct
19	3.7 Wall Effects
20	3.8 The Wall-Function-Method
21	The Dimensionless Quantities
23	Chapter Four : Numerical Solution
23	4.1 Introduction
23	4.2 Grid Generation
24	4.3 Momentum Equations
24	4.3.1 Numerical Formulation for Momentum Equation of Rectangular Duct
28	4.3.2 Numerical Formulation for Momentum Equation of Circular Duct
32	4.4 Numerical Formulation for Continuity Equation of Rectangular and Circular Duct
33	4.5 k-ε Model
33	4.5.1 Numerical Formulation for k-ε Model for Rectangular Duct
37	4.5.2 Numerical Formulation for k-ε Model for Circular Duct
39	4.6 Energy Equations
39	4.6.1 Energy Equations for Rectangular Duct
41	4.6.2 Energy Equations for Circular Duct
42	4.7 The Treatment of Singularity in the Center of Circular Duct

٤٦	٤.٨ Calculation of Boundary Values
٤٧	٤.٩ Calculation of Mean Velocity
٤٩	٤.١٠ Calculation of Bulk Temperature
٥١	٤.١١ Calculation of Reynolds Stresses
٥١	٤.١٢ Calculation of Turbulent Heat Flux
٥٢	٤.١٣ Calculation of Coefficient of Friction
٥٢	٤.١٤ Calculation of Nussult Number
٥٤	٤.١٥ Steps of Numerical Solution
٥٧	٤.١٦ Computer Program
٥٨	٤.١٧.١ Input Data
٥٨	٤.١٧.٢ Output Data
٥٩	٤.١٧.٣ Specifications of The Computer Program
٦١	Chapter Five : Results and Discussion
٦١	٥.١ Introduction
٦١	٥.٢ Numerical Solutions Limitations
٦٢	٥.٣ Developments of Velocity Profiles
٦٣	٥.٤ Developments of Kinetic Energy of Turbulence
٦٣	٥.٥ Axial Reynolds Stress
٦٤	٥.٦ Coefficient of friction
٦٤	٥.٧ Average Coefficient of friction
٦٤	٥.٨ Temperature Distribution
٦٥	٥.٩ Overall Heating
٦٦	٥.١٠ Turbulent Heat Flux
٦٦	٥.١١ Nussult Number
٦٧	٥.١٢ Verification of Results
٩٨	Chapter Six : Conclusions and Recommendations
٩٨	٦.١ Conclusions
٩٩	٦.٢ Recommendations
١٠٠	References
A-١	Appendix A : Derivation of the Governing Equations for Turbulent flows in terms of Cartesian Coordinates
B-١	Appendix B : Derivation of Finite Difference Equation for First Derivative of Dependent Variable $\Psi$ with Clustering
C-١	Appendix C : Flowcharts of Computer Programs for Rectangular and Circular Duct

Symbol	Definition	Unit
$A_c$	Cross-Sectional Area	m <sup>2</sup>
$a$	Width of Rectangular Duct	m
$C_f$	Coefficient of Friction	
$C_\mu, C_{\varepsilon 1}, C_{\varepsilon 2}$	Coefficients of Turbulence Model	
$D$	Diameter of Circular Duct	m
$D_h$	Hydraulic Diameter of Rectangular duct	m
$E$	Constant Used in Wall Function	
$G$	Generation Term	kg/m.s <sup>3</sup>
$H$	Height of Rectangular Duct	m
$k$	Turbulent Kinetic Energy for Unit of Mass	m <sup>2</sup> /s <sup>2</sup>
$L$	Length of the Duct	m
$M$	Number of Grid Nodes in the Axial Direction	
$\dot{m}$	Mass Flow Rate	kg/s
$N$	Number of Grid Nodes in the Radial Direction	
$Nu$	Local Nussult Number	
$P$	Pressure	N/m <sup>2</sup>
$Pee$	Pee Function	
$P_r, P_{r_t}$	Laminar and Turbulent Prandtl Number	
$q_w$	Constant Heat Flux	W/m <sup>2</sup>
$r$	Radial Direction of Circular Duct	m
$R$	Radius of Circular Duct	m
$\Delta r$	The Distance Between Two Nodal Points in the Radial Direction	m
$Re$	Reynolds Number	
$T$	Temperature	°C
$T_b$	Bulk Temperature	°C
$T_{in}$	Temperature at Inlet	°C
$u_b$	Bulk Velocity	m/s
$u$	Mean Velocity in Axial Direction of Rectangular Duct	m/s
$u_{in}$	Velocity at Inlet	m/s
$u_r$	Mean Velocity in Radial Direction of Circular Duct	m/sec
$u_x$	Mean Velocity in Axial Direction of Circular Duct	m/s
$v$	Transverse Mean Velocity of Rectangular Duct	m/s
$x$	Axial Direction of the Duct	m
$\Delta x$	The Distance Between Two nodal Points in the Axial Direction of the Duct	m
$y$	Transverse Direction of Rectangular Duct	m

$y_p$	The Normal Distance from the Wall Surface to Nodal Point Neighboring to the Wall	m
$y^+$	Dimensionless Distance from the Wall	—

## Greek Symbols

Symbol	Definition	Unit
$\lambda$	Conduction Heat Transfer Coefficient of Fluid	W/m.c
$\Gamma_{wall}$	Diffusion Coefficient at Wall	kg/m.s
$\varepsilon$	Dissipation Rate of Kinetic Energy of Turbulence	$m^2/s^3$
$\kappa$	Von Karman Constant	
$\mu$	Dynamic Viscosity	kg/m.s
$\mu_t$	Turbulent Viscosity	kg/m.s
$\mu_{eff}$	Effective Viscosity	kg/m.s
$\rho$	Density of Fluid	$kg/m^3$
$\tau_w$	Shear Stress at Wall	$N/m^2$

## Superscripts

Symbol	Definition	Unit
—	Mean	—
◊	Fluctuation	—
q	Number of Iterations	—

## Subscripts

Symbol	Definition	Unit
i,j	The index increment along the Axial and Radial Direction	—
t	Refers to Turbulent Flow	—
k	Refers to Kinetic Energy of Turbulence	—
$\varepsilon$	Refers to Dissipation Rate of Kinetic Energy of Turbulence	—
in	Inlet	—

## Supervisors Certificate

We certify that this thesis entitled “**Developing Turbulent Flow and Heat Transfer through Ducts of Rectangular and Circular Cross Section**” which is prepared by “**Ali Nu'man Ibrahim**” had been carried out completely under our supervision at Babylon University in partial fulfillment of the requirements for the degree of Master of Science in Mechanical Engineering.

Signature:

Name: Ass. Pro.

**Dr. Ihsan Y. Hussain**

Date: / / ٢٠٠٥

Signature:

Name: Ass. Pro.

**Dr. Emad S. Ali**

Date: / / ٢٠٠٥

## Chapter One

# INTRODUCTION

### 1.1 General:-

Any fluid flowing in a pipe had to enter the pipe at some location. The region of flow near where the fluid enters the pipe is termed the entrance region and illustrated in figure (1.1). The fluid typically enters the pipe with a nearly uniform velocity profile at section (1). As the fluid moves through the pipe, viscous effects cause it to stick to the pipe wall (the no slip boundary condition). This is true whether the fluid is relatively inviscid air or a very viscous oil. Thus, a boundary layer in which viscous effects are important is produced along the pipe wall such that the initial velocity profile changes with distance along the pipe,  $x$ , until the fluid reaches the end of the entrance length, section (2), beyond which the velocity profile does not vary with  $x$ . The boundary layer has grown in thickness to completely fill the pipe. The shape of the velocity profile in the pipe depends on whether the flow is laminar or turbulent, as does the entrance length,  $le$ . Typical entrance lengths are given by

$$\frac{le}{D} = 0.06 Re \quad \text{for laminar flow}$$

and

$$\frac{le}{D} = 4.4 Re^{1/6} \quad \text{for turbulent flow}$$

Once the fluid reaches the end of the entrance region, section (2) of fig. (1.1), the flow is simpler to describe because the velocity is a function of only the distance from the pipe centerline,  $r$ , and independent of  $x$  [2].

Fluid flow through tubes, pipes, or ducts is commonly used in practice in heating and cooling applications. The fluid in such applications is forced to flow

by a fan or pump through a tube which should be sufficiently long to accomplish the desired heat transfer application.

Turbulence in these applications is generated by friction forces at fixed walls, so it is called wall turbulence (while free turbulence is generated by the flow of layers of fluids with different velocities past or over one another). In the case of real viscous fluids, viscosity effects will result in the conversion of kinetic energy of flow into heat; thus turbulent flow is dissipative in nature. Other effects of viscosity are to make the turbulence more homogeneous and to make it less dependent on direction. In the extreme case, turbulence has quantitatively the same structure in all parts of the flow field; the turbulence is said to be homogeneous. The turbulence is called isotropic if its statistical features have no preference for any direction. If the turbulence is isotropic, no average shear stress can occur and, consequently, no gradient of the mean velocity. This mean velocity, if it occurs, is constant throughout the field. In all other cases, where the mean velocity shows a gradient, the turbulence will be nonisotropic, or anisotropic. Since this gradient in the mean velocity is associated with occurrence of an average shear stress, the expression “shear-flow turbulence” is often used to designate this class of flow. Wall turbulence and an isotropic free turbulence fall into this class [3].

For determination of the points with all desired important fluid flow features through duct, for a solution of questions of the operating reliability of heat transfer equipment with relatively short ducts, it is not sufficient and so expensive to measure these data experimentally. Besides; the experiments of turbulent flow are held on measuring either shear stress or velocity distribution which will be used to calculate the other required fluid flow features from the mathematical relations. These drawbacks of experiment made the researcher tend to rely on Computational Fluid Dynamics (CFD) in calculating all fluid flow and heat transfer features computationally with reliable results, for different boundary conditions, in very short time without economical cost. Hence, the CFD can

predict all fluid flow and heat transfer features numerically with noting that in all problems the number of unknowns is exactly equal to the number of equations. The lack in equations from the unknowns in many problems will be substituted by using the concept of modeling. In other words, in many physical problems there is no frank mathematical relation for calculating some physical properties like turbulent viscosity. Thus, the modeling comes to present a semi-empirical mathematical relation for calculating these properties.

In connection with increasing the rate of convective heat transfer in many industrial installations, there is a substantially increased interest in the study of convective heat transfer in the entrance region of a duct. The demand for more detailed knowledge and for more systematic methods of development was also apparent, particularly in such important applications as the cooling and heating processes in nuclear reactors, gas turbines, all kinds of waste-heat recovery, chemical and other process and power plant [4].

In the present work, developing turbulent flow and heat transfer in the entrance region of rectangular and circular duct as shown in figures (1.2) and (1.3) respectively, will be studied. The governing continuity, momentum, and energy equations will be numerically solved by using the Finite Difference Method. Two heating boundary conditions will be applied for each duct, constant wall temperature (CWT) and constant heat flux (CHF). The model which is used in this study is the  $k - \varepsilon$  model. FORTRAN 90 program is used for each duct to compute all the required fluid flow and heat transfer features.

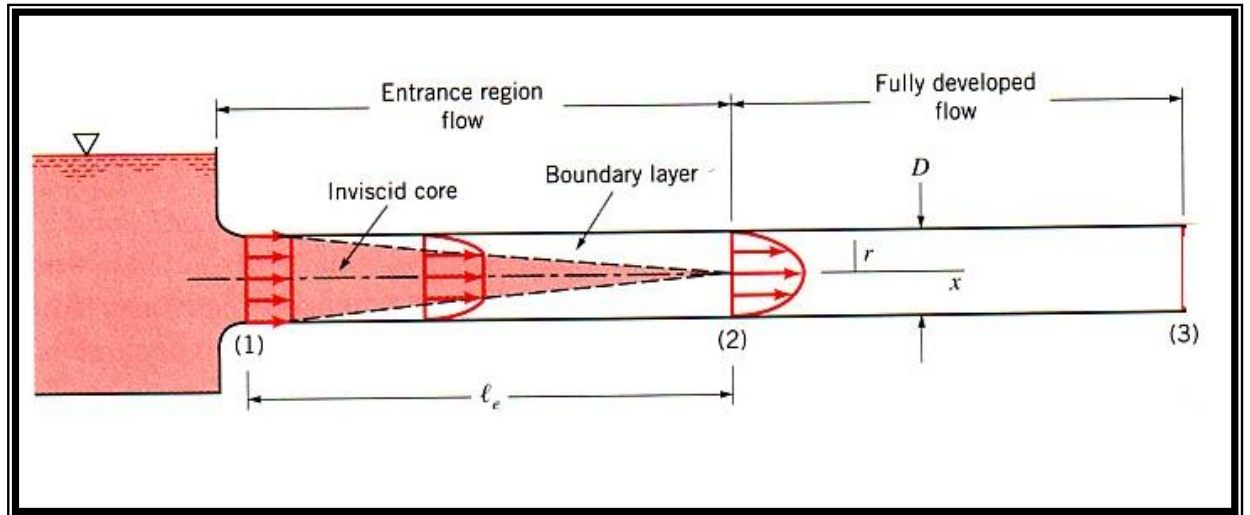


FIGURE (1.1): Entrance region, developing flow, and fully developed flow in a pipe as depicted in Ref. [1].

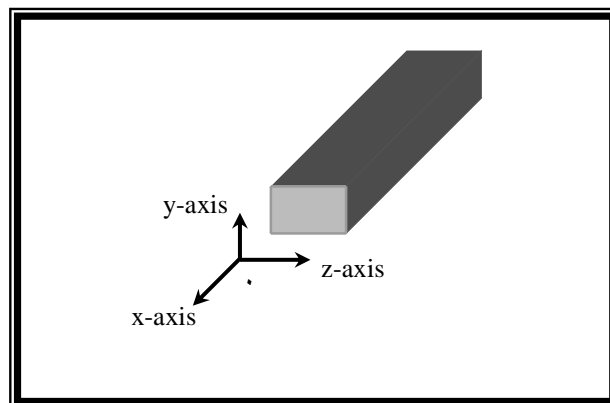


FIGURE (1.2): Rectangular Duct

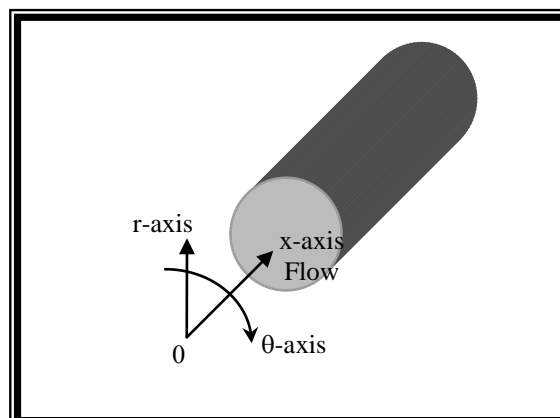


FIGURE (1.3): Circular Duct

**1.2 Objectives:-**

The main objectives of the present work are as follows:-

1. Mathematical modeling of turbulent developing flow and heat transfer through two dimensional rectangular and circular duct respectively.
2. Numerical solution of the governing equations for rectangular and circular duct by using Finite Difference Method.
3. Solving the problem for two types of thermal boundary conditions, constant wall temperature and constant heat flux.
4. Discussion of the results for final conclusions.

## Chapter Two

# LITERATURE SURVEY

### 2.1 Introduction:-

Developing turbulent flow and heat transfer in Circular and rectangular duct are very important especially in cooling and heating processes in nuclear reactors, gas turbines, all kinds of waste-heat recovery, chemical and other process and power plant. In the present chapter, the relevant works will be reviewed.

### 2.2 Survey of Literature:-

**Seban et. al** (1951) [5], investigated analytically the case of heat transfer to an incompressible fluid of constant properties flowing turbulently within a pipe having linear variation of wall temperature. The results compared heat-transfer coefficients as obtained under conditions of constant wall temperature and linear variation of wall temperature and they showed that for fluids of low Prandtl number the effect of wall-temperature profile was significant.

**Peter and Stuart** (1960) [6], measured experimentally the temperature profile and the local heat transfer from the wall of circular tube at  $X/D$  values of 0.403, 1.13, 4.12, and 9.97 respectively. This was achieved at the thermal entrance region for air in fully developed turbulent flow at Reynolds numbers of 10,000 and 70,000 in a 1.0 in tube. The velocity profile and pressure were also measured at the previous  $x/d$  values. Radial and longitudinal temperature gradients, radial heat fluxes, and eddy diffusivities for heat and momentum transfer were computed from the measurements. The longitudinal temperature gradients at all radii were found to differ significantly from the mixed mean temperature gradient. The eddy diffusivity for heat transfer was found to be independent of length in the thermal entrance region and hence a function only of the fluid motion.

The local heat transfer characteristics for air flowing turbulently in the entrance region of a circular duct had been determined experimentally over a flow Reynolds number range of  $10^4$  to  $10^5$  by **Mills** (1962) [7]. A wall - boundary heating condition of uniform heat flux was imposed. The entrance configuration investigated included a long calming section, bellmouth, orifice plate arrangements, and various entries of practical significance-elbow, T-piece, etc. A correlation of heat transfer under fully developed conditions was included together with the discussion of the effects of the fluid property variation in an axial direction. Entrance region heat transfer data were presented in the form of local heat transfer film coefficients and as the dimensionless ratio  $N_{U_x}/N_{U_\infty}$ , this quantity was defined in such a manner as to eliminate the effects of the fluid property variation in an axial direction. Data for average heat transfer over tubes of lengths from  $1/4$  to  $32$  diameters were presented in the form of the ratio  $N_{U_a}/N_{U_\infty}$ . In the case of the long calming section the results comparison with both experimental and theoretical previous investigation was satisfactory.

**Yang and Yu** (1974) [8], investigated numerically the  $2D$  entrance problem of convective magnetohydrodynamic channel flow between two parallel vertical plates subjected simultaneously to an axial temperature gradient and a pressure gradient. Both constant heat flux and constant wall temperature were considered. The solution matched to the fully developed solutions after a certain entrance length. It was found that an applied transverse magnetic field may reduce the entrance length of the velocity considerably, but has little effect on the temperature development.

**Stephenson** (1976) [9], predicted turbulent fluid flow and heat transfer in a circular tube and between parallel and diverging plates by the use of a finite-difference procedure. A turbulence model involving the solution of partial differential equations for two turbulence quantities had been employed. At the pipe or duct inlet, a finite velocity boundary-layer thickness,  $\delta$ , was assumed together with a power-law velocity profile. Except for close to the wall, the

turbulent kinetic energy,  $k$ , was assumed to vary linearly across the boundary-layer. The dissipation,  $\varepsilon$ , was calculated from  $k$  and from an assumed mixing-length distribution. The enthalpy was assumed uniform across the pipe or duct inlet.

**Emery and Gessner** (1976)[10], computed the velocity and temperature profiles for turbulent flow, both in the entrance region and the fully developed state in a duct with heated parallel plates. They started the calculations at the duct inlet and used a finite difference technique and a three-dimensional mixing length originally defined for corner flows, so it was possible to predict axial flow behavior and the non-asymptotic approach to fully developed flow with and without associated heat transfer. The used boundary conditions were ( $u(0, y) = u_{in}$ ,  $u(x, 0) = 0$ ,  $v(x, 0) = 0$  for  $x \geq 0$ ).

**Emery et. al** (1980)[11], computed velocity and temperature profiles for developing steady turbulent flow in a square duct with constant wall temperature, constant heat flux or asymmetric heating. The computations utilized an explicit numerical differencing scheme and an algebraic closure model based upon a three dimensional mixing length. The computed local and fully-developed shear stresses and heat transfer were shown to be in good agreement with measured data and with predictions using the  $k - \varepsilon$  closure model. The equations of the system were effected by means of the inlet conditions,  $u(0, y, z) = u_{in}$  and  $v(0, y, z) = w(0, y, z) = 0$ , with all Reynolds stress components equal to zero at the inlet and with the boundary conditions at the wall of  $u = v = w = 0$  and either  $T_w = 0$  for constant wall temperature, or  $-k \frac{\partial T}{\partial n} = q_w$  for constant heat flux. The

law of the wall, in conjunction with the seventh power law velocity profile was applied at all axial positions to determine the wall shear stress which was then used in evaluating the axial velocity at the first nodal point from the wall.

**Chen and Chiou** (1981) [12], studied laminar and turbulent heat transfer in pipe flow for liquid metals. Three flow regions, namely fully-developed,

developing thermal, and developing thermal and velocity regions were considered. The Van Driest mixing length hypothesis was adapted to model the turbulent shear stress, and the Cebeci model was extended to model the turbulent thermal conductivity of liquid metal flows. The thermal damping constant was redetermined in the study for the fully-developed region as well as other developing regions. Correlation for heat transfer calculation was given for boundary conditions at constant heat flux and constant wall temperature. The effect of the variation of physical properties was also studied. Coefficient of heat transfer calculation when the property is variable was given in a simple form of a liquid sodium NaK eutectic.

**Emery and Gessner** (1981) [13], made comparisons between experimental data and numerical predictions based on a three-dimensional length-scale model applicable to developing turbulent flow in rectangular duct of arbitrary aspect ratio. There was an underprediction in the friction factor behavior calculation at Reynolds numbers ( $Re < 10,000$ ) and overprediction in the axial centerline velocity calculation when ( $x/Dh \geq 10$ ) for the same previous range of Re. The cause of these discrepancies was probably attributable to the length-scale model employed according to the authors' point of view.

**Jicha and Ramik** (1982) [14], solved the heat transfer in the very short entrance region by  $L/d \approx 1$  in the circular tube of the inner diameter  $d = 0.5$  mm in which the air was flowing with Reynolds numbers from  $10^4$  to  $10^5$ . They suggested a simple mathematical model to calculate the universal temperature distribution or dimensionless temperature,  $T^+ = ((T_w - T) / (q_w / (\rho c_p \sqrt{\tau_w / \rho})))$  and the heat transfer coefficient in the developing thermal turbulent boundary layer. The problem was formulated mathematically by means of the time-averaged partial differential energy equation for turbulent boundary layer. The fully-developed velocity profile for the inner region of the boundary layer was desired by the  $\tau$ -layer scheme in the form of the universal velocity,  $u^+ (u^+ / \sqrt{\tau_w / \rho})$  as follows:-

$$u^+ = y^+ \text{ for } y^+ \leq 5$$

$$u^+ = 5 \ln y^+ - 3.05 \text{ for } 5 \leq y^+ \leq 30$$

$$u^+ = 2.78 \ln y^+ + 3.8 \text{ for } y^+ \geq 30$$

Where  $y^+$  is the dimensionless distance from the wall and equal to  $\rho y \sqrt{\tau_w / \rho} / \mu$ .

The Boussinesq concept of the turbulent thermal diffusivity ( $\alpha_t$ ) was used to express the turbulent heat flux density ( $-\rho c_p \overline{T'V'}$ ) as  $-\rho c_p \overline{T'V'} = \rho c_p \alpha_t \partial \overline{T} / \partial y$ . The turbulent thermal diffusivity was defined in two ways both based on the analogy with the momentum transport by using the turbulent Prandtl number. In the first way,  $P_{rt}$  was taken equal to 0.85 and 1. For the second way,  $P_{rt}$  was calculated from the relation  $P_{rt} = A_1(1 - \text{EXP}(-y/A)) / B_1(1 - \text{EXP}(-y/B))$ . Where  $A_1 = 0.41$ ,

$$B_1 = 0.44, A = \frac{26\mu}{\rho \sqrt{\tau_w / \rho}} \text{ and } B = \frac{35\mu}{\rho \sqrt{\tau_w / \rho}}. \text{ From this relation it was evident that}$$

$P_{rt}$  for small distance from the wall ( $y$ ) is dependent on this distance. For greater distance  $P_{rt}$  reaches a constant value of 0.93. The energy equation was solved numerically with the explicit non-iterative Dufort-Frankel method in the form of dimensionless temperature  $\theta$  where  $\theta = (T_w - T) / (T_w - T_\infty)$  and  $T_\infty$  is the free stream temperature. The comparison of the results with the data published in the literature was done in a limited way because of the lack of the experimental and specially calculated data at this time.

**Mousa** (1989) [15], studied the fully developed flow, steady, and one dimensional momentum equation in a circular duct far from the entrance. He also studied the Constant heat flux state. A one equation turbulent kinetic energy model similar to that proposed by Prandtl was used.

Numerical analysis had been performed for three-dimensional developing turbulent flow in the U-bend of strong curvature with rib-roughened walls by using an algebraic Reynolds stress model by **Sugiyama** and **watanabe** (2002)(16). In this calculation, the algebraic Reynolds stress model was adopted in order to predict precisely Reynolds stresses and boundary fitted-coordinate system was

introduced as the method for coordinate transformation to set exactly boundary conditions along complicated shape in rib-roughed walls. Calculated results of mean velocity and Reynolds stresses were compared with the experimental data in order to examine the validity of the presented numerical method and the algebraic Reynolds stress model. It had been pointed out as a characteristic feature from the experimental result that the maximum velocity appears near the inner wall of curved duct, which phenomenon was not recognized in mild curved duct. The present method could predict such velocity profiles correctly and reproduce the separated flow generated near the outlet cross section of curved duct. Adding to this, calculated results showed clearly that the generation of maximum velocity near the inner wall was caused by pressure driven secondary flow which moves to inner wall from outer wall along symmetrical axis. As for the comparison of Reynolds stresses, the used turbulent model relatively predicted the experimental data well except for the flow separated region which was located near the outlet cross section of curved duct.

### **۲.۳ Scope of the Present Work:-**

In the present work, the hydrodynamic and thermal boundary layer are considered to develop simultaneously, where this consideration is achieved by assuming uniform velocity and temperature profile at entrance of two dimensional circular and rectangular duct respectively. The clustering of the grid in the radial direction was used in the numerical solution for each duct and the thermal boundary conditions applied to the numerical solution are CWT and CHF for the two ducts. Mathematical modeling of the flow is accomplished by using the two equations of the (k- $\epsilon$ ) turbulence model.

## Chapter Three

# MATHEMATICAL MODEL

### 3.1 Introduction

In this chapter, the mathematical analysis is presented for the Partial Differential Equations (PDES) which describe developing turbulent fluid flow and heat transfer in two geometrical shapes. These shapes are rectangular and circular respectively. Incompressible and constant property flow is assumed throughout each duct.  $k - \varepsilon$  model is employed for predicting developing velocity and temperature profiles in the entrance region of each duct.

### 3.2 Geometrical Shapes and System Coordinates

The following study deals with developing turbulent fluid flow and heat transfer through ducts of two cross sections, rectangular (as shown in figure (1.1)) and circular (as shown in figure (1.2)) respectively. The first will be expressed in Cartesian Coordinates System, but the second in Cylindrical. This study will be achieved for two cases, Constant Heat Flux and Constant Wall Temperature respectively.

### 3.3 Assumptions and Governing Equations of Rectangular Duct

For two dimensional developing, steady state, incompressible turbulent flow in large aspect ratio  $\left( w = 0, \frac{\partial}{\partial z} = 0 \right)$  rectangular duct, with negligible body force, without free convection and heat generation and negligible viscous dissipation ( $\Phi = 0$ ), the continuity, momentum and energy equations which were reported in appendix A will be simplified as follows:-

*Continuity equation:*

$$\frac{\partial u}{\partial x} + \frac{\partial v}{\partial y} = 0 \quad \dots (3.1)$$

*X-momentum:*

$$\rho u \frac{\partial u}{\partial x} + \rho v \frac{\partial u}{\partial y} = -\frac{\partial p}{\partial x} + \frac{\partial}{\partial x} \left( \mu_{eff} \frac{\partial u}{\partial x} \right) + \frac{\partial}{\partial y} \left( \mu_{eff} \frac{\partial u}{\partial y} \right) + \frac{\partial}{\partial x} \left( \mu_t \frac{\partial u}{\partial x} \right) \quad \dots (3.2)$$

The mixed term  $\frac{\partial}{\partial y} \left( \mu_t \frac{\partial u}{\partial x} \right)$  is so small; hence it was canceled in equation (3.2).

$$\mu_{eff} = \mu + \mu_t \quad \dots (3.3)$$

$\mu$ ,  $\mu_t$  and  $\mu_{eff}$  are laminar, turbulent and effective viscosity respectively for turbulent fluid.

*Energy equation:*

$$\left[ \rho u \frac{\partial T}{\partial x} + \rho v \frac{\partial T}{\partial y} = \frac{\partial}{\partial x} \left( \frac{\mu_{eff}}{P_{reff}} \frac{\partial T}{\partial x} \right) + \frac{\partial}{\partial y} \left( \frac{\mu_{eff}}{P_{reff}} \frac{\partial T}{\partial y} \right) \right] \quad \dots (3.4)$$

Where:-

$$\frac{\mu_{eff}}{P_{reff}} = \frac{\mu}{P_r} + \frac{\mu_t}{P_{r_t}} \quad \dots (3.5)$$

$P_r$ ,  $P_{r_t}$  and  $P_{reff}$  are laminar, turbulent and effective Prandtl number respectively for turbulent fluid.

### 3.4 Assumptions and Governing Equations of Circular Duct

The governing equations for steady, axis-symmetric, incompressible turbulent fluid flow and heat transfer without heat generation and with neglected body forces, buoyancy effects, and dissipation function are as reported in Ref. [17], as follows:

*Continuity*

$$\frac{1}{r} \frac{\partial (ru_r)}{\partial r} + \frac{\partial u_x}{\partial x} = 0 \quad \dots (3.6)$$

*Momentum**X-direction:*

$$\rho \left( u_r \frac{\partial u_x}{\partial r} + u_x \frac{\partial u_x}{\partial x} \right) = -\frac{\partial \bar{P}}{\partial x} + \left[ \frac{1}{r} \frac{\partial}{\partial r} \left( r \mu_{eff} \frac{\partial u_x}{\partial r} \right) + \frac{\partial}{\partial x} \left( \mu_{eff} \frac{\partial u_x}{\partial x} \right) \right] + \frac{1}{r} \frac{\partial}{\partial r} \left( \mu_t r \frac{\partial u_r}{\partial x} \right) + \frac{\partial}{\partial x} \left( \mu_t \frac{\partial u_x}{\partial x} \right) - \frac{2}{3} \rho \frac{\partial k}{\partial x} \quad \dots (3.7)$$

*Energy Equation:*

$$\rho \left( u_r \frac{\partial T}{\partial r} + u_x \frac{\partial T}{\partial x} \right) = \left[ \frac{1}{r} \frac{\partial}{\partial r} \left( r \frac{\mu_{eff}}{P_{r_{eff}}} \frac{\partial T}{\partial r} \right) + \frac{\partial}{\partial x} \left( \frac{\mu_{eff}}{P_{r_{eff}}} \frac{\partial T}{\partial x} \right) \right] \quad \dots (3.8)$$

**3.0 Turbulence Model**

The  $k - \varepsilon$  model is the more common active model for turbulent fluid flow problems. It is also called the two equations model, where it characterizes the local state of turbulence by two parameters: the turbulent kinetic energy,  $k$ , and the rate of its dissipation  $\varepsilon$ . The absolute viscosity is related to these parameters by kolmogorov Prandtl expression:-

$$\mu_t = \rho C_\mu \frac{k^2}{\varepsilon} \quad \dots (3.9)$$

Where  $c_\mu$  is an empirical constant, which is equal (0.09) as reported in Ref. [14].

This model is chosen for modeling the two geometries according to the semi-empirical transport equations for  $k$  and  $\varepsilon$  as described below.

**3.0.1  $k - \varepsilon$  Model for Rectangular Duct**

The two equations turbulent models for Cartesian coordinates which were reported in Ref. [18] are:-

$$\rho u \frac{\partial k}{\partial x} + \rho v \frac{\partial k}{\partial y} + \rho w \frac{\partial k}{\partial z} = \frac{\partial}{\partial x} \left( \frac{\mu_t}{\sigma_k} \frac{\partial k}{\partial x} \right) + \frac{\partial}{\partial y} \left( \frac{\mu_t}{\sigma_k} \frac{\partial k}{\partial y} \right) + \frac{\partial}{\partial z} \left( \frac{\mu_t}{\sigma_k} \frac{\partial k}{\partial z} \right) + \rho G - \rho \varepsilon \quad \dots (3.10)$$

$$\rho u \frac{\partial \varepsilon}{\partial x} + \rho v \frac{\partial \varepsilon}{\partial y} + \rho w \frac{\partial \varepsilon}{\partial z} = \frac{\partial}{\partial x} \left( \frac{\mu_t}{\sigma_\varepsilon} \frac{\partial \varepsilon}{\partial x} \right) + \frac{\partial}{\partial y} \left( \frac{\mu_t}{\sigma_\varepsilon} \frac{\partial \varepsilon}{\partial y} \right) + \frac{\partial}{\partial z} \left( \frac{\mu_t}{\sigma_\varepsilon} \frac{\partial \varepsilon}{\partial z} \right) + \rho c_{1\varepsilon} \frac{\varepsilon}{k} G - \rho c_{2\varepsilon} \frac{\varepsilon^2}{k} \quad \dots (3.11)$$

Where  $G$  is the generation term and is equal to

$$G = \mu_t \left[ 2 \left( \left( \frac{\partial u}{\partial x} \right)^2 + \left( \frac{\partial v}{\partial y} \right)^2 + \left( \frac{\partial w}{\partial z} \right)^2 \right) + \left( \frac{\partial u}{\partial y} + \frac{\partial v}{\partial x} \right)^2 + \left( \frac{\partial u}{\partial z} + \frac{\partial w}{\partial x} \right)^2 + \left( \frac{\partial v}{\partial z} + \frac{\partial w}{\partial y} \right)^2 \right] \quad \dots (3.12)$$

In the two equations (3.11) and (3.12), there are four empirical constants and its values as indicated in Ref. [19] are:-

$$(C_{1\varepsilon} = 1.44), (C_{2\varepsilon} = 1.92), (\sigma_k = 1) \text{ and } (\sigma_\varepsilon = 1.3).$$

These two equations will be changed after applying the previous assumptions for rectangular geometry as follows:

$$\rho u \frac{\partial k}{\partial x} + \rho v \frac{\partial k}{\partial y} = \frac{\partial}{\partial x} \left( \frac{\mu_t}{\sigma_k} \frac{\partial k}{\partial x} \right) + \frac{\partial}{\partial y} \left( \frac{\mu_t}{\sigma_k} \frac{\partial k}{\partial y} \right) + \rho G - \rho \varepsilon \quad \dots (3.13)$$

$$\rho u \frac{\partial \varepsilon}{\partial x} + \rho v \frac{\partial \varepsilon}{\partial y} = \frac{\partial}{\partial x} \left( \frac{\mu_t}{\sigma_\varepsilon} \frac{\partial \varepsilon}{\partial x} \right) + \frac{\partial}{\partial y} \left( \frac{\mu_t}{\sigma_\varepsilon} \frac{\partial \varepsilon}{\partial y} \right) + \rho C_{1\varepsilon} \frac{\varepsilon}{k} G - \rho C_{2\varepsilon} \frac{\varepsilon^2}{k} \quad \dots (3.14)$$

$$G = \mu_t \left[ 2 \left( \frac{\partial u}{\partial x} \right)^2 + 2 \left( \frac{\partial v}{\partial y} \right)^2 + \left( \frac{\partial u}{\partial y} \right)^2 \right] \quad \dots (3.15)$$

### 3.5.2 $k - \varepsilon$ Model for Cylindrical Coordinates

The two equations models for cylindrical coordinates as reported in Ref. [19] are:-

$$\rho \left( u_r \frac{\partial k}{\partial r} + u_x \frac{\partial k}{\partial x} \right) = \left[ \frac{1}{r} \frac{\partial}{\partial r} \left( r \frac{\mu_t}{\sigma_k} \frac{\partial k}{\partial r} \right) + \frac{\partial}{\partial x} \left( \frac{\mu_t}{\sigma_k} \frac{\partial k}{\partial x} \right) \right] + \rho G - \rho \varepsilon \quad \dots (3.16)$$

$$\rho \left( u_r \frac{\partial \varepsilon}{\partial r} + u_x \frac{\partial \varepsilon}{\partial x} \right) = \left[ \frac{1}{r} \frac{\partial}{\partial r} \left( r \frac{\mu_t}{\sigma_\varepsilon} \frac{\partial \varepsilon}{\partial r} \right) + \frac{\partial}{\partial x} \left( \frac{\mu_t}{\sigma_\varepsilon} \frac{\partial \varepsilon}{\partial x} \right) \right] + \rho C_{\varepsilon 1} \frac{\varepsilon}{k} G - C_{\varepsilon 2} \rho \frac{\varepsilon^2}{k} \quad \dots (3.17)$$

Where:-

$$G = \mu_t \left\{ 2 \left[ \left( \frac{\partial u_r}{\partial r} \right)^2 + \left( \frac{\partial u_x}{\partial x} \right)^2 \right] + \left( \frac{\partial u_r}{\partial x} + \frac{\partial u_x}{\partial r} \right)^2 \right\} \quad \dots (3.18)$$

### 3.6 Boundary Conditions

The requirement that the dependent variable or its derivative must be satisfied on the boundary of the partial differential equation (Ref. [10]) is called the boundary condition. The boundary conditions represent the statements of physical facts at specified values of the independent variable. Any fluid moves over a surface whose temperature differs from it, will lead to transfer of heat by convection. Hence, the thermal and hydrodynamic boundary layer considerations will be encountered. These considerations should be precisely treated especially when turbulent boundary layer is faced. In order to achieve this purpose, suitable boundary conditions should be applied on the selected problem. Therefore; the boundary conditions according to the geometry will be written as follows:

#### 3.6.1 Boundary Conditions for Rectangular Duct

##### Entrance region Boundary Conditions:

Uniform temperature and velocity profile at the entrance region of rectangular duct is assumed. Likewise the  $k-\varepsilon$  model boundary condition and temperature are assumed uniform at entrance. All entrance boundary conditions can be written as follows:

$$\left. \begin{aligned} u &= u_{in} \\ p &= 101325 \\ v &= 0 \\ T &= T_{in} \\ k_{in} &= C_k u_{in}^2 \\ \varepsilon_{in} &= C_\mu k_{in}^{3/2} / (0.5 D_h C_\varepsilon) \end{aligned} \right\} \dots (3.19)$$

Where  $C_\varepsilon$  and  $C_k$  are constants ( $C_\varepsilon = 0.075$  &  $C_k = 0.075$ ) as indicated in Ref. [11].

$D_h$  represent hydraulic diameter where  $D_h = 4A/p$ ;

A is the area of rectangle.

p is wetted perimeter.

Exit region Boundary Conditions:

At exit the boundary conditions will be as taken in Ref. [17] as follows:-

$$\left. \begin{aligned} \frac{\partial u}{\partial x} = \frac{\partial v}{\partial x} = \frac{\partial k}{\partial x} = \frac{\partial \varepsilon}{\partial x} = 0 \\ \frac{\partial T}{\partial x} = \text{cons.} \\ \frac{\partial p}{\partial x} = \text{cons.} \end{aligned} \right\} \dots (3.20)$$

Wall Boundary Conditions:

All velocity components are zero at the walls, hence:-

$$u = v = 0 \dots (3.21)$$

The boundary condition of the kinetic energy, k, and its dissipation is:-

$$\left. \begin{aligned} k = 0 \\ \frac{\partial \varepsilon}{\partial y} = 0 \end{aligned} \right\} \dots (3.22)$$

For the constant wall temperature, the boundary condition will be:-

$$T = T_w$$

For the constant heat flux, the boundary condition will be:-

$$\frac{\partial T}{\partial y} = \pm \frac{q_w}{\lambda} \dots (3.23)$$

+ve sign is applied at the upper wall and -ve sign at the lower wall.

$\lambda$  represents thermal conductivity of the fluid.

**3.6.2 Boundary Conditions for Circular Duct**Entrance region Boundary Conditions:

Uniform temperature and velocity profile at the circular duct entrance is assumed as follows:

$$\left. \begin{aligned} u_r = 0 \\ u_x = u_{in} \\ T = T_{in} \end{aligned} \right\} \dots (3.24)$$

The entrance profile for the kinetic energy of turbulence and its rate of dissipation are assumed to be calculated from the following relations:

$$\left. \begin{aligned} k_{in} &= C_k u_{in}^2 \\ \varepsilon_{in} &= C_\mu k_{in}^{3/2} / (0.5DC_\varepsilon) \end{aligned} \right\} \dots (3.20)$$

Where  $C_\varepsilon$  and  $C_k$  are constants ( $C_\varepsilon = 0.075$  &  $C_k = 0.075$ ).

Exit region Boundary Conditions:

For fully developed turbulent fluid flow at exit, the velocity components gradient in the axial direction is zero. The presence of heat transfer by convection between the surface and fluid will keep fluid temperature changes with distance. This means that the temperature gradient in the axial direction will not equal zero ( $\frac{\partial T}{\partial x} \neq 0$ ). Therefore; the boundary conditions for velocity components, temperature, and pressure at exit can be written as follows (Ref. [17]):

$$\left. \begin{aligned} \frac{\partial u_x}{\partial x} = \frac{\partial u_r}{\partial x} &= 0 \\ \frac{\partial T}{\partial x} &= cons. \\ \frac{\partial p}{\partial x} &= cons. \end{aligned} \right\} \dots (3.26)$$

$k - \varepsilon$  model boundary condition at exit will be written as:-

$$\frac{\partial k}{\partial x} = \frac{\partial \varepsilon}{\partial x} = 0 \dots (3.27)$$

Wall Boundary Conditions:

All velocity components are zero at the walls, hence:-

$$u_x = u_r = 0 \dots (3.28)$$

The boundary condition of the kinetic energy, k and its dissipation is:-

$$\left. \begin{aligned} k &= 0 \\ \frac{\partial \varepsilon}{\partial r} &= 0 \end{aligned} \right\} \dots (3.29)$$

For the constant temperature wall, the boundary condition will be:-

$$T = T_w \quad \dots (3.30)$$

For the constant heat flux, the boundary condition will be:-

$$\frac{\partial T}{\partial r} = \frac{q_w}{\lambda} \quad \dots (3.31)$$

### 3.7 Wall Effects

The turbulent velocity boundary layer can be divided into three zones of flow. The zone immediately adjacent to the wall is the layer of fluid that, because of the damping effect of the wall, remains relatively laminar even though most of the flow in the boundary layer is turbulent. This very thin layer is called the viscous sublayer or laminar sublayer where the laminar transport properties have a predominant influence of the flow, and momentum and heat transfer can be largely accounted for by simple mechanisms of viscous shear ( $\tau = \mu \frac{\partial u}{\partial y}$ ) and molecular conduction ( $q = k \frac{\partial T}{\partial y}$ ). The second zone is called the transitional zone which is the zone between the laminar sublayer and the third zone which is called the fully turbulent region. In this zone the viscous and the turbulence inertia effects are of the same order of magnitude. The turbulent region comprises most of the boundary layer, where the viscous shear is negligible. The near wall region comprises the laminar sublayer, the transitional region and the initial part of the fully turbulent region but the core region comprises the external part of fully turbulent region.

The form of the model which has been presented previously for the two geometries is valid for turbulent region where the gradients of the flow properties are usually not very steep. Hence a moderately fine finite difference grid yields acceptable solutions [11]. Close to the solid walls and some other interfaces there are inevitably regions where the local Reynolds number ( $\equiv \rho k^{0.5} l / \mu$ , where  $l \equiv k^{1.5} / \varepsilon$ ) is so small that the viscous effects predominate over turbulent ones and the variations of the flow properties are much steeper. There are two methods of accounting for these regions in numerical methods for

computing turbulent flow; the wall-function-method; and the –low-Reynolds-number-modeling method [19]. For the two geometries, the wall-function-method will be used.

### 3.8 The Wall-Function-Method

This method is the one which has been most widely used, and which is indeed still to be preferred for many practical purposes. Its merits are two: it economizes computer time and storage and it allows the introduction of additional empirical information in special cases, as when the wall is rough [19].

Wall function is a method which is used for calculating the effective exchange coefficient,  $\Gamma_{wall}$ . Effective exchange coefficient represents the diffusion coefficient in the energy and momentum equations. The table (3.1) summarizes the expressions for  $\Gamma_{wall}$  for the different dependent variables [22].

Table (3.1) Wall Function

$g$	$\Gamma_w$	Notes
Velocity components normal to the wall	.	
Velocity components parallel to the wall	$\frac{\mu y^+}{1/\kappa \ln(Ey^+)}$	for $y^+ > 11.5$
	$\mu$	for $y^+ \leq 11.5$
$k_p, \varepsilon_p$	Not required	
$T_p$	$\frac{\mu}{p_r} \frac{y^+}{(1/\kappa \ln(Ey^+) + p_{ee})}$	for $y^+ > 11.5$
	$\frac{\mu}{p_r}$	for $y^+ \leq 11.5$

The following equation is used for calculating the kinetic energy of turbulence ( $k$ ) and its rate of dissipation  $\varepsilon$ , to the nodal point neighboring to the wall [33]:

$$k_p = \frac{\tau_w}{\rho C_\mu^{1/2}} \quad \dots (3.22)$$

$$\varepsilon_p = \frac{C_\mu^{1/4} k_p^{3/4}}{\kappa y_p} \quad \dots (3.23)$$

The important new variables and constants which appear in the above table and the two equations (3.22) and (3.23) are:-

The dimensionless amount  $y^+$  which appears in the above table is defined as follows:

$$y^+ = \frac{\rho y_p C_\mu^{1/4} k_p^{1/2}}{\mu} \quad \dots (3.24)$$

$y_p$  is the normal distance from the wall surface to nodal point neighboring to the wall.

$\kappa$  is the Von Karman constant and equal to (0.4188) and E is integration constant and equal to (9.793).

$p_{ee}$  is the Pee function which is the function for laminar and turbulent Prandtl number and can be calculated from the following relation which was reported by Ref. [34]

$$p_{ee} = 9.24 \left[ \left( \frac{p_{r_i}}{p_r} \right)^{0.75} - 1 \right] * \left\{ 1 + 0.28 \exp \left[ -0.007 \left( \frac{p_{r_i}}{p_r} \right) \right] \right\} \quad \dots (3.25)$$

**३.१ THE DIMENSIONLESS QUANTITIES**

The following dimensionless quantities will be used in the present work:

१. Reynolds number

(a) For rectangular duct

$$Re = \frac{\rho D_h U_{in}}{\mu} \quad \dots (३.३६)$$

(b) For circular duct

$$Re = \frac{\rho D U_{in}}{\mu} \quad \dots (३.३७)$$

२. Nussult number

(a) For rectangular duct

$$Nu = \frac{h D_h}{\lambda} \quad \dots (३.३८)$$

(b) For circular duct

$$Nu = \frac{h D}{\lambda} \quad \dots (३.३९)$$

## Chapter Four

# NUMERICAL SOLUTION

### 4.1 INTRODUCTION

The numerical solution procedures for governing differential equation which are described in chapter three are given in this chapter. The transformation of governing non-linear partial differential equations to the algebraic equations is achieved by using finite difference method.

### 4.2 GRID GENERATION

The governing equations for the present study will be solved by using the Explicit Finite Differences Method. The calculation region shown in figure (4.1) for rectangular duct and in figure (4.2) for circular duct (where clustering for all nodal points of each geometry was done) is divided into finite regions, in which the nodal points are specified by using the two indexes, (i) in the axial direction (x) and (j) in the lateral direction. The lateral direction is represented by y in rectangular duct and r in circular duct. For each node in rectangular duct, the coordinates will be  $(x = i\Delta x, y = y_{i,j})$ , where  $i = 0, M, j = 0, N$  and for circular duct will be  $(x = i\Delta x, r = r_{i,j})$ , where  $i = 0, M, j = -N, N$ . Therefore, the upper and lower walls for rectangular duct are represented by the two lines  $j = 0$  and  $j = N$  while the upper and lower walls for circular duct are represented by the two lines  $j = -N$  and  $j = N$  with center which is represented by the line  $j = 0$ . The inlet and exit for rectangular and circular duct are represented by the two lines  $i = 0$  and  $i = M$  respectively.

The dimensions which were taken for checking the result of studying the developing turbulent flow and heat transfer through rectangular and circular duct are  $(H = 0.05 \text{ m}, a = 0.002 \text{ m}, L = 3 \text{ Dh})$  for rectangular duct and  $(D = 0.001 \text{ m},$

$L=2D$ ) for circular duct. With this dimensions the numerical solution was accomplished by taking  $(M=10, N=10)$  for rectangular duct and  $(M=12, N=3)$  for circular duct. The grid generation for each duct is achieved by making the transverse nodal spacing varied across the duct height but constant down the duct. Hence, the nodal spacing was much denser near the duct wall than at the centerline.

To transform the partial terms in the partial differential equations to algebraic terms the nodal points shown in figure (4.3) will be considered. After transforming the governing equations from partial to algebraic form, it will be simultaneously solved by using Tri-Diagonal Matrix Algorithm (TDMA) except the momentum equation which will be solved by using Gauss- Seidel method as indicated in this chapter. The resulting algebraic forms for all equations presented in this chapter are solved by using a FORTRAN 90 Program.

### 4.3 MOMENTUM EQUATIONS

The Explicit Finite Differences Method will be used to solve the momentum equations. The momentum equation is a non-linear partial differential equation consists of the terms on the left-hand side which are called the convection terms, and the pressure gradient term and diffusion terms on the right-hand side. In turbulent flow the conversion of convective terms into algebraic form is accomplished by using Upwind Difference [20], where the Backward Difference is used in this method. But the diffusion terms will be converted into algebraic form by using Central Differences.

#### 4.3.1 NUMERICAL FORMULATION FOR MOMENTUM EQUATION OF RECTANGULAR DUCT

The Backward Difference is used to convert the convection terms and the pressure gradient term for rectangular duct into algebraic form as follows [20]:-

$$\rho u \frac{\partial u}{\partial x} \Big|_{i,j} = \rho u_{i,j} \frac{u_{i,j} - u_{i-1,j}}{\Delta x} \quad \dots (4.1)$$

$$\rho v \frac{\partial u}{\partial y} \Big|_{i,j} = \rho v_{i,j} \frac{u_{i,j} - u_{i,j-1}}{\Delta y_{i,j}} \quad \dots (\xi.2)$$

$$-\frac{\partial p}{\partial x} \Big|_i = -\frac{p_i - p_{i-1}}{\Delta x} \quad \dots (\xi.3)$$

But the Central Differences are used to convert the diffusion terms as indicated in Ref. [36] as follows:

$$\frac{\partial}{\partial x} \left( \mu_{eff} \frac{\partial u}{\partial x} \right) \Big|_{i,j} = \frac{1}{\Delta x} \left( \mu_{eff_{i+0.5,j}} \frac{u_{i+1,j} - u_{i,j}}{\Delta x} - \mu_{eff_{i-0.5,j}} \frac{u_{i,j} - u_{i-1,j}}{\Delta x} \right) \quad \dots (\xi.4)$$

$$\frac{\partial}{\partial y} \left( \mu_{eff} \frac{\partial u}{\partial y} \right) \Big|_{i,j} = \frac{2}{(\Delta y_{i,j} + \Delta y_{i,j+1})} \left( \mu_{eff_{i,j+0.5}} \frac{u_{i,j+1} - u_{i,j}}{\Delta y_{i,j+1}} - \mu_{eff_{i,j-0.5}} \frac{u_{i,j} - u_{i,j-1}}{\Delta y_{i,j}} \right) \quad \dots (\xi.5)$$

$$\frac{\partial}{\partial x} \left( \mu_t \frac{\partial u}{\partial x} \right) \Big|_{i,j} = \frac{1}{\Delta x} \left( \mu_{t_{i+0.5,j}} \frac{u_{i+1,j} - u_{i,j}}{\Delta x} - \mu_{t_{i-0.5,j}} \frac{u_{i,j} - u_{i-1,j}}{\Delta x} \right) \quad \dots (\xi.6)$$

By substituting the algebraic equations (xi.1), (xi.2), (xi.3), (xi.4), (xi.5) and (xi.6) into equation (3.2), the following equation will result:-

$$a_{1u_{i,j}} u_{i,j} = a_{2u_{i,j}} u_{i-1,j} + a_{3u_{i,j}} u_{i,j-1} + a_{4u_{i,j}} u_{i+1,j} + a_{5u_{i,j}} u_{i,j+1} - \frac{p_i - p_{i-1}}{\Delta x} \quad \dots (\xi.7)$$

Where:-

$$\left. \begin{aligned} a_{1u_{i,j}} &= \left( \frac{\rho u_{i,j}}{\Delta x} + \frac{\rho v_{i,j}}{\Delta y_{i,j}} + \frac{\mu_{eff_{i+0.5,j}} + \mu_{eff_{i-0.5,j}}}{\Delta x^2} + \frac{\mu_{t_{i+0.5,j}} + \mu_{t_{i-0.5,j}}}{\Delta x^2} + \frac{\mu_{eff_{i,j+0.5}}}{(\Delta y_{i,j+1}^2 + \Delta y_{i,j} \Delta y_{i,j+1})} \right. \\ &\quad \left. + \frac{\mu_{eff_{i,j-0.5}}}{(\Delta y_{i,j}^2 + \Delta y_{i,j} \Delta y_{i,j+1})} \right) \\ a_{2u_{i,j}} &= \left( \frac{\rho u_{i,j}}{\Delta x} + \frac{\mu_{eff_{i-0.5,j}} + \mu_{t_{i-0.5,j}}}{\Delta x^2} \right) \\ a_{3u_{i,j}} &= \left( \frac{\rho v_{i,j}}{\Delta y_{i,j}} + \frac{\mu_{eff_{i,j-0.5}}}{(\Delta y_{i,j}^2 + \Delta y_{i,j} \Delta y_{i,j+1})} \right) \\ a_{4u_{i,j}} &= \left( \frac{\mu_{eff_{i+0.5,j}} + \mu_{t_{i+0.5,j}}}{\Delta x^2} \right) \\ a_{5u_{i,j}} &= \left( \frac{\mu_{eff_{i,j+0.5}}}{(\Delta y_{i,j+1}^2 + \Delta y_{i,j} \Delta y_{i,j+1})} \right) \end{aligned} \right\} \dots (\xi.8)$$

Where:-

$$\left. \begin{aligned} \mu_{eff,i,j+0.5} &= \frac{\mu_{eff,i,j+1} + \mu_{eff,i,j}}{2} \\ \mu_{eff,i,j-0.5} &= \frac{\mu_{eff,i,j} + \mu_{eff,i,j-1}}{2} \\ \mu_{eff,i+0.5,j} &= \frac{\mu_{eff,i+1,j} + \mu_{eff,i,j}}{2} \\ \mu_{eff,i-0.5,j} &= \frac{\mu_{eff,i,j} + \mu_{eff,i-1,j}}{2} \\ \mu_{t,i+0.5,j} &= \frac{\mu_{t,i+1,j} + \mu_{t,i,j}}{2} \\ \mu_{t,i-0.5,j} &= \frac{\mu_{t,i,j} + \mu_{t,i-1,j}}{2} \end{aligned} \right\} \dots (\xi.9)$$

The equation (ξ.9) can be written as:

$$u_{i,j} = \alpha_{i,j} + \beta_{i,j} (\bar{P}_i - \bar{P}_{i-1}) \dots (\xi.10)$$

Where:-

$$\left. \begin{aligned} \alpha_{i,j} &= \left( \frac{a_{2u_{i,j}} u_{i-1,j} + a_{3u_{i,j}} u_{i,j-1} + a_{4u_{i,j}} u_{i+1,j} + a_{5u_{i,j}} u_{i,j+1}}{a_{1u_{i,j}}} \right) \\ \beta_{i,j} &= \frac{-1}{a_{1u_{i,j}} \Delta x} \end{aligned} \right\} \dots (\xi.11)$$

The mean pressure difference  $(\bar{P}_i - \bar{P}_{i-1})$  which appears in equation (ξ.10) is calculated by using the Mass Conservation Method [20]. By integrating equation (ξ.10) over the cross section of the rectangular duct, the result will be:-

$$\dot{m} = \int_0^H \rho u_{i,j} a dy = \int_0^H \rho \alpha_{i,j} a dy + (\bar{P}_i - \bar{P}_{i-1}) \int_0^H \rho \beta_{i,j} a dy \dots (\xi.12)$$

Where

Rearrange equation (ξ.12), to get:-

$$\bar{P}_i = \bar{P}_{i-1} + \frac{\dot{m} - \rho \int_0^H \alpha_{i,j} a dy}{\rho \int_0^H \beta_{i,j} a dy} \dots (\xi.13)$$

The integration in equation (4.13) is accomplished by using the Numerical Integration by Trapezoidal Rule. In the present work the following form of the trapezoidal rule is derived to accomplish the integration of the non- uniform grid spacing:-

$$\bar{P}_{i,j} = \bar{P}_{i-1,j} + \frac{\dot{m} - \sum_{j=1}^{N-1} \rho a \alpha_{i,j} \frac{(\Delta y_{i,j+1} + \Delta y_{i,j})}{2}}{\sum_{j=1}^{N-1} \rho a \beta_{i,j} \frac{(\Delta y_{i,j+1} + \Delta y_{i,j})}{2}} \quad \dots$$

For j=1:-

$$\bar{P}_{i,j} = \bar{P}_{i-1,j} + \frac{\dot{m} - \left( \frac{1}{4} \rho a \alpha_{i,j} \frac{\Delta y_{i,j}}{2} + \rho a \alpha_{i,j} \frac{(\Delta y_{i,j+1} + \Delta y_{i,j})}{2} \right)}{\left( \frac{1}{4} \rho a \beta_{i,j} \frac{\Delta y_{i,j}}{2} + \rho a \beta_{i,j} \frac{(\Delta y_{i,j+1} + \Delta y_{i,j})}{2} \right)} \quad \dots \quad (4.14)$$

For j=N-1:-

$$\bar{P}_{i,j} = \bar{P}_{i-1,j} + \frac{\dot{m} - \left( \frac{1}{4} \rho a \alpha_{i,j} \frac{\Delta y_{i,j+1}}{2} + \rho a \alpha_{i,j} \frac{(\Delta y_{i,j+1} + \Delta y_{i,j})}{2} \right)}{\left( \frac{1}{4} \rho a \beta_{i,j} \frac{\Delta y_{i,j+1}}{2} + \rho a \beta_{i,j} \frac{(\Delta y_{i,j+1} + \Delta y_{i,j})}{2} \right)} \quad \dots \quad (4.15-B)$$

The velocity equation (4.16) is solved by using the point by point Gauss – Seidel Method which is one of the iteration methods used for solving the linear equations. In this method the value of the dependent variable (u) at the present iteration is calculated for each node in the nodal grid in terms of the adjacent nodal points at the present and the previous iteration to achieve a suitable convergence. Hence, in any new iteration the calculation is done by depending on different iteration planes until reaching the required convergence. In iterative solution of the algebraic equations it is desired to accelerate or decelerate the convergence from one iteration to another; this process is called Under or Over

Relaxation. In the present work the time and iterations required to reach the values of  $u$  and  $v$  for the entire domain with reasonable percent of error (like  $1.0 \times 10^{-3}$ ) are large, hence the under-relaxation method was used to accelerate the convergence in the solution. So equation (4.15) can be written as the following under-relaxation form:-

$$u_{i,j}^{q+1} = (1 - \omega)u_{i,j}^q + \omega(\alpha_{i,j} + \beta_{i,j}(p_i - p_{i-1})) \quad \dots (4.16)$$

Where  $u_{i,j}^q$  and  $u_{i,j}^{q+1}$  represent the values of calculated velocity at each nodal point at the previous and the present iteration planes respectively. The symbol  $\omega$  in equation (4.16) is called the Relaxation Coefficient and the selection of its typical value depends on different factors like the number of nodal points, the type of used error for solving problem ...etc. The range of under-relaxation factor lies between (0-1).

In the present work, the value of  $\omega$  used for solving  $u$  and  $v$  for rectangular duct was (0.33). Equation (4.13) was solved without relaxation [20].

**4.3.2 NUMERICAL FORMULATION FOR MOMENTUM EQUATION OF CIRCULAR DUCT**

The same procedure for converting the momentum equation from differential to algebraic form for rectangular duct will be achieved for circular duct as follows:-

$$\rho u_r \frac{\partial u_x}{\partial r} \Big|_{i,j} = \rho u_{r,i,j} \frac{u_{x_{i,j}} - u_{x_{i,j-1}}}{\Delta r_{i,j}} \quad \dots (4.17)$$

$$\rho u_x \frac{\partial u_x}{\partial x} \Big|_{i,j} = \rho u_{x_{i,j}} \frac{u_{x_{i,j}} - u_{x_{i-1,j}}}{\Delta x} \quad \dots (4.18)$$

$$-\frac{\partial p}{\partial x} \Big|_i = -\frac{p_i - p_{i-1}}{\Delta x} \quad \dots (4.19)$$

$$\frac{1}{r} \frac{\partial}{\partial r} \left( r \mu_{eff} \frac{\partial u_x}{\partial r} \right) \Big|_{i,j} = \frac{1}{r} \frac{\partial \phi}{\partial r} \Big|_{i,j} = \frac{1}{r_{i,j}} \frac{(\phi_{i,j+1/2} - \phi_{i,j-1/2})}{(\Delta r_{i,j+1} + \Delta r_{i,j})} \quad \dots (4.20)$$

where  $\frac{\partial \phi}{\partial r} = \frac{\partial}{\partial r} \left( r \mu_{eff} \frac{\partial u_x}{\partial r} \right)$

$$\left. \begin{aligned} \varphi_{i,j+1/2} &= r_{i,j+0.5} \mu_{eff,i,j+0.5} \frac{(u_{x_{i,j+1}} - u_{x_{i,j}})}{\Delta r_{i,j+1}} \\ \varphi_{i,j-1/2} &= r_{i,j-0.5} \mu_{eff,i,j-0.5} \frac{(u_{x_{i,j}} - u_{x_{i,j-1}})}{\Delta r_{i,j}} \end{aligned} \right\} \dots (\xi.20)$$

Substitute equation (ξ.20) into (ξ.19) to get:-

$$\frac{1}{r} \frac{\partial}{\partial r} \left( r \mu_{eff} \frac{\partial u_x}{\partial r} \right) \Big|_{i,j} = \frac{2}{r_{i,j} (\Delta r_{i,j+1} + \Delta r_{i,j})} \left[ r_{i,j+0.5} \mu_{eff,i,j+0.5} \frac{(u_{x_{i,j+1}} - u_{x_{i,j}})}{\Delta r_{i,j+1}} - r_{i,j-0.5} \mu_{eff,i,j-0.5} \frac{(u_{x_{i,j}} - u_{x_{i,j-1}})}{\Delta r_{i,j}} \right] \dots (\xi.21)$$

$$\frac{\partial}{\partial x} \left( \mu_{eff} \frac{\partial u_x}{\partial x} \right) \Big|_{i,j} = \mu_{eff_{i+0.5,j}} \frac{u_{x_{i+1,j}} - u_{x_{i,j}}}{\Delta x^2} - \mu_{eff_{i-0.5,j}} \frac{u_{x_{i,j}} - u_{x_{i-1,j}}}{\Delta x^2} \dots (\xi.22)$$

$$\frac{1}{r} \frac{\partial}{\partial r} \left( r \mu_t \frac{\partial u_r}{\partial x} \right) \Big|_{i,j} = \frac{1}{r} \frac{\partial \psi}{\partial r} \Big|_{i,j} = \frac{1}{r_{i,j} (\Delta r_{i,j+1} + \Delta r_{i,j})} (\psi_{i,j+1} - \psi_{i,j-1}) \dots (\xi.23)$$

where  $\frac{\partial \psi}{\partial r} = \frac{\partial}{\partial r} \left( r \mu_t \frac{\partial u_r}{\partial x} \right)$

$$\left. \begin{aligned} \psi_{i,j+1} &= r_{i,j+1} \mu_{t,i,j+1} \frac{(u_{r_{i+1,j+1}} - u_{r_{i-1,j+1}})}{2\Delta x} \\ \psi_{i,j-1} &= r_{i,j-1} \mu_{t,i,j-1} \frac{(u_{r_{i+1,j-1}} - u_{r_{i-1,j-1}})}{2\Delta x} \end{aligned} \right\} \dots (\xi.24)$$

Substitute equation (ξ.24) into (ξ.23) to get:-

$$\frac{1}{r} \frac{\partial}{\partial r} \left( r \mu_t \frac{\partial u_r}{\partial x} \right) \Big|_{i,j} = \frac{1}{r} \frac{\partial \psi}{\partial r} \Big|_{i,j} = \frac{1}{r_{i,j} (\Delta r_{i,j+1} + \Delta r_{i,j})} \left[ r_{i,j+1} \mu_{t,i,j+1} \frac{(u_{r_{i+1,j+1}} - u_{r_{i-1,j+1}})}{2\Delta x} - r_{i,j-1} \mu_{t,i,j-1} \frac{(u_{r_{i+1,j-1}} - u_{r_{i-1,j-1}})}{2\Delta x} \right] \dots (\xi.25)$$

$$\frac{\partial}{\partial x} \left( \mu_t \frac{\partial u_x}{\partial x} \right) \Big|_{i,j} = \mu_{t_{i+0.5,j}} \frac{u_{x_{i+1,j}} - u_{x_{i,j}}}{\Delta x^2} - \mu_{t_{i-0.5,j}} \frac{u_{x_{i,j}} - u_{x_{i-1,j}}}{\Delta x^2} \dots (\xi.26)$$

The term  $\left(\frac{\partial k}{\partial x}\right)$  in equation (3.7) will be converted to the numerical form

by using the Central Differences as follows:-

$$-\frac{2}{3}\rho\frac{\partial k}{\partial x}\Big|_{i,j} = -\frac{2}{3}\rho\frac{k_{i+1,j} - k_{i-1,j}}{2\Delta x} \quad \dots$$

(3.27)

By substituting the algebraic equations (3.16), (3.17), (3.18), (3.21), (3.22), (3.23), (3.26), and (3.27) into equation (3.7), the following equation will result:-

$$a_{1u_{x_i,j}} u_{x_i,j} = a_{2u_{x_i,j}} u_{x_{i,j+1}} + a_{3u_{x_i,j}} u_{x_{i+1,j}} + a_{4u_{x_i,j}} u_{x_{i,j-1}} + a_{5u_{x_i,j}} u_{x_{i-1,j}} - \frac{P_i - P_{i-1}}{\Delta x} + S_{u_{i,j}} \quad \dots (3.28)$$

Where:-

$$\left. \begin{aligned} a_{1u_{x_i,j}} &= \frac{\rho u_{r_{i,j}}}{\Delta r_{i,j}} + \frac{\rho u_{x_{i,j}}}{\Delta x} + \frac{\mu_{eff_{i-0.5,j}} + \mu_{eff_{i+0.5,j}}}{\Delta x^2} + \frac{\mu_{t_{i-0.5,j}} + \mu_{t_{i+0.5,j}}}{\Delta x^2} + \frac{2r_{i,j+0.5}\mu_{eff_{i,j+0.5}}}{r_{i,j}(\Delta r_{i,j} + \Delta r_{i,j+1})\Delta r_{i,j+1}} \\ &+ \frac{2r_{i,j-0.5}\mu_{eff_{i,j-0.5}}}{r_{i,j}(\Delta r_{i,j} + \Delta r_{i,j+1})\Delta r_{i,j}} \\ a_{2u_{x_i,j}} &= \frac{2r_{i,j+0.5}\mu_{eff_{i,j+0.5}}}{r_{i,j}(\Delta r_{i,j} + \Delta r_{i,j+1})\Delta r_{i,j+1}} \\ a_{3u_{x_i,j}} &= \frac{\mu_{eff_{i+0.5,j}} + \mu_{t_{i+0.5,j}}}{\Delta x^2} \\ a_{4u_{x_i,j}} &= \frac{\rho u_{r_{i,j}}}{\Delta r} + \frac{r_{i,j-0.5}\mu_{eff_{i,j-0.5}}}{r_{i,j}(\Delta r_{i,j} + \Delta r_{i,j+1})\Delta r_{i,j}} \\ a_{5u_{x_i,j}} &= \frac{\rho u_{x_{i,j}}}{\Delta x} + \frac{\mu_{eff_{i-0.5,j}} + \mu_{t_{i-0.5,j}}}{\Delta x^2} \\ S_{u_{i,j}} &= \frac{r_{i,j+1}\mu_{t_{i,j+1}}}{4r_{i,j}(\Delta r_{i,j} + \Delta r_{i,j+1})\Delta x} u_{r_{i+1,j+1}} - \frac{r_{i,j+1}\mu_{t_{i,j+1}}}{4r_{i,j}(\Delta r_{i,j} + \Delta r_{i,j+1})\Delta x} u_{r_{i-1,j+1}} - \frac{r_{i,j-1}\mu_{t_{i,j-1}}}{4r_{i,j}(\Delta r_{i,j} + \Delta r_{i,j+1})\Delta x} u_{r_{i+1,j-1}} \\ &+ \frac{r_{i,j-1}\mu_{t_{i,j-1}}}{4r_{i,j}(\Delta r_{i,j} + \Delta r_{i,j+1})\Delta x} u_{r_{i-1,j-1}} - \frac{1}{3}\rho\frac{k_{i+1,j} - k_{i-1,j}}{\Delta x} \end{aligned} \right\} \dots (3.29)$$

Where:-

$$\left. \begin{aligned} \mu_{eff_{i,j+0.5}} &= \frac{\mu_{eff_{i,j+1}} + \mu_{eff_{i,j}}}{2} \\ \mu_{eff_{i,j-0.5}} &= \frac{\mu_{eff_{i,j}} + \mu_{eff_{i,j-1}}}{2} \\ \mu_{eff_{i+0.5,j}} &= \frac{\mu_{eff_{i+1,j}} + \mu_{eff_{i,j}}}{2} \\ \mu_{eff_{i-0.5,j}} &= \frac{\mu_{eff_{i,j}} + \mu_{eff_{i-1,j}}}{2} \\ \mu_{t_{i+0.5,j}} &= \frac{\mu_{t_{i+1,j}} + \mu_{t_{i,j}}}{2} \\ \mu_{t_{i-0.5,j}} &= \frac{\mu_{t_{i,j}} + \mu_{t_{i-1,j}}}{2} \end{aligned} \right\} \dots (\xi.30)$$

The equation (ξ.28) can be written as:

$$u_{x_{i,j}} = \alpha_{i,j} + \beta_{i,j}(\bar{P}_i - \bar{P}_{i-1}) \dots (\xi.31)$$

Where

$$\left. \begin{aligned} \alpha_{i,j} &= \left( \frac{a_{2ux_{i,j}} u_{x_{i,j+1}} + a_{3ux_{i,j}} u_{x_{i+1,j}} + a_{4ux_{i,j}} u_{x_{i,j-1}} + a_{5ux_{i,j}} u_{x_{i-1,j}} + S_{u_{i,j}}}{a_{1ux_{i,j}}} \right) \\ \beta_{i,j} &= \frac{-1}{a_{1ux_{i,j}}} \end{aligned} \right\} \dots (\xi.32)$$

By the same way of calculating the mean pressure difference for rectangular duct, the mean pressure difference  $(\bar{P}_i - \bar{P}_{i-1})$  which appears in equation (ξ.28) is calculated by using the Mass Conservation Method. By integration for the equation (ξ.31), the result will be:-

$$\dot{m} = \int_0^R \rho u_{x_{i,j}} 2\pi r dr = \int_0^R \rho \alpha_{i,j} 2\pi r_{i,j} \Delta r_{i,j} + (\bar{P}_i - \bar{P}_{i-1}) \int_0^R \rho \beta_{i,j} 2\pi r_{i,j} \Delta r_{i,j} \dots (\xi.33)$$

Rearrange equation (ξ.33), to get:

$$\bar{P}_i = \bar{P}_{i-1} + \frac{\dot{m} - 2\pi\rho \int_0^R \alpha_{i,j} r_{i,j} \Delta r_{i,j}}{2\pi\rho \int_0^R \beta_{i,j} r_{i,j} \Delta r_{i,j}} \quad \dots (\xi.34)$$

The integration in equation (ξ.34) is accomplished by using the direct Integration to get:-

$$\bar{P}_i = \bar{P}_{i-1} + \frac{\dot{m} - \sum_{j=1}^M 2\pi\rho\alpha_{i,j}r_{i,j}(r_{i,j} - r_{i,j-1})}{\sum_{j=1}^M 2\pi\rho\beta_{i,j}r_{i,j}(r_{i,j} - r_{i,j-1})} \quad \dots (\xi.35)$$

The velocity equation (ξ.31) is solved by using the same sequence which was explained for equation (ξ.10) in article (ξ.3.1) for rectangular duct.

**ξ.4 NUMERICAL FORMULATION FOR CONTINUITY EQUATION OF RECTANGULAR AND CIRCULAR DUCT**

The Backward Finite Differences will be used for converting the two equations, (3.1) for rectangular duct and (3.6) for circular duct to algebraic form as follows:-

For rectangular duct:-

$$\frac{\partial u}{\partial x} \Big|_{i,j} = \frac{u_{i,j} - u_{i-1,j}}{\Delta x} \quad \dots (\xi.36)$$

$$\frac{\partial v}{\partial y} \Big|_{i,j} = \frac{v_{i,j} - v_{i,j-1}}{\Delta y_{i,j}} \quad \dots (\xi.37)$$

Substitute equation (ξ.36) and (ξ.37) into equation (3.1), and get the following equation:-

$$v_{i,j} = \frac{\Delta y_{i,j}}{\Delta x} (u_{i-1,j} - u_{i,j}) + v_{i,j-1} \quad \dots (\xi.38)$$

The relaxation for (ξ.38) was done with ω=0.37 by using the following equation:-

$$v_{i,j}^{q+1} = (1 - \omega)v_{i,j}^q + \omega \left( \frac{\Delta y_{i,j}}{\Delta x} (u_{i-1,j} - u_{i,j}) + v_{i,j-1} \right) \quad \dots (\xi.39)$$

For circular duct:-

$$\frac{1}{r} \frac{\partial (ru_r)}{\partial r} \Big|_{i,j} = \frac{\partial u_r}{\partial r} \Big|_{i,j} + \frac{u_r}{r} \Big|_{i,j} = \frac{u_{ri,j} - u_{ri,j-1}}{\Delta r_{i,j}} + \frac{u_{ri,j}}{r_{i,j}} \quad \dots (\xi.40)$$

$$\frac{\partial u_x}{\partial x} \Big|_{i,j} = \frac{u_{xi,j} - u_{xi-1,j}}{\Delta x} \quad \dots (\xi.41)$$

Substitute equation (ξ.40) and (ξ.41) into equation (3.6), to obtain:-

$$u_{ri,j} = \frac{r_{i,j} \Delta r_{i,j}}{(r_{i,j} + \Delta r_{i,j}) \Delta x} (u_{xi-1,j} - u_{xi,j}) + \frac{r_{i,j}}{(r_{i,j} + \Delta r_{i,j})} u_{ri,j-1} \quad \dots (\xi.42)$$

The relaxation process for equation (ξ.42) is similar to (ξ.39).

### ξ.5 k - ε MODEL

The conversion of the two equation turbulent model ( $k - \varepsilon$ ) to the numerical form is accomplished by using the Backward Differences for the convective terms and Central Differences for the diffusion terms for the two ducts.

#### ξ.5.1 NUMERICAL FORMULATION FOR $k - \varepsilon$ MODEL OF RECTANGULAR DUCT

The turbulent kinetic energy equation (3.13) is a PDE and can be converted to algebraic form as follows:-

$$\rho u \frac{\partial k}{\partial x} \Big|_{i,j} = \rho u_{i,j} \frac{k_{i,j} - k_{i-1,j}}{\Delta x} \quad \dots (\xi.43)$$

$$\rho v \frac{\partial k}{\partial y} \Big|_{i,j} = \rho v_{i,j} \frac{k_{i,j} - k_{i,j-1}}{\Delta y_{i,j}} \quad \dots (\xi.44)$$

$$\frac{\partial}{\partial x} \left( \frac{\mu_t}{\sigma_k} \frac{\partial k}{\partial x} \right) \Big|_{i,j} = \frac{1}{\Delta x} \left[ \frac{\mu_{t_{i+0.5,j}}}{\sigma_k} \frac{(k_{i+1,j} - k_{i,j})}{\Delta x} - \frac{\mu_{t_{i-0.5,j}}}{\sigma_k} \frac{(k_{i,j} - k_{i-1,j})}{\Delta x} \right] \quad \dots (\xi. \xi \circ)$$

$$\frac{\partial}{\partial y} \left( \frac{\mu_t}{\sigma_k} \frac{\partial k}{\partial y} \right) \Big|_{i,j} = \left( \frac{2}{\Delta y_{i,j} + \Delta y_{i,j+1}} \right) \left[ \frac{\mu_{t_{i,j+0.5}}}{\sigma_k} \frac{(k_{i,j+1} - k_{i,j})}{\Delta y_{i,j+1}} - \frac{\mu_{t_{i,j-0.5}}}{\sigma_k} \frac{(k_{i,j} - k_{i,j-1})}{\Delta y_{i,j}} \right] \quad \dots (\xi. \xi \imath)$$

But the generation term conversion from Equation (3.10) form to numerical form will be as follows:-

$$G \Big|_{i,j} = \mu_{t_{i,j}} \left[ 2 \left( \left( \frac{u_{i+1,j} - u_{i-1,j}}{2\Delta x} \right)^2 + \left( \frac{v_{i,j+1} - v_{i,j-1}}{\Delta y_{i,j} + \Delta y_{i,j+1}} \right)^2 \right) + \left( \frac{u_{i,j+1} - u_{i,j-1}}{\Delta y_{i,j} + \Delta y_{i,j+1}} \right)^2 \right] \quad \dots (\xi. \xi \nu)$$

And the dissipation term in equation (3.11) will be converted as follows:-

$$\rho \varepsilon \Big|_{i,j} = \rho \varepsilon_{i,j} \quad \dots$$

(\xi. \xi \lambda)

After substitution of the algebraic equations (\xi. \xi \rceil), (\xi. \xi \xi), (\xi. \xi \circ), (\xi. \xi \imath), (\xi. \xi \nu) and (\xi. \xi \lambda) in equation (3.12), the result will be:-

$$a_{1k_{i,j}} k_{i,j} = a_{2k_{i,j}} k_{i-1,j} + a_{3k_{i,j}} k_{i,j-1} + a_{4k_{i,j}} k_{i+1,j} + a_{5k_{i,j}} k_{i,j+1} + S_{k_{i,j}} \quad \dots (\xi. \xi \rho)$$

Where:-

$$\left. \begin{aligned} a_{1k_{i,j}} &= \left( \frac{\rho u_{i,j}}{\Delta x} + \frac{\rho v_{i,j}}{\Delta y_{i,j}} + \frac{2(\mu_{t_{i,j-0.5}} + \mu_{t_{i,j+0.5}})}{\sigma_k (\Delta y_{i,j} + \Delta y_{i,j+1}) \Delta y_{i,j+1}} + \frac{\mu_{t_{i-0.5,j}} + \mu_{t_{i+0.5,j}}}{\sigma_k \Delta x^2} \right) \\ a_{2k_{i,j}} &= \left( \frac{\rho u_{i,j}}{\Delta x} + \frac{\mu_{t_{i-0.5,j}}}{\sigma_k \Delta x^2} \right) \\ a_{3k_{i,j}} &= \left( \frac{\rho v_{i,j}}{\Delta y_{i,j}} + \frac{\mu_{t_{i,j-0.5}}}{\sigma_k (\Delta y_{i,j} + \Delta y_{i,j+1}) \Delta y_{i,j}} \right) \\ a_{4k_{i,j}} &= \left( \frac{\mu_{t_{i+0.5,j}}}{\sigma_k \Delta x^2} \right) \\ a_{5k_{i,j}} &= \left( \frac{\mu_{t_{i,j+0.5}}}{\sigma_k (\Delta y_{i,j} + \Delta y_{i,j+1}) \Delta y_{i,j+1}} \right) \\ S_{k_{i,j}} &= G_{i,j} - \rho \varepsilon_{i,j} \end{aligned} \right\} \quad \dots (\xi. \xi \sigma)$$

Where: -

$$\left. \begin{aligned} \mu_{t_{i,j+0.5}} &= \frac{\mu_{t_{i,j+1}} + \mu_{t_{i,j}}}{2} \\ \mu_{t_{i,j}} &= \frac{\mu_{t_{i,j}} + \mu_{t_{i,j-1}}}{2} \\ \mu_{t_{i+0.5,j}} &= \frac{\mu_{t_{i+1,j}} + \mu_{t_{i,j}}}{2} \\ \mu_{t_{i,j-0.5}} &= \frac{\mu_{t_{i,j}} + \mu_{t_{i-1,j}}}{2} \end{aligned} \right\} \dots (\xi.01)$$

The kinetic energy equation ( $\xi.\xi^9$ ) can be solved by using the point by point Gauss –Seidel Method. The principle of this method is based on formulating an ordered linear equation so that it is valid for calculating three unknowns of the dependent variables along a constant line (j=constant). According to this method, equation ( $\xi.\xi^9$ ) can be written as [ $\Upsilon^0$ ]:-

$$- a_{2k_{i,j}} k_{i-1,j} + a_{1k_{i,j}} k_{i,j} - a_{4k_{i,j}} k_{i+1,j} = a_{3k_{i,j}} k_{i,j-1} + a_{5k_{i,j}} k_{i,j+1} + S_{k_{i,j}} \dots (\xi.02)$$

The equation ( $\xi.02$ ) is used for all varying (i) nodal points at (j=constant). This equation can be solved by successive manner by using Tri-Diagonal Matrix Algorithm (TDMA) [ $\Upsilon^1$ ]. The calculation of the turbulent kinetic energy values (k) at nodal points can be done at constant calculation line (j). This calculation depends on the (k) values at the two calculation line sides which were calculated either from the boundary conditions of the problem or from the previous iteration. When the (k) calculation is done for all grid lines, a new iteration process will be started until reaching the required convergence. The equation ( $\xi.02$ ) was solved without relaxation (with relaxation factor of value  $\omega_k = 1$ ) according to the following criteria:-

$$k_{i,j}^{q+1} = (1 - \omega_k) k_{i,j}^q + \omega_k k_{i,j}^{q+1} \dots (\xi.03)$$

Where  $k_{i,j}^q$  and  $k_{i,j}^{q+1}$  are the values of calculated k at each nodal point at the previous and the present iteration planes respectively.

$$\rho u \left. \frac{\partial \varepsilon}{\partial x} \right|_{i,j} = \rho u_{i,j} \frac{\varepsilon_{i,j} - \varepsilon_{i-1,j}}{\Delta x} \dots (\xi.04)$$

$$\rho v \frac{\partial \varepsilon}{\partial y} \Big|_{i,j} = \rho v_{i,j} \frac{\varepsilon_{i,j} - \varepsilon_{i,j-1}}{\Delta y_{i,j}} \quad \dots (4.55)$$

$$\frac{\partial}{\partial x} \left( \frac{\mu_t}{\sigma_\varepsilon} \frac{\partial \varepsilon}{\partial x} \right) \Big|_{i,j} = \frac{1}{\Delta x} \left[ \frac{\mu_{t_{i+0.5,j}}}{\sigma_\varepsilon} \frac{(\varepsilon_{i+1,j} - \varepsilon_{i,j})}{\Delta x} - \frac{\mu_{t_{i-0.5,j}}}{\sigma_\varepsilon} \frac{(\varepsilon_{i,j} - \varepsilon_{i-1,j})}{\Delta x} \right] \quad \dots (4.56)$$

$$\frac{\partial}{\partial y} \left( \frac{\mu_t}{\sigma_\varepsilon} \frac{\partial \varepsilon}{\partial y} \right) \Big|_{i,j} = \left( \frac{2}{\Delta y_{i,j} + \Delta y_{i,j+1}} \right) \left[ \frac{\mu_{t_{i,j+0.5}}}{\sigma_\varepsilon} \frac{(\varepsilon_{i,j+1} - \varepsilon_{i,j})}{\Delta y_{i,j+1}} - \frac{\mu_{t_{i,j-0.5}}}{\sigma_\varepsilon} \frac{(\varepsilon_{i,j} - \varepsilon_{i,j-1})}{\Delta y_{i,j}} \right] \quad \dots (4.57)$$

$$C_{\varepsilon 1} G \frac{\varepsilon}{k} \Big|_{i,j} = C_{\varepsilon 1} G_{i,j} \frac{\varepsilon_{i,j}}{k_{i,j}} \quad \dots (4.58)$$

Where  $G_{i,j}$  is calculated from equation (4.57).

$$-C_{\varepsilon 2} \rho \frac{\varepsilon^2}{k} \Big|_{i,j} = -C_{\varepsilon 2} \rho \frac{\varepsilon_{i,j}^2}{k_{i,j}} \quad \dots (4.59)$$

After substitution of the algebraic equations (4.54), (4.55), (4.56), (4.57), (4.58) and (4.59) in equation (3.14), the result will be:-

$$a_{1\varepsilon_{i,j}} \varepsilon_{i,j} = a_{2\varepsilon_{i,j}} \varepsilon_{i-1,j} + a_{3\varepsilon_{i,j}} \varepsilon_{i,j-1} + a_{4\varepsilon_{i,j}} \varepsilon_{i+1,j} + a_{5\varepsilon_{i,j}} \varepsilon_{i,j+1} + S_{\varepsilon_{i,j}} \quad \dots (4.60)$$

Where:-

$$\left. \begin{aligned} a_{1\varepsilon_{i,j}} &= \left( \frac{\rho u_{i,j}}{\Delta x} + \frac{\rho v_{i,j}}{\Delta y_{i,j}} + \frac{\mu_{t_{i-0.5,j}} + \mu_{t_{i+0.5,j}}}{\sigma_\varepsilon \Delta x^2} + \frac{2(\mu_{t_{i,j-0.5}} + \mu_{t_{i,j+0.5}})}{\sigma_\varepsilon (\Delta y_{i,j} + \Delta y_{i,j+1}) \Delta y_{i,j+1}} + \rho C_{\varepsilon 2} \frac{\varepsilon_{i,j}}{k_{i,j}} \right) \\ a_{2\varepsilon_{i,j}} &= \left( \frac{\rho u_{i,j}}{\Delta x} + \frac{\mu_{t_{i-0.5,j}}}{\sigma_\varepsilon \Delta x^2} \right) \\ a_{3\varepsilon_{i,j}} &= \left( \frac{\rho v_{i,j}}{\Delta y_{i,j}} + \frac{\mu_{t_{i,j-0.5}}}{\sigma_\varepsilon (\Delta y_{i,j} + \Delta y_{i,j+1}) \Delta y_{i,j}} \right) \\ a_{4\varepsilon_{i,j}} &= \left( \frac{\mu_{t_{i+0.5,j}}}{\sigma_\varepsilon \Delta x^2} \right) \\ a_{5\varepsilon_{i,j}} &= \left( \frac{\mu_{t_{i,j+0.5}}}{\sigma_\varepsilon (\Delta y_{i,j} + \Delta y_{i,j+1}) \Delta y_{i,j+1}} \right) \\ S_{\varepsilon_{i,j}} &= C_{\varepsilon 1} G_{i,j} \frac{\varepsilon_{i,j}}{k_{i,j}} \end{aligned} \right\} \quad \dots (4.61)$$

The values of the turbulent viscosity at halve points like  $\mu_{t_{i,j-0.5}}$  are calculated from equation (4.51).

The generation and dissipation terms are treated as indicated in the two equations (4.58) and (4.59) respectively to attain the stability of the numerical solution [14].

The linear dissipation rate equation (4.60) is solved by using the Gauss – Seidel Method which was explained in detail in the kinetic energy equation. Hence equation (4.60) will become:-

$$-a_{2\varepsilon_{i,j}} \varepsilon_{i-1,j} + a_{1\varepsilon_{i,j}} \varepsilon_{i,j} - a_{4\varepsilon_{i,j}} \varepsilon_{i+1,j} = a_{3\varepsilon_{i,j}} \varepsilon_{i,j-1} + a_{5\varepsilon_{i,j}} \varepsilon_{i,j+1} + S_{\varepsilon_{i,j}} \quad \dots (4.62)$$

The equation (4.62) was solved without relaxation according to the following criteria

$$\varepsilon_{i,j}^{q+1} = (1 - \omega_{\varepsilon}) \varepsilon_{i,j}^q + \omega_{\varepsilon} \varepsilon_{i,j}^{q+1} \quad \dots (4.63)$$

**4.5.2 NUMERICAL FORMULATION FOR  $k - \varepsilon$  MODEL of CIRCULAR DUCT**

The same treatment for  $k - \varepsilon$  model of the rectangular duct will be done for the circular duct as follows:-

For k equation:

$$\rho u_r \frac{\partial k}{\partial r} \Big|_{i,j} = \rho u_{r_{i,j}} \frac{k_{i,j} - k_{i,j-1}}{\Delta r_{i,j}} \quad \dots (4.64)$$

$$\rho u_x \frac{\partial k}{\partial x} \Big|_{i,j} = \rho u_{x_{i,j}} \frac{k_{i,j} - k_{i-1,j}}{\Delta x} \quad \dots (4.65)$$

$$\frac{1}{r} \frac{\partial}{\partial r} \left( r \frac{\mu_t}{\sigma_k} \frac{\partial k}{\partial r} \right) \Big|_{i,j} = \frac{2}{r_{i,j} (\Delta r_{i,j} + \Delta r_{i,j+1})} \left[ r_{i,j+0.5} \frac{\mu_{t_{i,j+0.5}}}{\sigma_k} \frac{(k_{i,j+1} - k_{i,j})}{\Delta r_{i,j+1}} - r_{i,j-0.5} \frac{\mu_{t_{i,j-0.5}}}{\sigma_k} \frac{(k_{i,j} - k_{i,j-1})}{\Delta r_{i,j}} \right] \quad \dots (4.66)$$

$$\frac{\partial}{\partial x} \left( \frac{\mu_t}{\sigma_k} \frac{\partial k}{\partial x} \right) \Big|_{i,j} = \frac{1}{\Delta x} \left[ \frac{\mu_{t_{i+0.5,j}}}{\sigma_k} \frac{k_{i+1,j} - k_{i,j}}{\Delta x} - \frac{\mu_{t_{i-0.5,j}}}{\sigma_k} \frac{k_{i,j} - k_{i-1,j}}{\Delta x} \right] \quad \dots (4.67)$$

$$G|_{i,j} = \mu_{t_i,j} \left[ 2 \left( \left( \frac{u_{r_{i,j+1}} - u_{r_{i,j-1}}}{(\Delta r_{i,j} + \Delta r_{i,j+1})} \right)^2 + \left( \frac{u_{x_{i+1,j}} - u_{x_{i-1,j}}}{2\Delta x} \right)^2 \right) + \left( \frac{u_{r_{i+1,j}} - u_{r_{i-1,j}}}{2\Delta x} + \frac{u_{x_{i,j+1}} - u_{x_{i,j-1}}}{(\Delta r_{i,j} + \Delta r_{i,j+1})} \right)^2 \right] \dots (\xi.68)$$

$$\rho \varepsilon|_{i,j} = \rho \varepsilon_{i,j} \dots (\xi.69)$$

After rearranging the above equations for k, the following form can be written:

$$a_{1k_{j,i}} k_{j,i} = a_{2k_{j,i}} k_{j+1,i} + a_{3k_{j,i}} k_{j,i+1} + a_{4k_{j,i}} k_{j-1,i} + a_{5k_{j,i}} k_{j,i-1} + S_{k_{j,i}} \dots (\xi.70)$$

Where:-

$$\left. \begin{aligned} a_{1k_{i,j}} &= \left( \frac{\rho u_{i,j}}{\Delta x} + \frac{\rho v_{i,j}}{\Delta r_{i,j}} + \frac{2r_{i,j+0.5} \mu_{t_{i,j+0.5}}}{\sigma_k r_{i,j} (\Delta r_{i,j} + \Delta r_{i,j+1}) \Delta r_{i,j+1}} + \frac{2r_{i,j-0.5} \mu_{t_{i,j-0.5}}}{\sigma_k r_{i,j} (\Delta r_{i,j} + \Delta r_{i,j+1}) \Delta r_{i,j}} \right. \\ &\quad \left. + \frac{(\mu_{t_{i-0.5,j}} + \mu_{t_{i+0.5,j}})}{\sigma_k \Delta x^2} \right) \\ a_{2k_{i,j}} &= \left( \frac{2r_{i,j+0.5} \mu_{t_{i,j+0.5}}}{\sigma_k r_{i,j} (\Delta r_{i,j} + \Delta r_{i,j+1}) \Delta r_{i,j+1}} \right) \\ a_{3k_{i,j}} &= \left( \frac{\mu_{t_{i+0.5,j}}}{\sigma_k \Delta x^2} \right) \\ a_{4k_{i,j}} &= \left( \frac{\rho v_{i,j}}{\Delta r_{i,j}} + \frac{2r_{i,j-0.5} \mu_{t_{i,j-0.5}}}{\sigma_k r_{i,j} (\Delta r_{i,j} + \Delta r_{i,j+1}) \Delta r_{i,j}} \right) \\ a_{5k_{i,j}} &= \left( \frac{\rho u_{i,j}}{\Delta x} + \frac{\mu_{t_{i-0.5,j}}}{\sigma_k \Delta x^2} \right) \\ S_{k_{i,j}} &= G_{i,j} - \rho \varepsilon_{i,j} \end{aligned} \right\} \dots (\xi.71)$$

$$-a_{5k_{i,j}} k_{i-1,j} + a_{1k_{i,j}} k_{i,j} - a_{3k_{i,j}} k_{i+1,j} = a_{2k_{i,j}} k_{i,j+1} + a_{4k_{i,j}} k_{i,j-1} + S_{k_{i,j}} \dots (\xi.72)$$

For  $\varepsilon$  equation:-

$$\rho u_r \frac{\partial \varepsilon}{\partial r} |_{i,j} = \rho u_{r_{i,j}} \frac{\varepsilon_{i,j} - \varepsilon_{i,j-1}}{\Delta r_{i,j}} \dots (\xi.73)$$

$$\rho u_x \frac{\partial \varepsilon}{\partial x} \Big|_{i,j} = \rho u_{x_{i,j}} \frac{\varepsilon_{i,j} - \varepsilon_{i-1,j}}{\Delta x} \quad \dots (\xi. \vee \xi)$$

$$\frac{1}{r} \frac{\partial}{\partial r} \left( r \frac{\mu_t}{\sigma_\varepsilon} \frac{\partial \varepsilon}{\partial r} \right) \Big|_{i,j} = \frac{2}{r_{i,j} (\Delta r_{i,j} + \Delta r_{i,j+1})} \left[ r_{i,j+0.5} \frac{\mu_{t_{i,j+0.5}} (\varepsilon_{i,j+1} - \varepsilon_{i,j})}{\sigma_\varepsilon \Delta r_{i,j+1}} - r_{i,j-0.5} \frac{\mu_{t_{i,j-0.5}} (\varepsilon_{i,j} - \varepsilon_{i,j-1})}{\sigma_\varepsilon \Delta r_{i,j}} \right] \quad \dots (\xi. \vee \circ)$$

$$\frac{\partial}{\partial x} \left( \frac{\mu_t}{\sigma_\varepsilon} \frac{\partial \varepsilon}{\partial x} \right) \Big|_{i,j} = \frac{1}{\Delta x} \left[ \frac{\mu_{t_{i+0.5,j}} \varepsilon_{i+1,j} - \varepsilon_{i,j}}{\sigma_\varepsilon \Delta x} - \frac{\mu_{t_{i-0.5,j}} \varepsilon_{i,j} - \varepsilon_{i-1,j}}{\sigma_\varepsilon \Delta x} \right] \quad \dots (\xi. \vee \vee)$$

$$C_{\varepsilon 1} G \frac{\varepsilon}{k} \Big|_{i,j} = C_{\varepsilon 1} G_{i,j} \frac{\varepsilon_{i,j}}{k_{i,j}} \quad \dots (\xi. \vee \vee)$$

Where  $G_{i,j}$  is calculated from equation ( $\xi. \vee \wedge$ ).

$$-C_{\varepsilon 2} \rho \frac{\varepsilon^2}{k} \Big|_{i,j} = -C_{\varepsilon 2} \rho \frac{\varepsilon_{i,j}^2}{k_{i,j}} \quad \dots (\xi. \vee \wedge)$$

After rearranging the above equations for  $\varepsilon$ , the following form can be written:-

$$a_{1\varepsilon_{i,j}} \varepsilon_{i,j} = a_{2\varepsilon_{i,j}} \varepsilon_{i,j+1} + a_{3\varepsilon_{i,j}} \varepsilon_{i+1,j} + a_{4\varepsilon_{i,j}} \varepsilon_{i,j-1} + a_{5\varepsilon_{i,j}} \varepsilon_{i-1,j} + S_{\varepsilon_{i,j}} \quad \dots (\xi. \vee \vartheta)$$

Where:-

$$\left. \begin{aligned} a_{1\varepsilon_{i,j}} &= \left( \frac{\rho u_{r_{i,j}}}{\Delta r_{i,j}} + \frac{\rho u_{x_{i,j}}}{\Delta x} + \frac{2r_{i,j+0.5} \mu_{t_{i,j+0.5}}}{r_{i,j} \sigma_\varepsilon (\Delta r_{i,j} + \Delta r_{i,j+1}) \Delta r_{i,j+1}} + \frac{2r_{i,j-0.5} \mu_{t_{i,j-0.5}}}{r_{i,j} \sigma_\varepsilon (\Delta r_{i,j} + \Delta r_{i,j+1}) \Delta r_{i,j}} \right. \\ &\quad \left. + \frac{\mu_{t_{i+0.5,j}} + \mu_{t_{i-0.5,j}}}{\sigma_\varepsilon \Delta x^2} + C_{\varepsilon 2} \rho \frac{\varepsilon_{i,j}}{k_{i,j}} \right) \\ a_{2\varepsilon_{i,j}} &= \frac{2r_{i,j+0.5} \mu_{t_{i,j+0.5}}}{r_{i,j} \sigma_\varepsilon (\Delta r_{i,j} + \Delta r_{i,j+1}) \Delta r_{i,j+1}}; \quad a_{3\varepsilon_{i,j}} = \frac{\mu_{t_{i+0.5,j}}}{\sigma_\varepsilon \Delta x^2} \\ a_{4\varepsilon_{i,j}} &= \frac{\rho u_{r_{i,j}}}{\Delta r_{i,j}} + \frac{2r_{i,j-0.5} \mu_{t_{i,j-0.5}}}{r_{i,j} \sigma_\varepsilon (\Delta r_{i,j} + \Delta r_{i,j+1}) \Delta r_{i,j}}; \quad a_{5\varepsilon_{i,j}} = \frac{\rho u_{x_{i,j}}}{\Delta x} + \frac{\mu_{t_{i-0.5,j}}}{\sigma_\varepsilon \Delta x^2} \\ S_{\varepsilon_{i,j}} &= C_{\varepsilon 1} G_{i,j} \frac{\varepsilon_{i,j}}{k_{i,j}} \end{aligned} \right\} \quad \dots (\xi. \wedge \circ)$$

$$-a_{5\varepsilon_{i,j}} \varepsilon_{i-1,j} + a_{1\varepsilon_{i,j}} \varepsilon_{i,j} - a_{3\varepsilon_{i,j}} \varepsilon_{i+1,j} = a_{4\varepsilon_{i,j}} \varepsilon_{i,j-1} + a_{2\varepsilon_{i,j}} \varepsilon_{i,j+1} + S_{\varepsilon_{i,j}} \quad \dots (\xi. \wedge \vartheta)$$

The relaxation treatment for  $k - \varepsilon$  model of circular duct is similar to that of rectangular duct.

## 4.6 ENERGY EQUATIONS

By using the Backward Differences for convection terms and the Central Differences for diffusion terms, the energy equation for each of rectangular and circular duct can be converted to the algebraic form in the following two articles.

**4.7.1 ENERGY EQUATION FOR RECTANGULAR DUCT**

$$\rho u \left. \frac{\partial T}{\partial x} \right|_{i,j} = \rho u_{i,j} \frac{T_{i,j} - T_{i-1,j}}{\Delta x} \quad \dots (4.82)$$

$$\rho v \left. \frac{\partial T}{\partial y} \right|_{i,j} = \rho v_{i,j} \frac{T_{i,j} - T_{i,j-1}}{\Delta y_{i,j}} \quad \dots (4.83)$$

$$\frac{\partial}{\partial x} \left( \frac{\mu_{eff}}{P_{eff}} \frac{\partial T}{\partial x} \right) \Big|_{i,j} = \frac{1}{\Delta x} \left( \frac{\mu_{eff_{i+0.5,j}}}{P_{eff}} \frac{T_{i+1,j} - T_{i,j}}{\Delta x} - \frac{\mu_{eff_{i-0.5,j}}}{P_{eff}} \frac{T_{i-1,j} - T_{i,j}}{\Delta x} \right) \quad \dots (4.84)$$

$$\frac{\partial}{\partial y} \left( \frac{\mu_{eff}}{P_{eff}} \frac{\partial T}{\partial y} \right) \Big|_{i,j} = \left( \frac{1}{\Delta y_{i,j} + \Delta y_{i,j+1}} \right) \left( \frac{\mu_{eff_{i,j+0.5}}}{P_{eff}} \frac{T_{i,j+1} - T_{i,j}}{\Delta y_{i,j+1}} - \frac{\mu_{eff_{i,j-0.5}}}{P_{eff}} \frac{T_{i,j} - T_{i,j-1}}{\Delta y_{i,j}} \right) \quad \dots (4.85)$$

$$a_{1T_{i,j}} T_{i,j} = a_{2T_{i,j}} T_{i-1,j} + a_{3T_{i,j}} T_{i,j-1} + a_{4T_{i,j}} T_{i+1,j} + a_{5T_{i,j}} T_{i,j+1} \quad \dots (4.86)$$

Where:-

$$\left. \begin{aligned}
 a_{1T_{i,j}} &= \left( \frac{\rho u_{i,j}}{\Delta x} + \frac{\rho v_{i,j}}{\Delta y_{i,j}} + \frac{2 \frac{\mu_{eff_{i,j+0.5}}}{P_{reff}}}{(\Delta y_{i,j} + \Delta y_{i,j+1}) \Delta y_{i,j+1}} + \frac{2 \frac{\mu_{eff_{i,j-0.5}}}{P_{reff}}}{(\Delta y_{i,j} + \Delta y_{i,j+1}) \Delta y_{i,j}} + \frac{\left( \frac{\mu_{eff_{i+0.5,j}}}{P_{reff}} + \frac{\mu_{eff_{i-0.5,j}}}{P_{reff}} \right)}{\Delta x^2} \right) \\
 a_{2T_{i,j}} &= \left( \frac{\rho u_{i,j}}{\Delta x} + \frac{\mu_{eff_{i-0.5,j}}}{P_{reff} \Delta x^2} \right); \quad a_{3T_{i,j}} = \left( \frac{\rho v_{i,j}}{\Delta y_{i,j}} + \frac{2 \frac{\mu_{eff_{i,j-0.5}}}{P_{reff}}}{(\Delta y_{i,j} + \Delta y_{i,j+1}) \Delta y_{i,j}} \right) \\
 a_{4T_{i,j}} &= \left( \frac{\mu_{eff_{i+0.5,j}}}{P_{reff} \Delta x^2} \right); \quad a_{5T_{i,j}} = \left( \frac{2 \frac{\mu_{eff_{i,j+0.5}}}{P_{reff}}}{(\Delta y_{i,j} + \Delta y_{i,j+1}) \Delta y_{i,j+1}} \right)
 \end{aligned} \right\} \dots (\xi. \lambda \nu)$$

Where: -

$$\left. \begin{aligned}
 \frac{\mu_{eff_{i,j+0.5}}}{P_{reff}} &= \frac{1}{2} \left( \frac{\mu_{eff_{i,j}}}{P_{reff}} + \frac{\mu_{eff_{i,j+1}}}{P_{reff}} \right) \\
 \frac{\mu_{eff_{i,j-0.5}}}{P_{reff}} &= \frac{1}{2} \left( \frac{\mu_{eff_{i,j}}}{P_{reff}} + \frac{\mu_{eff_{i,j-1}}}{P_{reff}} \right) \\
 \frac{\mu_{eff_{i+0.5,j}}}{P_{reff}} &= \frac{1}{2} \left( \frac{\mu_{eff_{i,j}}}{P_{reff}} + \frac{\mu_{eff_{i+1,j}}}{P_{reff}} \right) \\
 \frac{\mu_{eff_{i-0.5,j}}}{P_{reff}} &= \frac{1}{2} \left( \frac{\mu_{eff_{i,j}}}{P_{reff}} + \frac{\mu_{eff_{i-1,j}}}{P_{reff}} \right)
 \end{aligned} \right\} \dots (\xi. \lambda \lambda)$$

The solution of the temperature equation (ξ.λν) is accomplished by using the point by point Gauss –Seidel Method which was explained previously in the kinetic energy equation. So equation (ξ. λν) will become:-

$$T_{i,j} = (a_{2T_{i,j}} T_{i-1,j} + a_{3T_{i,j}} T_{i,j-1} + a_{4T_{i,j}} T_{i+1,j} + a_{5T_{i,j}} T_{i,j+1}) / a_{1T_{i,j}} \dots (\xi. \lambda \rho)$$

Equation (ξ.λρ) was solved by using the following relaxation equation:-

$$T_{i,j}^{q+1} = (1 - \omega_T) T_{i,j}^q + \omega_T \left( (a_{2T_{i,j}} T_{i-1,j} + a_{3T_{i,j}} T_{i,j-1} + a_{4T_{i,j}} T_{i+1,j} + a_{5T_{i,j}} T_{i,j+1}) / a_{1T_{i,j}} \right) \dots (\xi. \lambda \sigma)$$

Where, the suitable relaxation factor for solving this equation was  $\omega_T = 0.956$ .

**ξ.λ.ϒ ENERGY EQUATION FOR CIRCULAR DUCT**

$$\rho u_r \frac{\partial T}{\partial r} \Big|_{i,j} = \rho u_{r_{i,j}} \frac{T_{i,j} - T_{i,j-1}}{\Delta r_{i,j}} \quad \dots (\xi.91)$$

$$\rho u_x \frac{\partial T}{\partial x} \Big|_{i,j} = \rho u_{x_{i,j}} \frac{T_{i,j} - T_{i-1,j}}{\Delta x} \quad \dots (\xi.92)$$

$$\frac{1}{r} \frac{\partial}{\partial r} \left( r \frac{\mu_{eff}}{P_{reff}} \frac{\partial T}{\partial r} \right) \Big|_{i,j} = \frac{2}{r_{i,j} (\Delta r_{i,j} + \Delta r_{i,j+1})} \left[ r_{i,j+0.5} \frac{\mu_{eff_{i,j+0.5}}}{P_{reff}} \frac{(T_{i,j+1} - T_{i,j})}{\Delta r_{i,j+1}} - r_{i,j-0.5} \frac{\mu_{eff_{i,j-0.5}}}{P_{reff}} \frac{(T_{i,j} - T_{i,j-1})}{\Delta r_{i,j}} \right] \quad \dots (\xi.93)$$

$$\frac{\partial}{\partial x} \left( \frac{\mu_{eff}}{P_{reff}} \frac{\partial T}{\partial x} \right) \Big|_{i,j} = \frac{1}{\Delta x} \left( \frac{\mu_{eff_{i+0.5,j}}}{P_{reff}} \frac{T_{i+1,j} - T_{i,j}}{\Delta x} - \frac{\mu_{eff_{i-0.5,j}}}{P_{reff}} \frac{T_{i,j} - T_{i-1,j}}{\Delta x} \right) \quad \dots (\xi.94)$$

After rearranging the above equations for T, the following form can be written: -

$$a_{1T_{i,j}} T_{i,j} = a_{2T_{i,j}} T_{i,j+1} + a_{3T_{i,j}} T_{i+1,j} + a_{4T_{i,j}} T_{i,j-1} + a_{5T_{i,j}} T_{i-1,j} \quad \dots (\xi.95)$$

$$\left. \begin{aligned} a_{1T_{i,j}} &= \frac{\rho u_{r_{i,j}}}{\Delta r_{i,j}} + \frac{\rho u_{x_{i,j}}}{\Delta x} + \frac{2r_{i,j+0.5} \frac{\mu_{eff_{i,j+0.5}}}{P_{reff}}}{r_{i,j} (\Delta r_{i,j} + \Delta r_{i,j+1}) \Delta r_{i,j+1}} + \frac{2r_{i,j-0.5} \frac{\mu_{eff_{i,j-0.5}}}{P_{reff}}}{r_{i,j} (\Delta r_{i,j} + \Delta r_{i,j+1}) \Delta r_{i,j}} + \frac{\frac{\mu_{eff_{i+0.5,j}}}{P_{reff}} + \frac{\mu_{eff_{i-0.5,j}}}{P_{reff}}}{\Delta x^2} \\ a_{2T_{i,j}} &= \frac{2r_{i,j+0.5} \frac{\mu_{eff_{i,j+0.5}}}{P_{reff}}}{r_{i,j} (\Delta r_{i,j} + \Delta r_{i,j+1}) \Delta r_{i,j+1}}; \quad a_{3T_{i,j}} = \frac{\mu_{eff_{i+0.5,j}}}{\Delta x^2} \\ a_{4T_{i,j}} &= \frac{\rho u_{r_{i,j}}}{\Delta r} + \frac{r_{i,j-0.5} \frac{\mu_{eff_{i,j-0.5}}}{P_{reff}}}{r_{i,j} \Delta r^2}; \quad a_{5T_{i,j}} = \frac{\rho u_{x_{i,j}}}{\Delta x} + \frac{\mu_{eff_{i-0.5,j}}}{\Delta x^2} \end{aligned} \right\} \quad \dots (\xi.96)$$

$$\left. \begin{aligned} \frac{\mu_{eff,i,j+0.5}}{P_{reff}} &= \frac{1}{2} \left( \frac{\mu_{eff,i,j}}{P_{reff_{i,j}}} + \frac{\mu_{eff,i,j+1}}{P_{reff_{i,j+1}}} \right) \\ \frac{\mu_{eff,i,j-0.5}}{P_{reff}} &= \frac{1}{2} \left( \frac{\mu_{eff,i,j}}{P_{reff_{i,j}}} + \frac{\mu_{eff,i,j-1}}{P_{reff_{i,j-1}}} \right) \\ \frac{\mu_{eff,i+0.5,j}}{P_{reff}} &= \frac{1}{2} \left( \frac{\mu_{eff,i,j}}{P_{reff_{i,j}}} + \frac{\mu_{eff,i+1,j}}{P_{reff_{i+1,j}}} \right) \\ \frac{\mu_{eff,i-0.5,j}}{P_{reff}} &= \frac{1}{2} \left( \frac{\mu_{eff,i,j}}{P_{reff_{i,j}}} + \frac{\mu_{eff,i-1,j}}{P_{reff_{i-1,j}}} \right) \end{aligned} \right\} \dots (\xi.97)$$

$$-a_{4T_{i,j}} T_{i,j-1} + a_{1T_{i,j}} T_{i,j} - a_{2T_{i,j}} T_{i,j+1} = a_{3T_{i,j}} T_{i+1,j} + a_{5T_{i,j}} T_{i-1,j} \dots (\xi.98)$$

The relaxation for energy equation of circular duct was similar to that of rectangular.

**ξ.9 THE TREATMENT OF SINGULARITY IN THE CENTER OF CIRCULAR DUCT:-**

In any application includes the solution of conservative equations in polar coordinates for duct laminar or turbulent flow, there is a problem will be faced in the center of this duct. This problem comes from getting the radius of the duct (r) the value zero at the center of the duct, which causes the division by zero or the “Singularity” at any term in the governing equation contains (r) in the denominator.

To overcome this problem, the L’Hopitals Rule should be used with any term in the governing equations contains (r) in the denominator (99). Most of the terms will be converted to the numerical form by using the Central Differences as follows:-

*Momentum Equation:*

$$\rho u_r \frac{\partial u_x}{\partial r} \Big|_{i,j} = \rho u_{ri,j} \left( \frac{u_{x_{i,j+1}} - u_{x_{i,j-1}}}{\Delta r_{i,j+1} + \Delta r_{i,j}} \right) \dots (\xi.99)$$

$$\rho u_x \left. \frac{\partial u_x}{\partial x} \right|_{i,j} = \rho u_{x_{i,j}} \frac{u_{x_{i+1,j}} - u_{x_{i-1,j}}}{2\Delta x} \quad \dots (\xi.1.09)$$

$$-\left. \frac{\partial p}{\partial x} \right|_i = -\frac{P_i - P_{i-1}}{\Delta x} \quad \dots (\xi.1.11)$$

By using the L'Hopitals Rule with the term  $\frac{1}{r} \frac{\partial}{\partial r} \left( r \mu_t \frac{\partial u_r}{\partial r} \right)$  to get:-

$$\begin{aligned} \lim_{r \rightarrow 0} \frac{1}{r} \frac{\partial}{\partial r} \left( r \mu_{eff} \frac{\partial u_x}{\partial r} \right) &= \lim_{r \rightarrow 0} \frac{\frac{\partial^2}{\partial r^2} \left( r \mu_{eff} \frac{\partial u_x}{\partial r} \right)}{\frac{\partial}{\partial r} (r)} \\ &= \lim_{r \rightarrow 0} \frac{\partial}{\partial r} \left( r \mu_{eff} \frac{\partial^2 u_x}{\partial r^2} + \frac{\partial u_x}{\partial r} \left( r \frac{\partial \mu_{eff}}{\partial r} + \mu_{eff} \right) \right) \\ &= 2\mu_{eff} \frac{\partial^2 u_x}{\partial r^2} + 2 \frac{\partial \mu_{eff}}{\partial r} \frac{\partial u_x}{\partial r} \quad \dots (\xi.1.12) \end{aligned}$$

$$\begin{aligned} \therefore \frac{1}{r} \frac{\partial}{\partial r} \left( r \mu_{eff} \frac{\partial u_x}{\partial r} \right) \Big|_{i,j} &= \left( 2\mu_{eff} \frac{\partial^2 u_x}{\partial r^2} + 2 \frac{\partial \mu_{eff}}{\partial r} \frac{\partial u_x}{\partial r} \right) \Big|_{i,j} = 2\mu_{eff_{i,j}} \frac{u_{x_{i,j+1}} - 2u_{x_{i,j}} + u_{x_{i,j-1}}}{\left( \frac{\Delta r_{i,j+1} + \Delta r_{i,j}}{2} \right)^2} \\ &+ 2 \frac{\mu_{eff_{i,j+1}} - \mu_{eff_{i,j-1}}}{\left( \Delta r_{i,j+1} + \Delta r_{i,j} \right)} \frac{u_{x_{i,j+1}} - u_{x_{i,j-1}}}{\left( \Delta r_{i,j+1} + \Delta r_{i,j} \right)} \quad \dots (\xi.1.13) \end{aligned}$$

$$\frac{\partial}{\partial x} \left( \mu_{eff} \frac{\partial u_x}{\partial x} \right) \Big|_{i,j} = \mu_{eff_{i+0.5,j}} \frac{u_{x_{i+1,j}} - u_{x_{i,j}}}{\Delta x^2} - \mu_{eff_{i-0.5,j}} \frac{u_{x_{i,j}} - u_{x_{i-1,j}}}{\Delta x^2} \quad \dots (\xi.1.14)$$

The same thing will be done for the term  $\frac{1}{r} \frac{\partial}{\partial r} \left( r \mu_t \frac{\partial u_r}{\partial x} \right)$  to get:-

$$\lim_{r \rightarrow 0} \frac{1}{r} \frac{\partial}{\partial r} \left( r \mu_t \frac{\partial u_r}{\partial x} \right) = 2\mu_t \frac{\partial^2 u_r}{\partial r \partial x} + 2 \frac{\partial \mu_t}{\partial r} \frac{\partial u_r}{\partial x} \quad \dots (\xi.1.15)$$

$$\frac{1}{r} \frac{\partial}{\partial r} \left( r \mu_t \frac{\partial u_r}{\partial x} \right) \Big|_{i,j} = \left( 2\mu_t \frac{\partial^2 u_r}{\partial r \partial x} + 2 \frac{\partial \mu_t}{\partial r} \frac{\partial u_r}{\partial x} \right) \Big|_{i,j} = 2\mu_t \frac{\partial}{\partial r} \left( \frac{\partial u_r}{\partial x} \right) \Big|_{i,j} + 2 \frac{\partial \mu_t}{\partial r} \frac{\partial u_r}{\partial x} \Big|_{i,j}$$

$$= 2\mu_{t_{i,j}} \frac{\frac{\partial u_r}{\partial x} \Big|_{i,j+1} - \frac{\partial u_r}{\partial x} \Big|_{i,j-1}}{\left( \Delta r_{i,j} + \Delta r_{i,j+1} \right)} + 2 \frac{\mu_{t_{i,j+1}} - \mu_{t_{i,j-1}}}{\left( \Delta r_{i,j} + \Delta r_{i,j+1} \right)} \frac{u_{r_{i-1,j}} - u_{r_{i+1,j}}}{2\Delta x} \quad \dots (\xi.1.16)$$

$$\frac{\partial}{\partial x} \left( \mu_t \frac{\partial u_x}{\partial x} \right) \Big|_{i,j} = \mu_{t_{i+0.5,j}} \frac{u_{x_{i+1,j}} - u_{x_{i,j}}}{\Delta x^2} - \mu_{t_{i-0.5,j}} \frac{u_{x_{i,j}} - u_{x_{i-1,j}}}{\Delta x^2} \quad \dots (\xi.1.17)$$

$$-\frac{2}{3}\rho\frac{\partial k}{\partial x}\Big|_{i,j} = -\frac{2}{3}\rho\frac{k_{i+1,j} - k_{i-1,j}}{2\Delta x} \quad \dots (\xi.1.08)$$

By substituting the algebraic equations (\xi.99), (\xi.100), (\xi.101), (\xi.103), (\xi.105), (\xi.106), (\xi.107), and (\xi.108) into equation (3.5), the algebraic equation for the momentum equation at the center of the circular duct will be:-

$$a_{1u_{x_i,j}} u_{x_i,j} = a_{2u_{x_i,j}} u_{x_{i,j+1}} + a_{3u_{x_i,j}} u_{x_{i+1,j}} + a_{4u_{x_i,j}} u_{x_{i,j-1}} + a_{5u_{x_i,j}} u_{x_{i-1,j}} - \frac{P_i - P_{i-1}}{\Delta x} + S_{u_{i,j}} \quad \dots (\xi.109)$$

Where:-

$$\left. \begin{aligned} a_{1u_{x_i,j}} &= \frac{4\mu_{eff_{i,j}}}{\left(\frac{\Delta r_{i,j} + \Delta r_{i,j+1}}{2}\right)^2} + \frac{\mu_{eff_{i+0.5,j}} + \mu_{eff_{i-0.5,j}}}{\Delta x^2} + \frac{\mu_{t_{i+0.5,j}} + \mu_{t_{i-0.5,j}}}{\Delta x^2} \\ a_{2u_{x_i,j}} &= \left(\frac{-\rho u_{r_{i,j}}}{\Delta r_{i,j} + \Delta r_{i,j+1}}\right) + \frac{2\mu_{eff_{i,j}}}{\left(\frac{\Delta r_{i,j} + \Delta r_{i,j+1}}{2}\right)^2} + 2\frac{\mu_{eff_{i,j+1}} - \mu_{eff_{i,j-1}}}{\left(\Delta r_{i,j} + \Delta r_{i,j+1}\right)^2} \\ a_{3u_{x_i,j}} &= \frac{-\rho u_{x_{i,j}}}{2\Delta x} + \frac{\mu_{eff_{i+0.5,j}} + \mu_{t_{i+0.5,j}}}{\Delta x^2} \\ a_{4u_{x_i,j}} &= \left(\frac{\rho u_{r_{i,j}}}{\Delta r_{i,j} + \Delta r_{i,j+1}}\right) + \frac{2\mu_{eff_{i,j}}}{\left(\frac{\Delta r_{i,j} + \Delta r_{i,j+1}}{2}\right)^2} - 2\frac{\mu_{eff_{i,j+1}} - \mu_{eff_{i,j-1}}}{\left(\Delta r_{i,j} + \Delta r_{i,j+1}\right)^2} \\ a_{5u_{x_i,j}} &= \frac{\rho u_{x_{i,j}}}{2\Delta x} + \frac{\mu_{eff_{i-0.5,j}} + \mu_{t_{i-0.5,j}}}{\Delta x^2} \\ S_{u_{i,j}} &= \frac{2\mu_{t_{j,i}}}{\Delta x(\Delta r_{i,j} + \Delta r_{i,j+1})} (u_{r_{i+1,j+1}} - u_{r_{i-1,j+1}} - u_{r_{i+1,j-1}} + u_{r_{i-1,j-1}}) \\ &+ 2\frac{\mu_{eff_{i,j+1}} - \mu_{eff_{i,j-1}}}{\left(\Delta r_{i,j} + \Delta r_{i,j+1}\right)^2} \frac{u_{r_{i+1,j}} - u_{r_{i-1,j}}}{2\Delta x} - \frac{1}{3}\rho\frac{k_{i+1,j} - k_{i-1,j}}{\Delta x} \end{aligned} \right\} \dots (\xi.110)$$

*k-ε and energy Equations at the center of the circular duct:*

The same procedure will be done to get the following algebraic equations for the k-ε and energy equations respectively as follows:-

For k Equation:-

$$a_{1k_{i,j}} k_{i,j} = a_{2k_{i,j}} k_{i,j+1} + a_{3k_{i,j}} k_{i+1,j} + a_{4k_{i,j}} k_{i,j-1} + a_{5k_{i,j}} k_{i-1,j} + S_{k_{i,j}} \quad \dots (\xi.111)$$

Where:-

$$\left. \begin{aligned}
 a_{1k_{i,j}} &= \frac{4\mu_{t_{i,j}}}{\sigma_k \left( \frac{(\Delta r_{i,j} + \Delta r_{i,j+1})}{2} \right)^2} + \frac{\mu_{t_{i+0.5,j}} + \mu_{t_{i-0.5,j}}}{\sigma_k \Delta x^2} \\
 a_{2k_{i,j}} &= \frac{-\rho u_{r_{i,j}}}{(\Delta r_{i,j} + \Delta r_{i,j+1})} + \frac{2\mu_{t_{i,j}}}{\sigma_k \left( \frac{(\Delta r_{i,j} + \Delta r_{i,j+1})}{2} \right)^2} + 2 \frac{\mu_{t_{i,j+1}} - \mu_{t_{i,j-1}}}{\sigma_k (\Delta r_{i,j} + \Delta r_{i,j+1})^2} \\
 a_{3k_{i,j}} &= \frac{-\rho u_{x_{i,j}}}{2\Delta x} + \frac{\mu_{t_{i+0.5,j}}}{\sigma_k \Delta x^2} \\
 a_{4k_{i,j}} &= \frac{\rho u_{r_{i,j}}}{\Delta r} + \frac{2\mu_{t_{i,j}}}{\sigma_k \left( \frac{(\Delta r_{i,j} + \Delta r_{i,j+1})}{2} \right)^2} - 2 \frac{\mu_{t_{i,j+1}} - \mu_{t_{i,j-1}}}{\sigma_k (\Delta r_{i,j} + \Delta r_{i,j+1})^2} \\
 a_{5k_{i,j}} &= \frac{\rho u_{x_{i,j}}}{2\Delta x} + \frac{\mu_{t_{i-0.5,j}}}{\sigma_k \Delta x^2} \\
 s_{k_{i,j}} &= G_{i,j} - \rho \varepsilon_{i,j}
 \end{aligned} \right\} \dots (\xi.112)$$

For  $\varepsilon$  equation:-

$$a_{1\varepsilon_{i,j}} \varepsilon_{i,j} = a_{2\varepsilon_{i,j}} \varepsilon_{i,j+1} + a_{3\varepsilon_{i,j}} \varepsilon_{i+1,j} + a_{4\varepsilon_{i,j}} \varepsilon_{i,j-1} + a_{5\varepsilon_{i,j}} \varepsilon_{i-1,j} + S_{\varepsilon_{i,j}} \dots (\xi.113)$$

Where:-

$$\left. \begin{aligned}
 a_{1\varepsilon_{j,i}} &= \frac{4\mu_{t_{i,j}}}{\sigma_\varepsilon \left( \frac{(\Delta r_{i,j} + \Delta r_{i,j+1})}{2} \right)^2} + \frac{\mu_{t_{i+0.5,j}} + \mu_{t_{i-0.5,j}}}{\sigma_\varepsilon \Delta x^2} + C_{\varepsilon 2} \rho \frac{\varepsilon_{i,j}}{k_{i,j}} \\
 a_{2\varepsilon_{j,i}} &= \frac{\rho u_{r_{i,j}}}{(\Delta r_{i,j} + \Delta r_{i,j+1})} + \frac{2\mu_{t_{i,j}}}{\sigma_\varepsilon \left( \frac{(\Delta r_{i,j} + \Delta r_{i,j+1})}{2} \right)^2} + 2 \frac{\mu_{t_{i,j+1}} - \mu_{t_{i,j-1}}}{\sigma_\varepsilon (\Delta r_{i,j} + \Delta r_{i,j+1})^2} \\
 a_{3\varepsilon_{j,i}} &= \frac{-\rho u_{x_{i,j}}}{2\Delta x} + \frac{\mu_{t_{i+0.5,j}}}{\sigma_\varepsilon \Delta x^2}; \quad a_{4\varepsilon_{j,i}} = \frac{-\rho u_{r_{i,j}}}{(\Delta r_{i,j} + \Delta r_{i,j+1})} + \frac{2\mu_{t_{i,j}}}{\sigma_\varepsilon \left( \frac{(\Delta r_{i,j} + \Delta r_{i,j+1})}{2} \right)^2} - 2 \frac{\mu_{t_{i,j+1}} - \mu_{t_{i,j-1}}}{\sigma_\varepsilon (\Delta r_{i,j} + \Delta r_{i,j+1})^2} \\
 a_{5\varepsilon_{j,i}} &= \frac{\rho u_{x_{i,j}}}{2\Delta x} + \frac{\mu_{t_{i-0.5,j}}}{\sigma_\varepsilon \Delta x^2}; \quad S_{\varepsilon_{i,j}} = C_{\varepsilon 1} G_{i,j} \frac{\varepsilon_{i,j}}{k_{i,j}}
 \end{aligned} \right\} \dots (\xi.114)$$

For Energy Equation:-

$$a_{1T_{i,j}} T_{i,j} = a_{2T_{i,j}} T_{i,j+1} + a_{3T_{i,j}} T_{i+1,j} + a_{4T_{i,j}} T_{i,j-1} + a_{5T_{i,j}} T_{i-1,j} \quad \dots (\xi.110)$$

Where:-

$$\left. \begin{aligned} a_{1T_{i,j}} &= \frac{4}{\left(\frac{\Delta r_{i,j} + \Delta r_{i,j+1}}{2}\right)^2} \left( \frac{\mu_{eff_{i,j}}}{P_{reff}} \right) + \frac{1}{\Delta x^2} \left( \frac{\mu_{eff_{i+0.5,j}}}{P_{reff}} + \frac{\mu_{eff_{i-0.5,j}}}{P_{reff}} \right) \\ a_{2T_{i,j}} &= \frac{-\rho u_{r_{i,j}}}{\left(\Delta r_{i,j} + \Delta r_{i,j+1}\right)} + \frac{2 \frac{\mu_{eff_{i,j}}}{P_{reff}}}{\left(\frac{\Delta r_{i,j} + \Delta r_{i,j+1}}{2}\right)^2} + 2 \frac{\frac{\mu_{eff_{i,j+1}}}{P_{reff}} - \frac{\mu_{eff_{i,j-1}}}{P_{reff}}}{\left(\Delta r_{i,j} + \Delta r_{i,j+1}\right)^2} \\ a_{3T_{i,j}} &= \frac{-\rho u_{x_{i,j}}}{2\Delta x} + \frac{1}{\Delta x^2} \left( \frac{\mu_{eff_{i+0.5,j}}}{P_{reff}} \right) \\ a_{4T_{i,j}} &= \frac{\rho u_{r_{i,j}}}{\left(\Delta r_{i,j} + \Delta r_{i,j+1}\right)} + \frac{2 \frac{\mu_{eff_{i,j}}}{P_{reff}}}{\left(\frac{\Delta r_{i,j} + \Delta r_{i,j+1}}{2}\right)^2} - 2 \frac{\frac{\mu_{eff_{i,j+1}}}{P_{reff}} - \frac{\mu_{eff_{i,j-1}}}{P_{reff}}}{\left(\Delta r_{i,j} + \Delta r_{i,j+1}\right)^2} \\ a_{5T_{i,j}} &= \frac{\rho u_{x_{i,j}}}{2\Delta x} + \frac{1}{\Delta x^2} \left( \frac{\mu_{eff_{i-0.5,j}}}{P_{reff}} \right) \end{aligned} \right\} \dots (\xi.116)$$

### ξ.11 CALCULATION OF BOUNDARY VALUES

Temperature at the walls of the rectangular duct for constant heat flux boundary condition can be calculated from the following equation:-

$$q_w = \lambda \frac{\partial T}{\partial y} \Big|_{y=H} \quad \dots (\xi.117)$$

By using the clustered backward difference for four nodal points from equation (B-16) of appendix B, the temperature derivative at the upper wall of rectangular duct will become:-

$$\frac{\partial T}{\partial y} \Big|_{i,N} = \frac{1.619999T_{i,N} - 2.69179T_{i,N-1} + 1.4227896T_{i,N-2} - 0.3964391T_{i,N-3} + 0.0454402T_{i,N-4}}{\Delta y}$$

... (ξ.118)

By substitution of equation (4.118) into (4.117) and doing some arrangement, the following equation will result:-

$$T_{i,N} = \frac{\frac{q_w \Delta y_{i,N}}{\lambda} + 2.69179T_{i,N-1} - 1.422789T_{i,N-2} + 0.396439T_{i,N-3} - 0.045440T_{i,N-4}}{1.619999} \dots (4.119)$$

By doing the same procedure at the lower wall of rectangular duct, the result will be:-

$$T_{i,0} = \frac{\frac{-q_w \Delta y_{i,1}}{\lambda} + 2.69179T_{i,1} - 1.422789T_{i,2} + 0.396439T_{i,3} - 0.045440T_{i,4}}{1.619999} \dots (4.120)$$

If the same procedure (which was done to get equations (4.119) and (4.120) for rectangular duct) is done for circular duct, the result will be the following two equations:-

$$T_{i,N} = \frac{\frac{q_w \Delta r_{i,N}}{\lambda} + 2.69179T_{i,N-1} - 1.422789T_{i,N-2} + 0.396439T_{i,N-3} - 0.045440T_{i,N-4}}{1.619999} \dots (4.121)$$

$$T_{i,-N} = \frac{\frac{-q_w \Delta r_{i,1-N}}{\lambda} + 2.69179T_{i,1-N} - 1.422789T_{i,2-N} + 0.396439T_{i,3-N} - 0.045440T_{i,4-N}}{1.619999} \dots (4.122)$$

**4.9 CALCULATION OF MEAN VELOCITY**

Since the velocity along the cross section is changed and there is no clear definition for the free stream velocity in internal flows, it is important to use the mean velocity concept to express the velocity in such flows. The mean velocity  $u_b$  is defined as the velocity which when multiplied by the fluid density ( $\rho$ ) and the cross sectional area ( $A_c$ ) the result will be the mass flow rate ( $\dot{m}$ ) over the cross section, where:-

$$\dot{m} = \rho u_b A_c \dots (4.123)$$

In which  $\dot{m}$  may be calculated from equation (ξ.12) for rectangular duct and from equation (ξ.13) for circular duct.

The benefit of calculating mean velocity resides in its constancy and the mass flow rate constancy with respect to axial direction when an incompressible fluid flows steadily in uniform cross sectional area , where  $\dot{m}$  and  $u_b$  are independent of x-direction. Thus  $u_b$  is used to describe the internal flow and can be calculated from the following equation:-

$$u_b = \frac{\int_{A_c} \rho u dA_c}{\int_{A_c} \rho dA_c} \quad \dots (\xi.124)$$

For rectangular duct:-

$$\dots (\xi.125) \quad u_b = \frac{\int_0^H u dy}{\int_0^H dy}$$

Mean velocity for rectangular duct can be calculated from equation (ξ.125), by taking the integration at each location of the axial direction from knowing the velocity profile at this location as follows:-

$$u_{bi} = \frac{\sum_{j=1}^{N-1} \sum_{i=0}^M u_{i,j} \frac{(\Delta y_{i,j} + \Delta y_{i,j+1})}{2}}{\sum_{j=1}^{N-1} \sum_{i=0}^M \Delta y_{i,j}} \quad \dots (\xi.126)$$

For j=1:

$$u_{bi} = \frac{\frac{1}{4} u_{i,1} \frac{\Delta y_{i,1}}{2} + u_{i,1} \frac{(\Delta y_{i,1} + \Delta y_{i,2})}{2}}{\sum_{j=1}^{N-1} \sum_{i=0}^M \Delta y_{i,j}} \quad \dots (\xi.126-A)$$

For  $j=N-1$ :

$$u_{bi} = \frac{\frac{1}{4} u_{i,N-1} \frac{\Delta y_{i,N}}{2} + u_{i,N-1} \frac{(\Delta y_{i,N-1} + \Delta y_{i,N})}{2}}{\sum_{j=1}^{N-1} \Delta y_{i,j}} \quad \dots (\xi.126-B)$$

For circular duct:-

$$u_b = \frac{\int_0^R u_x r dr}{\int_0^R r dr} \quad \dots (\xi.127)$$

In the numerical form equation (ξ.127) will become:-

$$u_{b_i} = \frac{\sum_{j=1}^{N-1} u_{x_{i,j}} r_{i,j} \Delta r_{i,j}}{\sum_{j=1}^{N-1} r_{i,j} dr_{i,j}} \quad \dots (\xi.128)$$

**ξ.10. CALCULATION OF BULK TEMPERATURE**

The absence of the constant free stream temperature implies the use of the bulk temperature concept. The bulk temperature in any cross section can be defined in terms of the thermal energy transport and the bulk motion of the fluid when it passes in this section. It can be calculated as follows:-

$$T_b = \frac{\int_{A_c} \rho C_p u T dA_c}{\int_{A_c} \rho C_p u dA_c} = \frac{\int_{A_c} u T dA_c}{\int_{A_c} u dA_c} \quad \dots (\xi.129)$$

For rectangular duct:-

$$T_b = \frac{\int_0^H u T dy}{\int_0^H u dy} \quad \dots (\xi.130)$$

In the numerical form equation (٤.١٣٠) will become:-

$$T_{b_i} = \frac{\sum_{j=1}^{N-1} \sum_{i=0}^M u_{i,j} T_{i,j} \Delta y_{i,j}}{\sum_{j=1}^{N-1} \sum_{i=0}^M u_{i,j} \Delta y_{i,j}} \quad \dots (٤.١٣١)$$

For j= ١:

$$T_{b_i} = \frac{\frac{1}{4} u_{i,1} T_{i,1} \frac{\Delta y_{i,1}}{2} + u_{i,1} T_{i,1} \frac{(\Delta y_{i,1} + \Delta y_{i,2})}{2}}{\frac{1}{4} u_{i,1} \frac{\Delta y_{i,1}}{2} + u_{i,1} \frac{(\Delta y_{i,1} + \Delta y_{i,2})}{2}} \quad \dots (٤.١٣١-A)$$

For j=N-١:

$$T_{b_i} = \frac{\frac{1}{4} u_{i,N-1} T_{i,N-1} \frac{\Delta y_{i,N}}{2} + u_{i,N-1} T_{i,N-1} \frac{(\Delta y_{i,N-1} + \Delta y_{i,N})}{2}}{\frac{1}{4} u_{i,N-1} \frac{\Delta y_{i,N}}{2} + u_{i,N-1} \frac{(\Delta y_{i,N-1} + \Delta y_{i,N})}{2}} \quad \dots (٤.١٣١-B)$$

For circular duct:-

$$T_b = \frac{\int_0^R u_x T r dr}{\int_0^R u_x r dr} \quad \dots (٤.١٣٢)$$

In the numerical form:-

$$T_{b_i} = \frac{\sum_{j=1-N}^{N-1} \sum_{i=0}^M u_{i,j} r_{i,j} T_{i,j} \frac{(\Delta r_{i,j} + \Delta r_{i,j+1})}{2}}{\sum_{j=1-N}^{N-1} \sum_{i=0}^M u_{i,j} r_{i,j} \frac{(\Delta r_{i,j} + \Delta r_{i,j+1})}{2}} \quad \dots (٤.١٣٣)$$

For j= ١-N:

$$T_{b_i} = \frac{\frac{1}{4} u_{i,1-N} T_{i,1-N} \frac{\Delta r_{i,1-N}}{2} + u_{i,1-N} T_{i,1-N} \frac{(\Delta r_{i,1-N} + \Delta r_{i,2-N})}{2}}{\frac{1}{4} u_{i,1-N} r_{i,1-N} \frac{\Delta r_{i,1-N}}{2} + u_{i,1-N} r_{i,1-N} \frac{(\Delta r_{i,1-N} + \Delta r_{i,2-N})}{2}} \quad \dots (٤.١٣٣-A)$$

For  $j=N-1$ :

$$T_{bi} = \frac{\frac{1}{4} u_{i,N-1} T_{i,N-1} \frac{\Delta r_{i,N}}{2} + u_{i,N-1} T_{i,N-1} \frac{(\Delta r_{i,N-1} + \Delta r_{i,N})}{2}}{\frac{1}{4} u_{i,N-1} r_{i,N-1} \frac{\Delta r_{i,N}}{2} + u_{i,N-1} r_{i,N-1} \frac{(\Delta r_{i,N-1} + \Delta r_{i,N})}{2}} \quad \dots (\xi.133-B)$$

Unlike the bulk velocity, the bulk temperature changes with the axial direction because of the presence of convection from and to the fluid along the flow. Hence, for calculating bulk temperature for rectangular and circular duct, equations (ξ.131) and (ξ.133) respectively can be used.

### ξ.11 CALCULATION OF REYNOLDS STRESSES

Reynolds stress for rectangular duct from equation (A.50) in the appendix A can be calculated by using the central Difference as follows:-

$$-\rho \overline{u'v'} = -\mu_{t,i,j} \left( \frac{2(u_{i,j+1} - u_{i,j-1})}{(\Delta y_{i,j} + \Delta y_{i,j+1})} + \frac{(v_{i+1,j} - v_{i-1,j})}{2\Delta x} \right) \quad \dots (\xi.134)$$

For circular duct:-

$$-\rho \overline{u'_x u'_r} = -\mu_{t,i,j} \left( \frac{2(u_{xi,j+1} - u_{xi,j-1})}{(\Delta y_{i,j} + \Delta y_{i,j+1})} + \frac{(u_{ri+1,j} - u_{ri-1,j})}{2\Delta x} \right) \quad \dots (\xi.135)$$

### ξ.12 CALCULATION OF TURBULENT HEAT FLUX

By using the central Difference for turbulent heat flux for rectangular duct in the axial and radial direction of (A.50) in the appendix A the result will be:-

$$-\rho \overline{u'T'} = \frac{-\mu_{t,i,j}}{p_{r_i}} \left( \frac{(T_{i+1,j} - T_{i-1,j})}{2\Delta x} \right) \quad \dots (\xi.136)$$

$$-\rho \overline{v'T'} = \frac{-2\mu_{t,i,j}}{p_{r_i}} \left( \frac{(T_{i,j+1} - T_{i,j-1})}{(\Delta y_{i,j} + \Delta y_{i,j+1})} \right) \quad \dots (\xi.137)$$

For circular duct:

$$-\overline{\rho u'_x T'} = \frac{-\mu_{t,i,j}}{\rho r_i} \left( \frac{(T_{i+1,j} - T_{i-1,j})}{2\Delta x} \right) \quad \dots (4.138)$$

$$-\overline{\rho u'_r T'} = \frac{-2\mu_{t,i,j}}{\rho r_i} \left( \frac{(T_{i,j+1} - T_{i,j-1})}{(\Delta r_{i,j} + \Delta r_{i,j+1})} \right) \quad \dots (4.139)$$

### 4.13 CALCULATION OF COEFFICIENT OF FRICTION

The local coefficient of friction can be calculated from the following equation:-

$$C_f = \frac{\tau_w}{\frac{1}{2}\rho u_b^2} \quad \dots (4.140)$$

Where the shear stress,  $\tau_w$  can be calculated from the wall function in terms of kinetic energy of turbulence ( $\nu^*$ ) as follows:-

$$\tau_w = \frac{\rho k C_\mu^{1/4} u_p k_p^{1/2}}{\ln(Ey_{plus})} \quad \dots (4.141)$$

The average coefficient of friction can be calculated by taking the integration for the local coefficient of friction of (4.141) along the length of the duct as follows:-

$$\overline{C_f} = \frac{1}{L} \int_0^L C_f dx \quad \dots (4.142)$$

### 4.14 CALCULATION OF NUSSULT NUMBER

The local Nussult number can be defined as:-

$$Nu = \frac{hD_h}{\lambda} \quad \dots (4.143)$$

For rectangular duct:

$$h(T_w - T_b) = \lambda \left. \frac{\partial T}{\partial y} \right|_{y=H}$$

Or

$$h = \frac{\lambda \left. \frac{\partial T}{\partial y} \right|_{y=H}}{(T_w - T_b)} \quad \dots (\xi.1 \xi \xi)$$

Substitute  $(\xi.1 \xi \xi)$  in  $(\xi.1 \xi \text{v})$  to get:

$$Nu = \frac{\left. \frac{\partial T}{\partial y} \right|_{y=H} D_h}{(T_w - T_b)} \quad \dots (\xi.1 \xi \circ)$$

If the same procedure is done for circular duct the result will be:-

$$Nu = \frac{\left. \frac{\partial T}{\partial r} \right|_{r=R} D}{(T_w - T_b)} \quad \dots (\xi.1 \xi \text{v})$$

If constant heat flux boundary condition is substituted in  $(\xi.1 \xi \circ)$  and  $(\xi.1 \xi \text{v})$  respectively, they will become:-

$$Nu = \frac{q_o D_h}{\lambda(T_w - T_b)} \quad \dots (\xi.1 \xi \text{v})$$

$$Nu = \frac{q_o D}{\lambda(T_w - T_b)} \quad \dots (\xi.1 \xi \wedge)$$

Where,  $T_w$  in equations  $(\xi.1 \xi \text{v})$  and  $(\xi.1 \xi \wedge)$  should be expressed in the numerical form (like  $T_{i,N}$ ) of the calculated wall temperature which is not constant.

But for constant wall temperature condition, equations  $(\xi.1 \xi \text{v})$  and  $(\xi.1 \xi \wedge)$  will be:-

$$Nu = \frac{D_h}{(T_w - T_b)} \left. \frac{\partial T}{\partial y} \right|_{y=H} \quad \dots (\xi.1 \xi \text{v})$$

$$Nu = \frac{D}{(T_w - T_b)} \left. \frac{\partial T}{\partial r} \right|_{r=R} \quad \dots (\xi.1 \circ \circ)$$

By using the backward difference for four nodal points from equation (B-16) in appendix B to  $(\xi.1 \xi \text{v})$  and to  $(\xi.1 \circ \circ)$  respectively to get:-

$$Nu = \frac{D_h}{(T_w - T_b)} \frac{1.619999T_{i,N} - 2.69179T_{i,N-1} + 1.4227896T_{i,N-2} - 0.3964391T_{N-3} + 0.0454402T_{i,N-4}}{\Delta y_{i,N}} \dots (\xi.101)$$

$$Nu = \frac{D}{(T_w - T_b)} \frac{1.619999T_{i,N} - 2.69179T_{i,N-1} + 1.4227896T_{i,N-2} - 0.3964391T_{N-3} + 0.0454402T_{i,N-4}}{\Delta r_{i,N}} \dots$$

(ξ.102)

The average Nussult number can be calculated by doing the integration for local Nussult number along the duct length as follows:-

$$\overline{Nu} = \frac{1}{L} \int_0^L Nu dx \dots (\xi.103)$$

Where, the integration of (ξ.103) will be done by using the numerical integration by using Simpson’s Rule.

**ξ.10 STEPS OF NUMERICAL SOLUTION**

The numerical solution steps for all equations of this chapter can be summarized as follows:-

1. Starting from initial guessed values for all dependent variables.
2. Calculation of momentum equation coefficients by using equation (ξ.8) for rectangular duct and (ξ.29) for circular duct.
3. Calculation of pressure difference in the axial direction by using equation (ξ.18) for rectangular duct and (ξ.30) for circular duct. This equation of pressure difference was solved by using the point by point Gauss –Seidel Method.
4. Calculation of the axial velocity component for all interior nodes by using equation (ξ.10) for rectangular duct and (ξ.31) for circular duct. The updating of the coefficients of (ξ.8) for rectangular duct and (ξ.29) for circular duct for the raw of the nodal points which are parallel to wall should be accomplished by using the law of the wall. The Under-Relaxation Method was used for solving (ξ.10) and (ξ.31).

٥. Calculation of the radial velocity component for all interior nodes by using equation (٤.٣٩) for rectangular duct and (٤.٤٢) for circular duct. The Nodal Gauss –Seidel Method was used for doing this calculation.
٦. Computation of the coefficients of the kinetic energy of turbulence equation by using equation (٤.٥٠) for rectangular duct and (٤.٧١) for circular duct for all interior nodal points except for the points neighboring to the wall where its values should be calculated by using the wall function. Solving of k-equation (equation (٤.٥٣) for rectangular duct and (٤.٧٢) for circular duct) was done by using TDMA to calculate the values of k for all interior nodes.
٧. Calculation of the coefficients of the dissipation rate of kinetic energy of turbulence equation by using equation (٤.٦١) for rectangular duct and (٤.٨٠) for circular duct for all interior nodal points except for the points neighboring to the wall where its values should be calculated by using the wall function. Solving of  $\varepsilon$ -equation (equation (٤.٦٣) for rectangular duct and (٤.٨١) for circular duct) was done by using TDMA to calculate the values of  $\varepsilon$  for all interior nodes.
٨. Calculation of turbulent viscosity,  $\mu_t$  and mean effective viscosity,  $\mu_{eff}$
٩. Calculation of the coefficients of the energy equation by using equation (٤.٨٧) for rectangular duct and (٤.٩٦) for circular duct for all interior nodal points except for the points neighboring to the wall where its values should be calculated by using the wall function of T. Solving of T-equation (equation (٤.٩٠) for rectangular duct and (٤.٩٨) for circular duct) was done by using TDMA to calculate the values of T for all interior nodes.
١٠. Calculation of temperatures at walls for rectangular and circular duct with CHF boundary condition from equations (٤.١١٩), (٤.١٢٠), (٤.١٢١), and (٤.١٢٢) respectively.
١١. Update the coefficients of equations (٤.٨), (٤.٢٩), (٤.٥٠), (٤.٧١), (٤.٦١), (٤.٨٠), (٤.٨٧), and (٤.٩٦).

12. The steps from 11 to 12 should be repeated until reaching the required convergence. To ensure the reaching of the required values for all dependent variables, the numerical iterative method was used with the following criteria:-

$$\text{Error} = (\text{Error} + \text{summation of errors for all dependent variables}) \leq 10^{-4}$$

Where error for each dependent variable,  $\phi$  is calculated from the following relation which is similar to that in [11]:-

$$\text{Error } \phi = \frac{\sum_{i=0}^N \sum_{j=0}^M |\phi_{i,j}^k - \phi_{i,j}^{k-1}|}{\sum_{i=0}^N \sum_{j=0}^M |\phi_{i,j}^{k-1}|} \quad \text{where k is the present iteration.}$$

13. Calculation of the axial mean velocity from (2.126) for rectangular duct, and for circular duct from (2.128).

14. Calculation of the bulk temperature for rectangular duct and circular duct from (2.131), and (2.133) respectively.

15. Calculation of the local Nussult number for CHF boundary condition by using (2.147) for rectangular duct and (2.148) for circular duct, and the local Nussult number for CWT boundary condition by using (2.151) for rectangular duct and (2.152) for circular duct.

16. Calculation of the average Nussult number by using (2.153) for rectangular and circular duct.

17. Calculation of the local coefficient of friction by using (2.149) for rectangular and circular duct and the average coefficient of friction for each one of the two ducts is calculated from (2.154).

18. Calculation of the Reynolds stress from (2.134) for rectangular duct and (2.136) for circular duct.

۱۹. The turbulent heat fluxes are calculated from (۴.۱۳۶) and (۴.۱۳۷) for rectangular duct, and from (۴.۱۳۸) and (۴.۱۳۹) for circular duct.

#### ۴.۱۶ COMPUTER PROGRAM

Two FORTRAN ۹۰ language programs were built to execute all the numerical steps which are described in the previous article, one for the rectangular duct, and the other for circular. Each one is a general program consists of ۹ subroutines for solving the flow in the duct and heat transfer with CWT and CHF boundary condition. The main program for each duct includes the input data, the subroutines calling instructions, and the output data. The subroutines for each duct are:-

۱. Subroutine for grid generation which includes clustering to the radial direction in each duct.
۲. Subroutine for calculating the axial pressure difference, [equation (۴.۱۴) for rectangular duct and (۴.۳۰) for circular duct] and the axial and radial velocity components [two equations (۴.۱۰) and (۴.۳۹) respectively for rectangular duct and two equations (۴.۳۱) and (۴.۴۲) respectively for circular duct].
۳. Subroutine for calculating the kinetic energy,  $k$  [equation (۴.۰۳) for rectangular duct and (۴.۷۲) for circular duct].
۴. Subroutine for calculating the dissipation rate of kinetic energy,  $\varepsilon$  [equation (۴.۶۳) for rectangular duct and (۴.۸۱) for circular duct].
۵. Subroutine for calculating temperature,  $T$  [equation (۴.۹۰) for rectangular duct and (۴.۹۸) for circular duct].
۶. Subroutine for calculating the axial mean, [equation (۴.۱۲۶) for rectangular duct and (۴.۱۲۸) for circular duct].
۷. Subroutine for calculating bulk temperature, [equation (۴.۱۳۱) for rectangular duct and (۴.۱۳۳) for circular duct].

٨. Subroutine for calculating the local Nussult number and average Nussult number [equation (٤.١٤٧) for rectangular duct and (٤.١٤٨) for circular duct for CHF or equation (٤.١٥١) for rectangular duct and (٤.١٥٢) for circular duct for CWT and average Nussult number from (٤.١٥٣) for the two ducts].

٩. Subroutine for calculating TDMA.

The Reynolds stress, the turbulent heat fluxes, and local and average coefficient of friction are also calculated. At the end of the main program the printing of results is accomplished.

The two programs can be used for the calculations of the two dimensional laminar and turbulent flow with heat transfer for arbitrary cross sections by doing the adequate modifications. Where, the rectangular duct program is valid for Cartesian coordinates and the circular duct program is valid for Polar coordinates.

The important steps of execution for each program were described in appendix C which represents the flow chart for each program.

#### ٤.١٧.١ INPUT DATA

The input constants which are required for rectangular and circular duct programs execution include:-

١. Geometrical shape dimensions which comprise the length and the radius (or height and width) of the duct.
٢. Grid dimensions which involve the number of nodal grid points in the axial and radial direction.
٣. The fluid properties and the  $k - \varepsilon$  model constants.
٤. The maximum value of error which is  $10^{-\varepsilon}$ .
٥. The boundary conditions.

#### ٤.١٧.٢ OUTPUT DATA

The program of each duct prints the result of calculations for the last step of the numerical iteration which embraces:-

١. The values of the components of velocities, kinetic energy of turbulence, dissipation rate of kinetic energy of turbulence, temperatures, turbulent viscosity, and mean eddy viscosity for each nodal point with the position of the nodal point ((x,y) or (x,r)) in the dimensionless or dimensional form according to the need.
٢. The values of the mean velocity and bulk temperature at each location in the axial direction.
٣. The values of the local Nussult number and local coefficient of friction at each location in the axial direction.
٤. The values of the average Nussult number and average coefficient of friction.
٥. The values of the dimensionless distance  $y_{plus}$  at each location in the axial direction.
٦. The components of the Reynolds stress and turbulent heat flux for all nodal points with position of each nodal point.

#### ٤.١٧.٣ SPECIFICATIONS OF THE COMPUTER PROGRAM

FORTRAN ٩٥ language was used for formation of the present study programs. The execution was done on (Pentium ٤) computer by using the compiler (Microsoft Developer Studio) or (FORTRAN Power Station ٤.٠) which is an operation program doing under windows with high precise performance. The time required for execution was about (٧ minutes) for each duct.

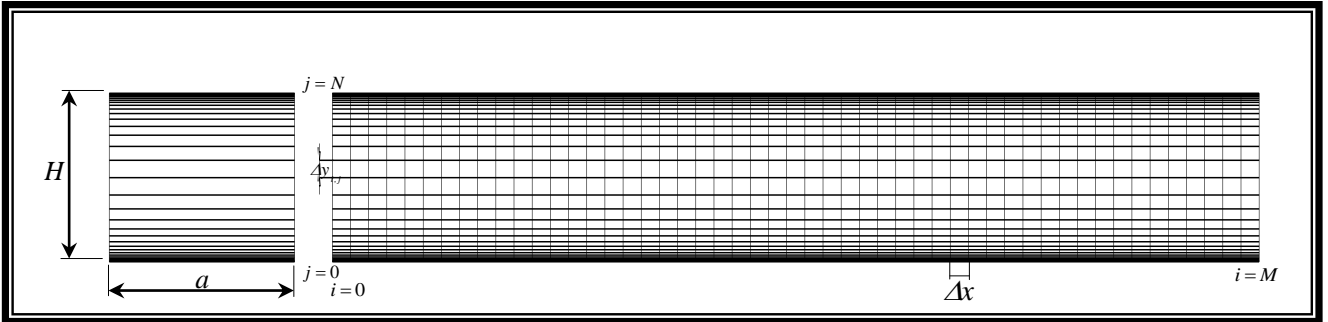


FIGURE (4.1): Nodal Grid for Rectangular

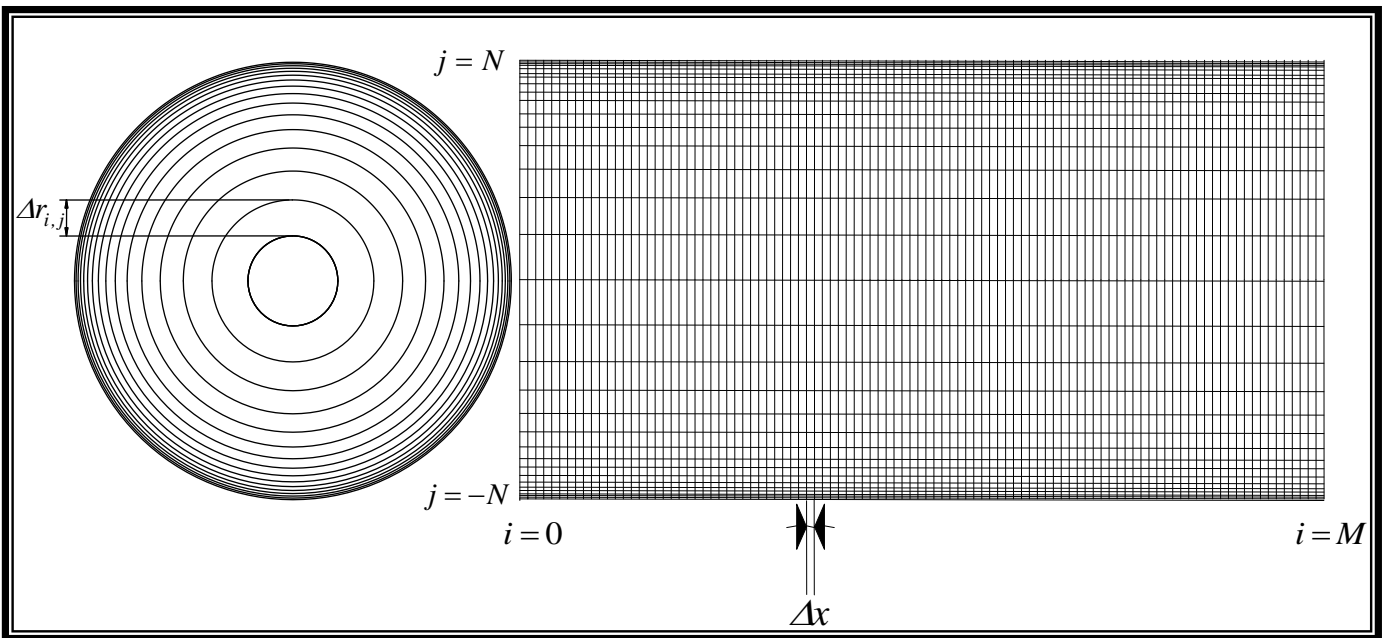


FIGURE (4.2): Nodal Grid for Circular Duct

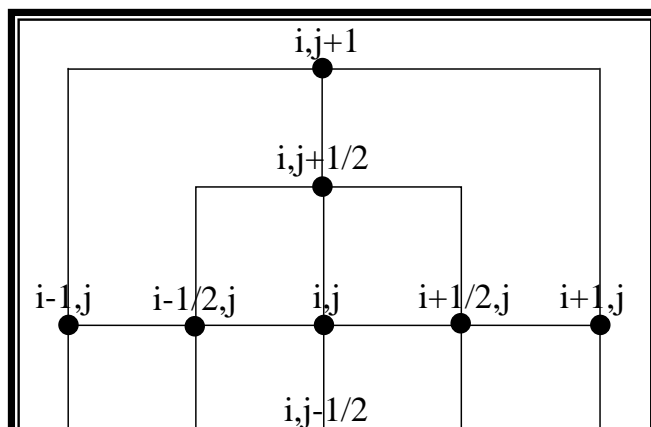


FIGURE (4.3): Nodal Points

## RESULTS AND DISCUSSION

### 5.1 INTRODUCTION

The numerical results will be reviewed in this chapter for the two geometries which were studied in the preceding chapters. The rectangular duct dimensions are ( $H=0.1\text{ m}$ ), ( $a=0.166\text{ m}$ ) with length ( $L=3\text{ Dh}$ ). The circular duct dimensions are ( $D=0.2\text{ m}$ ) and ( $L=3\text{ D}$ ). The Prandtl number is ( $0.707$ ) for all results but two values were selected for Reynolds number ( $Re=1000$ ) and ( $Re=12000$ ) for two cases of heating, CHF and CWT for rectangular duct and CWT for circular duct. The results reliability will be verified for thermal behavior of fluid flowing through each duct for CWT case by comparing results of the present work with previous works. No results are available for flow behavior of the two ducts for comparison.

### 5.2 NUMERICAL SOLUTION LIMITATIONS

The results in this chapter were obtained from the numerical solution (which was explained in chapter four) by using the computer program which was prepared for this purpose. The transverse nodal spacing varied across the radial direction of each duct but was constant across the axial direction. The nodal spacing was much denser near the walls than at midpoints to permit acceptable definition of the boundary layer thickness. ( $N*M$ ) represents the number of nodal points for rectangular duct but  $((3*N+1)*M)$  represents the number of nodal points for circular duct. At first, the rectangular duct problem was solved with ( $M=100$ ,  $N=0$ ) but the circular was solved with ( $M=120$ ,  $N=3$ ). When the number of nodes in the radial

direction increases, the required total percent of error will be obtained with less number of iterations, but if the number of nodes decreases, more number of iterations will be required to reach the same percent of error. The compromise is to choose the number of iterations which ensure a reasonable definition of boundary layer especially near the walls and ensure good results for thermal behavior of fluid flowing through each duct. Finally, the rectangular duct problem was solved with  $(M=20, N=20)$  but the circular was solved with  $(M=20, N=25)$ .

### 5.3 DEVELOPMENT OF VELOCITY PROFILES

Figures (5.1), (5.2), (5.3), (5.4), (5.5), (5.6), (5.7) and (5.8) show the velocity vectors which manifest stages of developing of the hydrodynamic boundary layer for Reynolds numbers  $(Re=1000)$  and  $(Re=12000)$  at different sections of rectangular and circular duct respectively. After improving the solution for each duct by reducing the number of nodal grid points, the stages of developing of the hydrodynamic boundary layer for the two ducts were described in figures (5.9-a), (5.9-b), (5.9-c) and (5.9-d).

All figures from (5.1) to (5.9) show that the values of velocity near walls are high and this may belong to the used wall function and to the small size of spacing between the clustered nodal points.

The effects of the viscosity forces are very important when the fluid is in contact with the surface where the boundary layer grows with increasing the distance in the axial direction. The velocity vectors (which were shown for each duct) elucidate that the shape of the boundary layer will be fixed after a certain distance from the entrance, which is the so-called "The Hydrodynamic Entry length". There is a noticeable deformation in some vectors of velocity near the entrance. This deformation may be attributed to

the small value of the selected velocity at entrance of each duct, which may be not adequate to make the flow turbulent with prescribed conditions. For example ( $U_{in} = 0.01$  m/sec) for circular duct with ( $Re = 1000$ ) where this value of velocity is very small to cause flow turbulence, so there should be a disturbances in the entrance to cause turbulence. Hence the mathematical model was compelled to assume that there are disturbances in the form of deformation in the near centerline velocity vectors at entrance during the treatment of the solution.

Figures (0.10-a), (0.10-b), (0.11-a) and (0.11-b) represent the behavior of the velocity profiles for Reynolds numbers ( $Re = 1000$ ) and ( $Re = 12000$ ) at different selected sections of rectangular and circular duct respectively. It is noted that the hydrodynamic entrance length increases with increasing of Reynolds number and the flatness of velocity profiles for circular duct is clearer than that of rectangular.

#### 0.4 DEVELOPMENT OF KINETIC ENERGY OF TURBULENCE

Figures (0.12-a), (0.12-b), (0.13-a) and (0.13-b) show the development of dimensionless kinetic energy of turbulence ( $\frac{1}{2}k/u_b^2$ ) of rectangular and circular duct for Reynolds numbers ( $Re = 1000$ ) and ( $Re = 12000$ ) respectively. It is clear from the two figures that the maximum values of kinetic energy of turbulence are near the walls and decrease toward the central region for each duct. This behavior of turbulent kinetic energy is attributed to the decrease of axial velocity near the walls. There is another observation from the two figures that the decrease of turbulent kinetic energy occurs with increasing the value of Reynolds number because of the depression of axial velocity profile with increasing Reynolds number value.

### 5.5 AXIAL REYNOLDS STRESS

The axial Reynolds stress developing stages for Reynolds numbers ( $Re=10000$ ) and ( $Re=120000$ ) of rectangular and circular duct at five selected sections respectively are shown in figures (5.14-a), (5.14-b), (5.15-a) and (5.15-b). The two figures show that the axial Reynolds stress is equal zero at the maximum value of velocity and reaches the maximum and minimum values near the upper and lower walls respectively. The axial Reynolds stress values range lies between  $-0.7$  and  $0.7$ .

### 5.6 COEFFICIENT OF FRICTION

Figures (5.16-a), (5.16-b), (5.17-a) and (5.17-b) show the axial development of local coefficient of friction for Reynolds numbers ( $Re=10000$ ) and ( $Re=120000$ ) of rectangular and circular duct respectively. From the two figures it is observed that the coefficient of friction follows the same behavior for the two ducts. Where its levels decrease with increasing the Reynolds number due to two causes: the first is decreasing the kinetic energy of turbulence which enters in calculation of shear stress (which is calculated from wall function) and the second is decreasing the boundary layer thickness with increasing Reynolds number. The length at which the flow becomes fully developed increases with increasing Reynolds number.

### 5.7 AVERAGE COEFFICIENT OF FRICTION

The effect of Reynolds number upon the average coefficient of friction for circular and rectangular duct is shown in the two figures (5.18-a) and (5.18-b). With increasing Reynolds number; the average coefficient of friction will be decreased for the same reasons mentioned in the previous article for coefficient of friction.

### 5.8 TEMPERATURE DISTRIBUTION

Figures (5.19-a), (5.19-b), (5.20-a) and (5.20-b) show the isothermal contour maps of temperature in rectangular and circular duct exposed to constant wall temperature ( $T_w = 100^\circ\text{C}$ ) for Reynolds numbers ( $Re = 6000$ ) and ( $Re = 12000$ ) respectively. Figure (5.19-a) shows that the temperature increases in the axial and lateral direction until reaching a constant value at a certain length from entrance “Thermal Entry Length”. It is observed from this figure that the thermal entry length is very small, i.e. the developing of thermal boundary layer is so fast because the very high heat transfer coefficients which belongs to the very small height (H) and the other reason is the using of wall function with small size of spacing between the clustered nodal points which leads to very high velocities near walls. Because of the symmetric boundary conditions and geometry for each duct, the temperature contour behaves as parabola at entrance. The rest of figures behave the same as figure (5.19-a).

Figures (5.21-a), (5.21-b) show the isothermal contour maps of temperature in rectangular Duct with walls exposed to constant heat flux ( $q_w = 480.3476 \text{ W/m}^2$ ) for Reynolds numbers ( $Re = 6000$ ) and ( $Re = 12000$ ) respectively. The behavior of temperature in the two figures is the same as that of constant wall temperature case. The results of the CHF case for circular duct were not satisfactory, because the temperature distribution is not symmetric; hence it was not presented in this chapter.

### 5.9 OVERALL HEATING

Figures (5.22-a) and (5.22-b) show the axial distribution of overall heating (axial distribution of bulk temperature of fluid flowing through duct) for rectangular and circular duct respectively with Reynolds numbers

( $Re=6000$ ) and ( $Re=12000$ ). Figure (5.22-a) for  $Re=12000$  shows that the bulk temperature increases linearly in the developing region until reaching the fully developed region at  $x/Dh \approx 1.5$ . In the fully developed region, the bulk temperature increases slightly until reaching  $x/Dh \approx 1.7$  to reach finally a constant value (zero slope of bulk temperature). The zero slope of bulk temperature means that there is no heat transfer ( $\Delta T \approx 0$ ) because of reaching the fluid temperature to a value close to wall temperature. The same behavior of figure (5.22-a) is noted for figure (5.22-b).

### 5.1. TURBULENT HEAT FLUX

The lateral distribution of turbulent heat flux for rectangular and circular duct for CWT case with Reynolds numbers ( $Re=6000$ ) and ( $Re=12000$ ) at different sections respectively is shown in figures (5.23-a), (5.23-b), (5.24-a), and (5.24-b). The lateral turbulent heat flux for each of these figures starts at maximum value near the upper wall (The top of circular duct) and then falls to minimum value in a sinusoidal behavior at half section of each duct, and then it increases to maximum value near the lower wall (The bottom of circular duct). Note that the maximum value occurs near the heated walls, and decreases toward the central region of the duct.

Figures (5.25-a), (5.25-b) show the radial distribution of turbulent heat flux for rectangular duct for CHF case with Reynolds numbers ( $Re=6000$ ) and ( $Re=12000$ ) at different sections. The same behavior of CWT case is noted for CHF case.

### 5.11 NUSSULT NUMBER

Figures (5.26-a) and (5.26-b) show the axial development of local Nussult number of circular and rectangular duct with Reynolds numbers ( $Re=6000$ ) and ( $Re=12000$ ) for CWT case respectively. Figure (5.27) shows the axial development of local Nussult number of rectangular duct with Reynolds numbers ( $Re=6000$ ) and ( $Re=12000$ ) for CHF case. In these figures, Nussult number has the maximum value at the start of entrance region of each duct and then decreases gradually until close to thermal fully developed region. The boundary layer thickness is zero at the start of entrance region; hence there is no resistance against heat transfer which leads to raise the heat transfer coefficient value to maximum. So the heat transfer coefficient decreases when the boundary layer begins the process of developing until reaching a constant value. The length at which the thermal boundary layer is fully developed increases with increasing Reynolds Number. Figure (5.26-a) for  $Re=12000$ , show that the thermal boundary layer becomes fully developed at  $x/Dh \approx 1.5$  and this value represents very small value with respect to  $x/Dh=30$ . This very small value of thermal entrance length is attributed to the very high heat transfer coefficients which belong to very high velocities near walls. These high velocities may result from the using of wall function with small size of spacing between the clustered nodal points. Another reason of getting very small value of thermal entrance length is the very small geometry of the duct which also permits very high heat transfer coefficients or very high Nussult numbers. The same behavior is observed for the other figures with note that; some of the values of the local Nussult Numbers close to zero after the thermal entrance length and this because of reaching the fluid to temperature(s) closed to that (or those) of wall , i.e. there is no heat transfer.

## 5.12 VERIFICATION OF RESULTS

The thermal results were verified according to the following:-

### 1. Constant Wall Temperature Case:

The solution of CWT problem for each duct is checked by using the following criteria:-

There is a suitable correlation for Nussult number of turbulent thermal entry region as indicated in reference [30], expressed by the following mathematical expression:-

$$Nu = 0.036 Re^{0.8} Pr^{1/3} \left( \frac{D}{L} \right)^{0.055} \quad \text{for } 10 < \frac{L}{D} < 400$$

This correlation is valid for circular and noncircular ducts. For present work, when  $L=30D$ ,  $Pr=0.707$  and  $Re=6000$  are substituted in the above correlation, the value of Nussult number will be  $Nu=170.2940$ , and for Reynolds number  $Re=12000$ , Nussult number will become  $Nu=300.12$ . The results obtained from numerical solution for Nussult number at  $L=30D$  are  $Nu=170.6328$  with  $Re=6000$  and  $Nu=300.1189$  with  $Re=12000$ .

By comparing the Nussult number values obtained from the numerical solution of the present work with that calculated from the above given correlation, it is found that there is very good agreement between the two results.

### 2. Constant heat flux Case:

There is no criterion to check the CHF problem for rectangular duct. Hence it was solved by:

1. Taking the temperature distribution obtained from CWT solution as guessed values.

٢. Using the average  $q_w$  which is calculated from CWT solution in CHF solution. The average  $q_w$  is calculated from CWT results according to the following relations:-

$$q_w = \frac{q_{w1} + q_{w2} + q_{w3} + \dots + q_{wi}}{i}$$

Where:  $i$  is the number of selected sections to calculate  $q_w$ .

$q_{wi}$  is calculated as follows:

$$\text{For Rectangular duct: } q_{wi} = k \left. \frac{\partial T}{\partial y} \right|_N = k \frac{T_{i,N} - T_{i,N-1}}{\Delta y_{i,N}}$$

The results of CHF were acceptable because the temperature gradient is reasonable and the temperature distribution close to CWT temperature distribution as addition to good Nussult number results, where the trend of local Nussult number is similar and higher than that of CWT and this agrees with the physical picture of the problem.

## **CONCLUSIONS AND RECOMMENDATIONS**

### **6.1 CONCLUSIONS**

From the results of the numerical solution of the present work for rectangular with CWT and CHF boundary conditions and with CWT boundary conditions of circular duct, the following conclusions are deduced:-

1. The effect of the fluid flow features on the heat transfer behavior appears clearly in calculating bulk temperature, where the bulk temperature increases linearly in the developing and the fully developed region of thermal boundary layer because of the very high velocities near walls. In the fully developed region, the bulk temperature increases slightly until its slope become zero. The zero slope of bulk temperature means that there is no heat transfer ( $\Delta T \approx 0$ ) because of reaching the fluid temperature to a value close to wall temperature.
2. Decreasing of local coefficient of friction with increasing Reynolds stress because of decreasing the kinetic energy of turbulence which enters in calculation of shear stress and decreasing the boundary layer thickness with increasing Reynolds number. The steep variations of local coefficient of friction may belong to the clustering of the nodal points with very small size of spacing especially near walls.

- ϣ. The level of kinetic energy of turbulence ( $\gamma k/u_b^\gamma$ ) decreases away from the walls but the axial Reynolds stress ( $2(u'v')/\rho u_b^2$ ) decreases away from the near walls.
- ξ. Turbulent heat flux has the maximum values near walls and decreases toward the core of the duct until reaching minimum values near half section of the duct in the developing region.
- ο. Thermal Entry Length lies between,  $x/D$  (1.4-1.6) for the two ducts which means that the developing of thermal boundary layer is so fast because the very high heat transfer coefficients which result from very high velocities near walls and the very small selected dimensions of each duct. The very high velocities near walls may result from the using of wall function with very small size of spacing between the clustered nodal points especially near walls.

### 6.2 SUGGESTION FOR FUTURE WORK

- 1. Performing a three-dimensional study for turbulent flow and heat transfer at the entrance region of triangular duct by using Finite Element Method or Boundary Element with  $k - \varepsilon$  model.
- ϣ. Performing an experimental study by using the hot wire measure for studying developing turbulent flow for triangular duct.
- ϣ. Performing a three-dimensional study for turbulent flow and heat transfer at the entrance region of square duct by using Finite Element Method with  $k - \varepsilon$  model.
- ξ. Performing an experimental study by using the hot wire measure for studying developing turbulent flow for square duct.

- . Performing a three-dimensional study for studying developing turbulent flow over an object through square duct by using Finite Element Method with  $k - \varepsilon$  model.

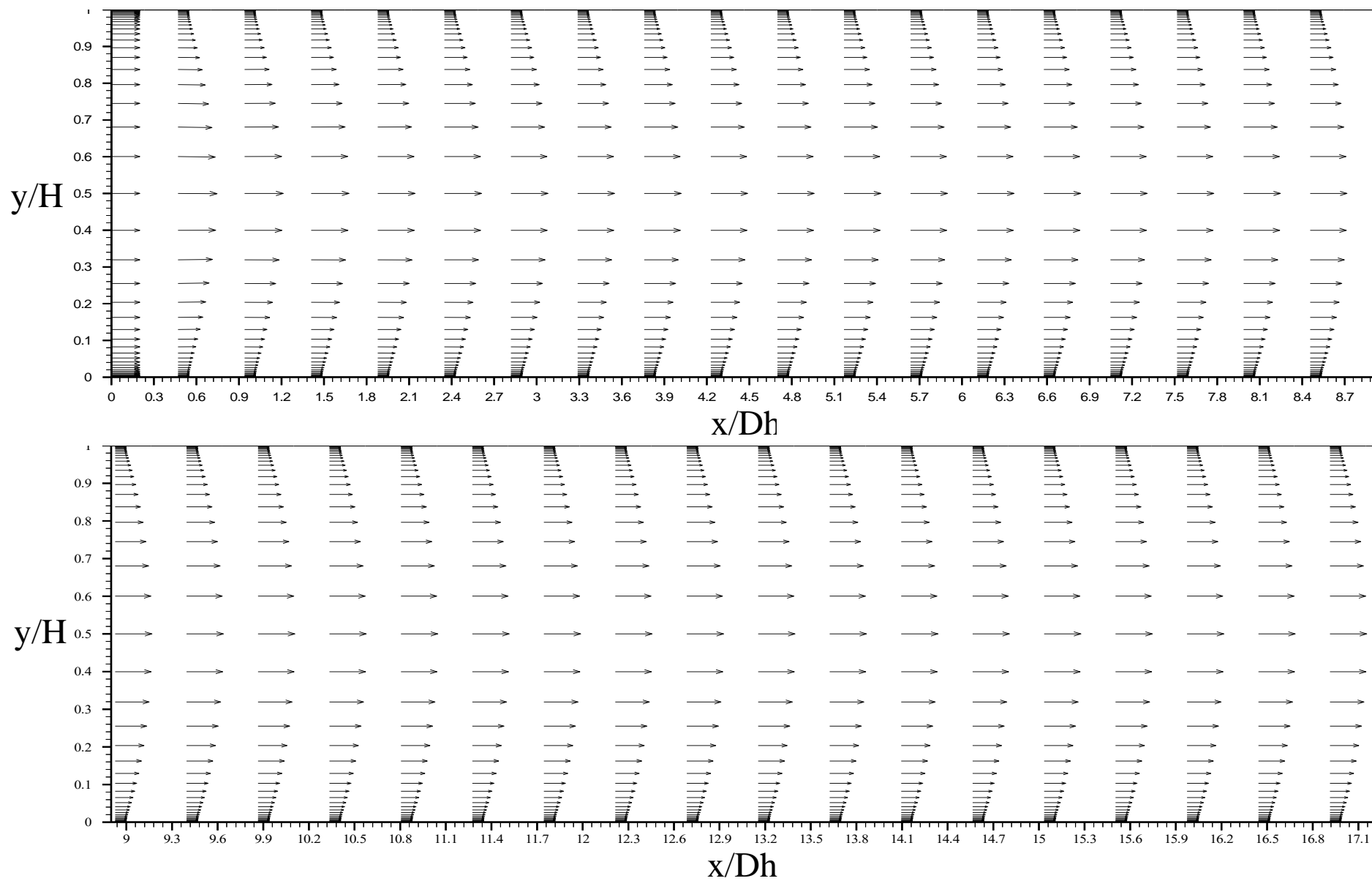


FIGURE (0.1): Development of Turbulent Hydrodynamic Boundary layer of Rectangular Duct for  $Re=6000$

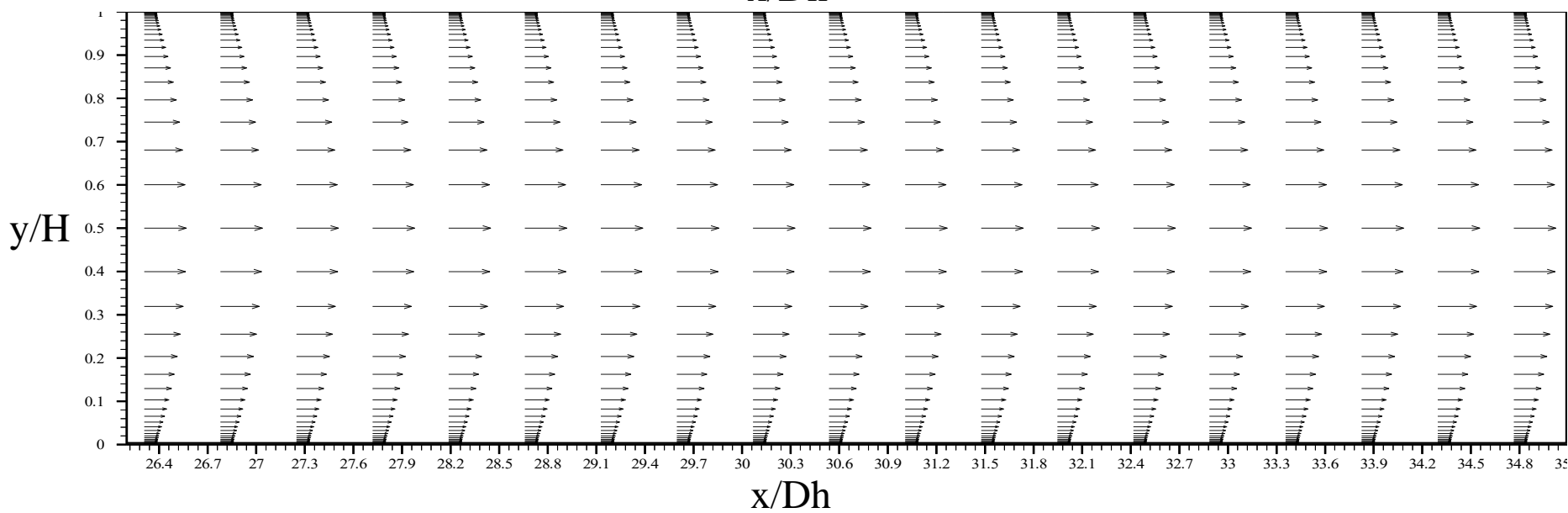
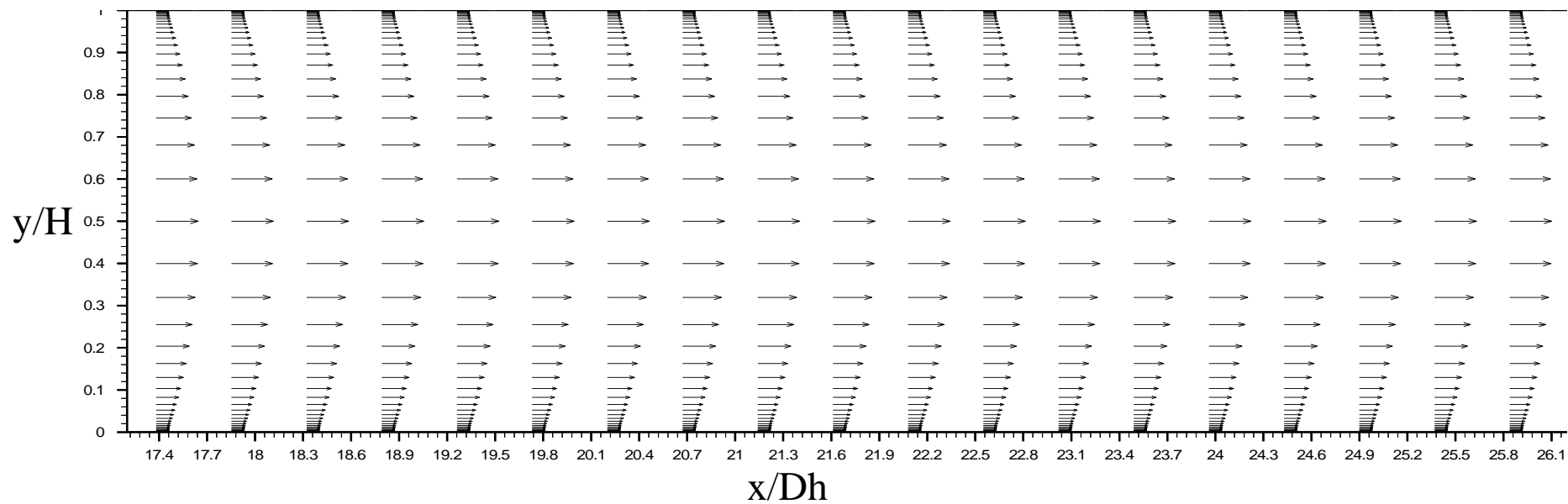


FIGURE (e.1): Development of Turbulent Hydrodynamic Boundary layer of Rectangular Duct for  $Re=1000$

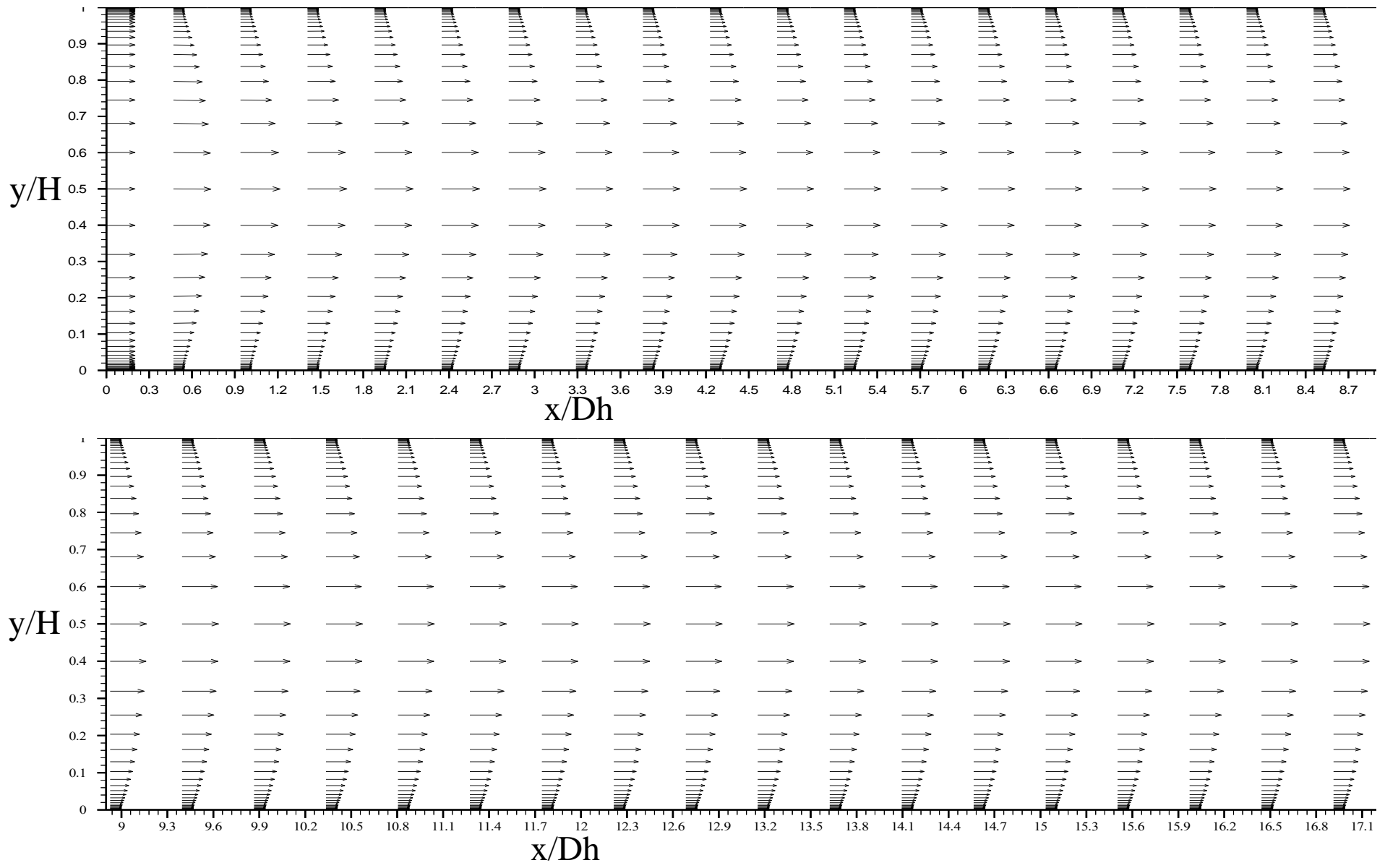


FIGURE (6.3): Development of Turbulent Hydrodynamic Boundary layer of Rectangular Duct for  $Re=12000$

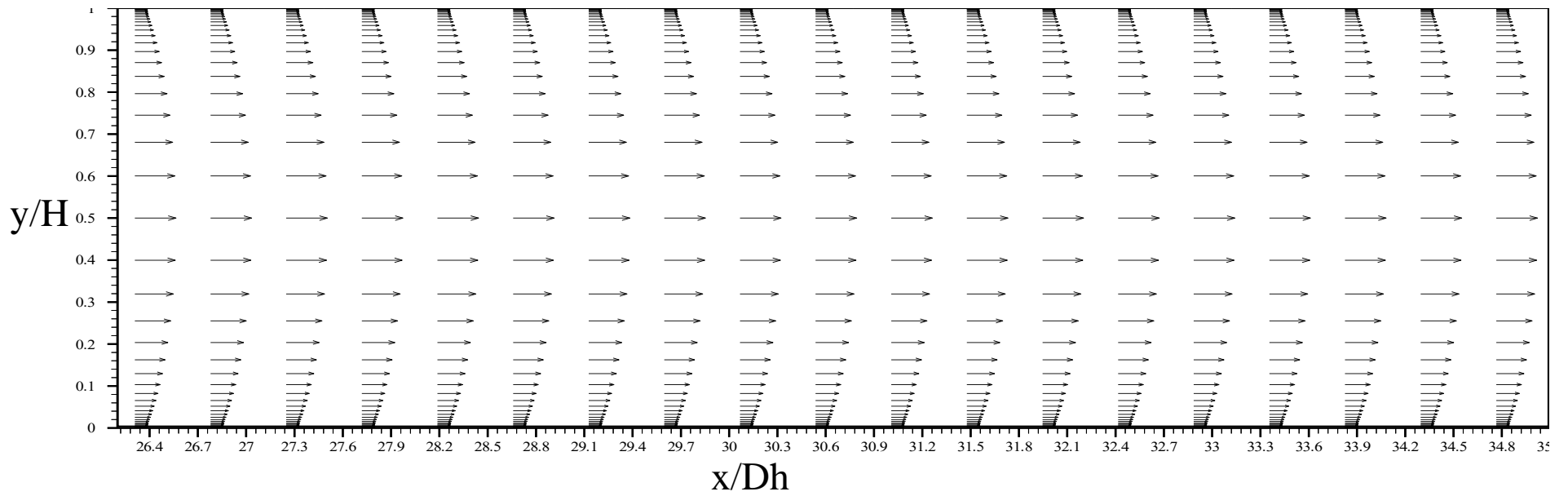
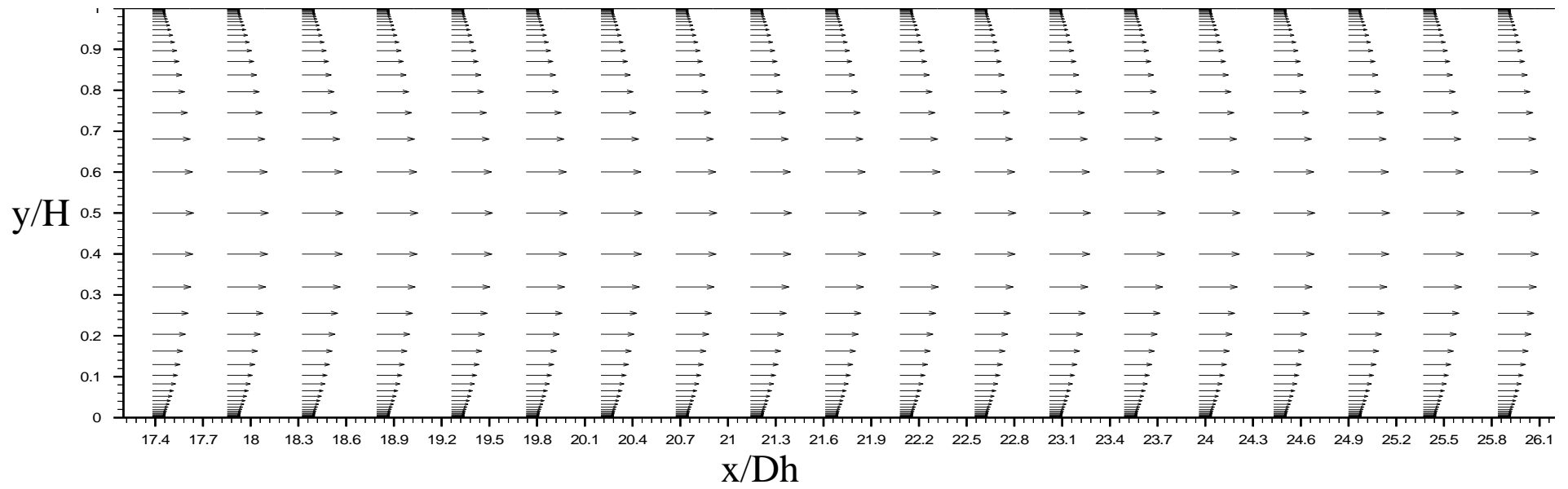


FIGURE (٥.٤): Development of Turbulent Hydrodynamic Boundary layer of Rectangular Duct for  $Re=12000$

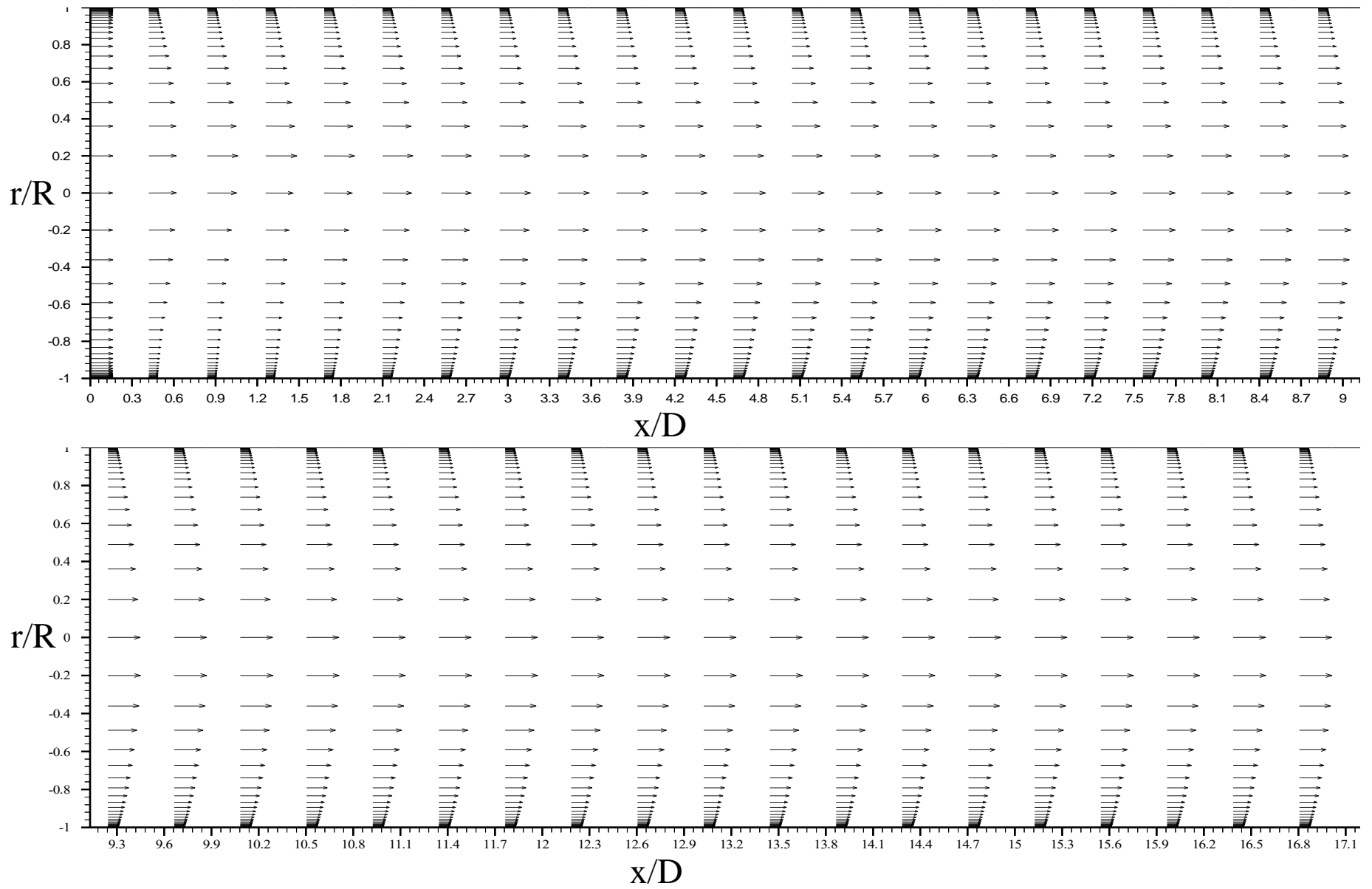


FIGURE (◦.◦): Development of Turbulent Hydrodynamic Boundary layer of Circular Duct for  $Re=7000$

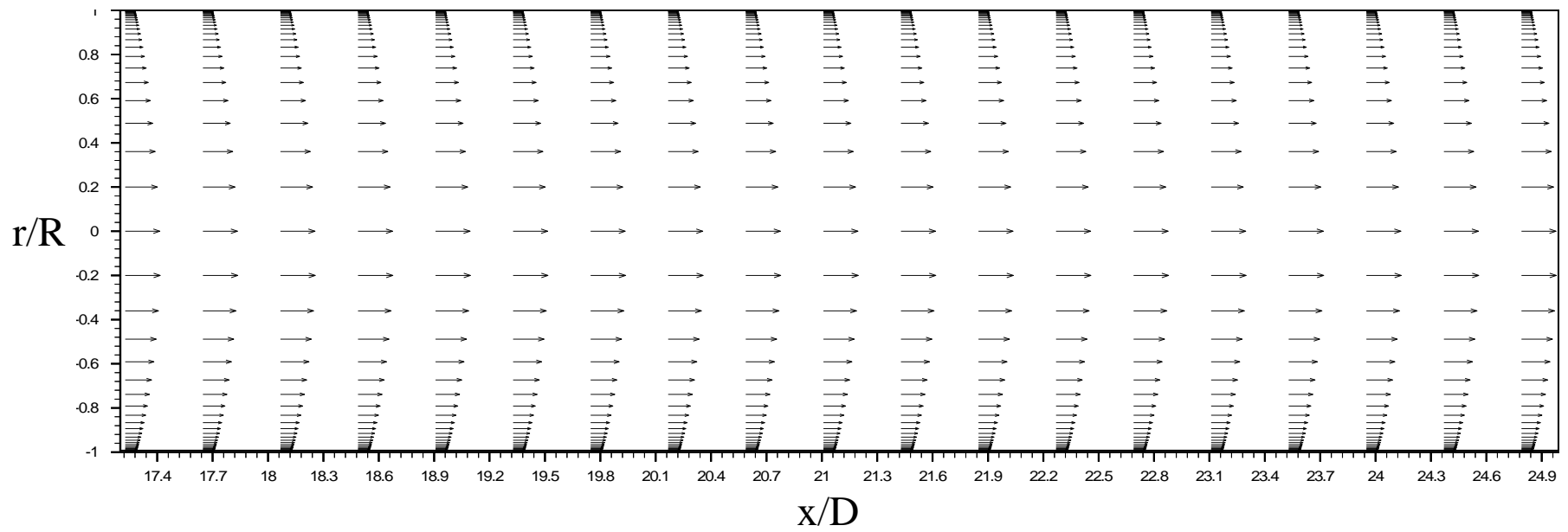


FIGURE (5.6): Development of Turbulent Hydrodynamic Boundary layer of Circular Duct for  $Re=6000$

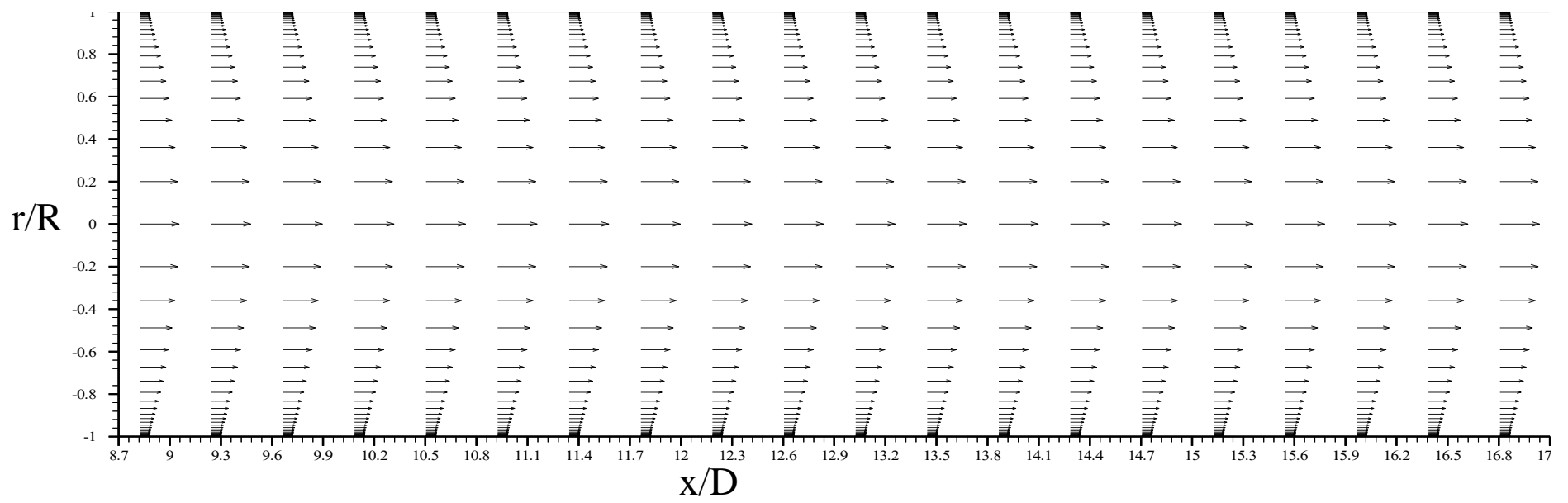
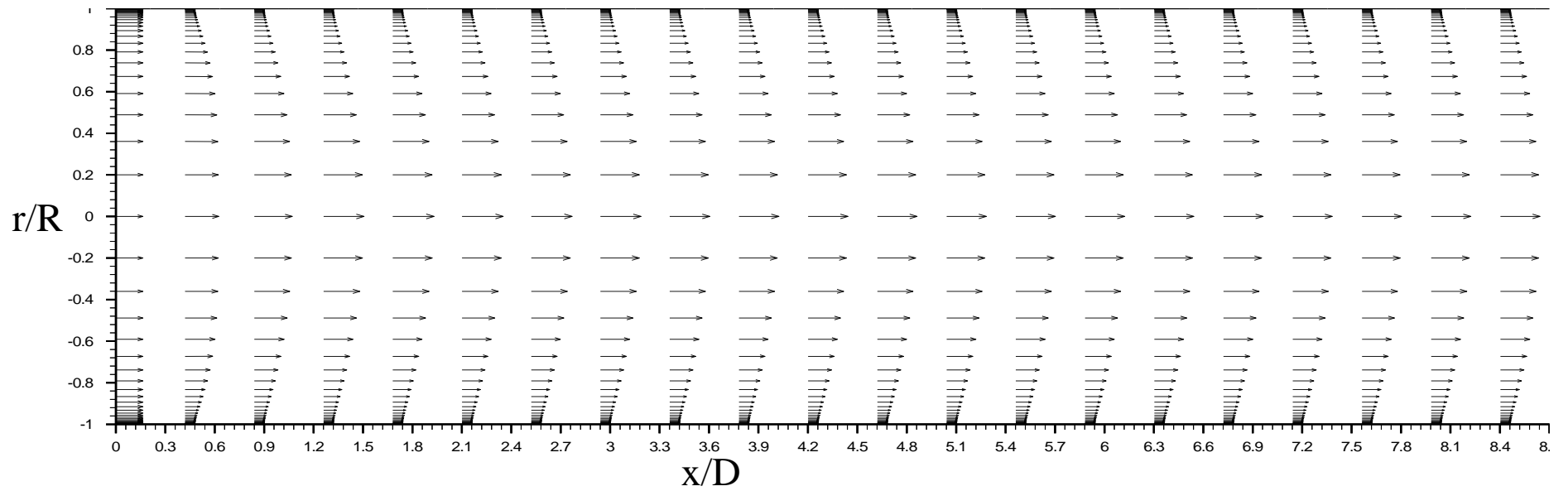


FIGURE (e.v): Developing of Turbulent Hydrodynamic Boundary layer of Circular Duct for  $Re=12000$

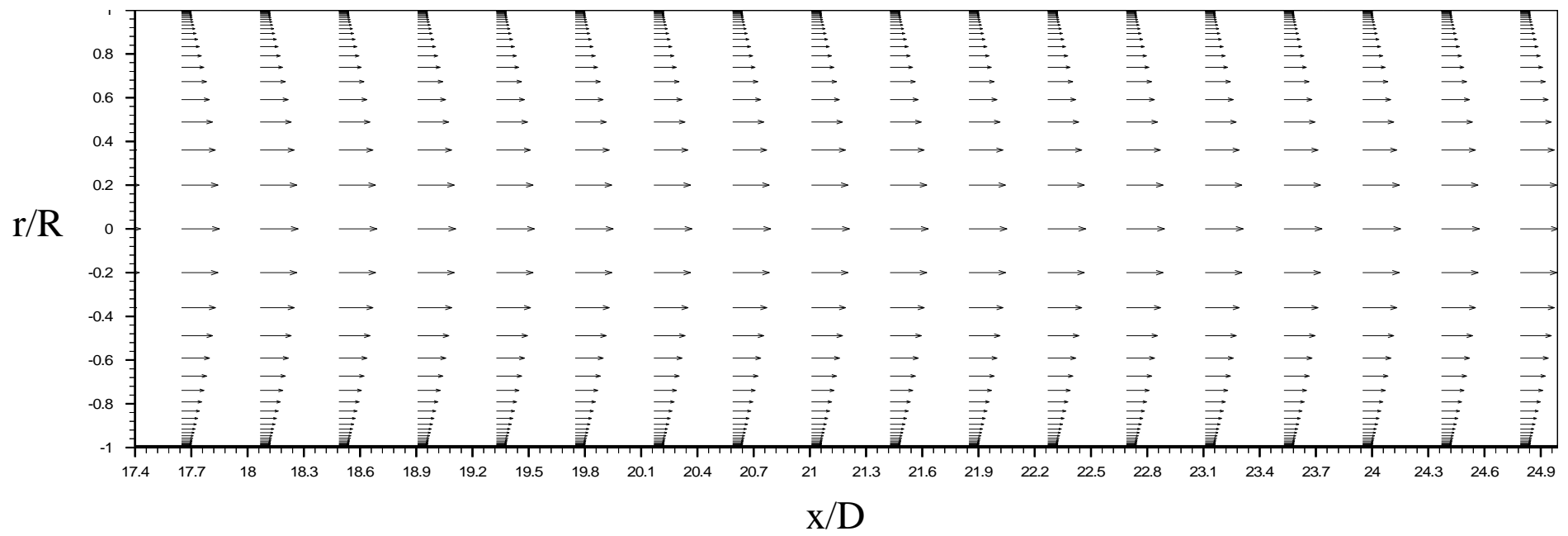


FIGURE (◦.Λ): Developing of Turbulent Hydrodynamic Boundary layer of Circular Duct for  $Re=12000$

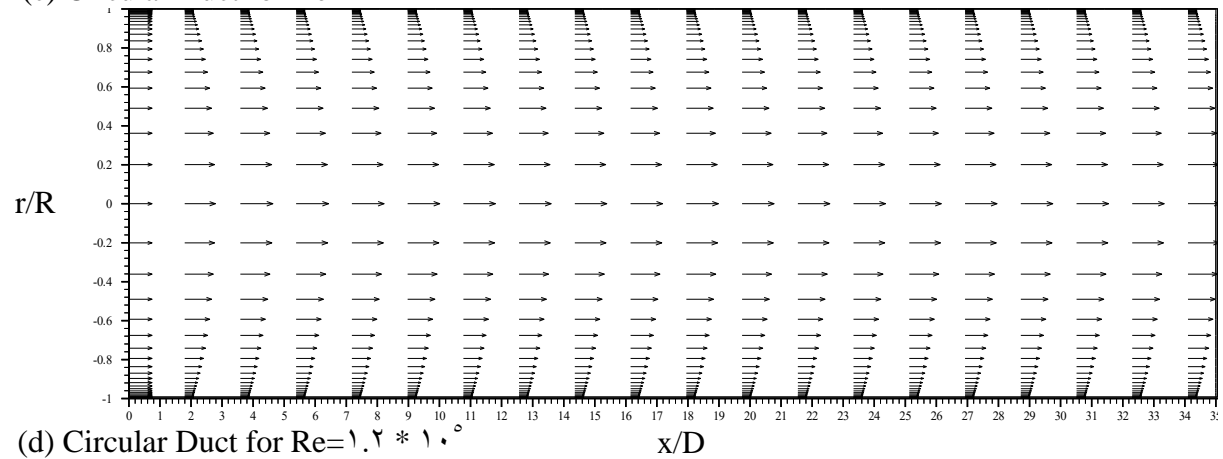
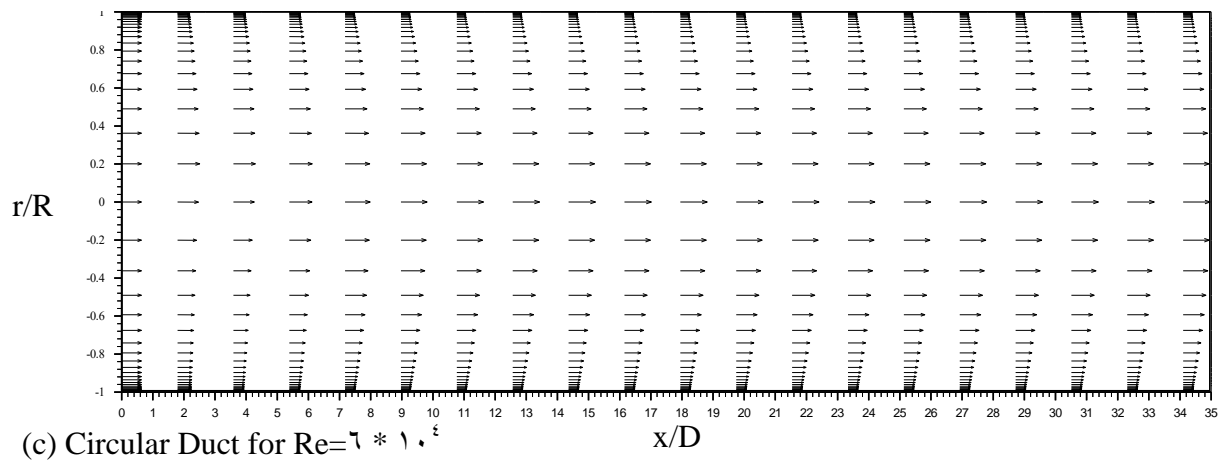
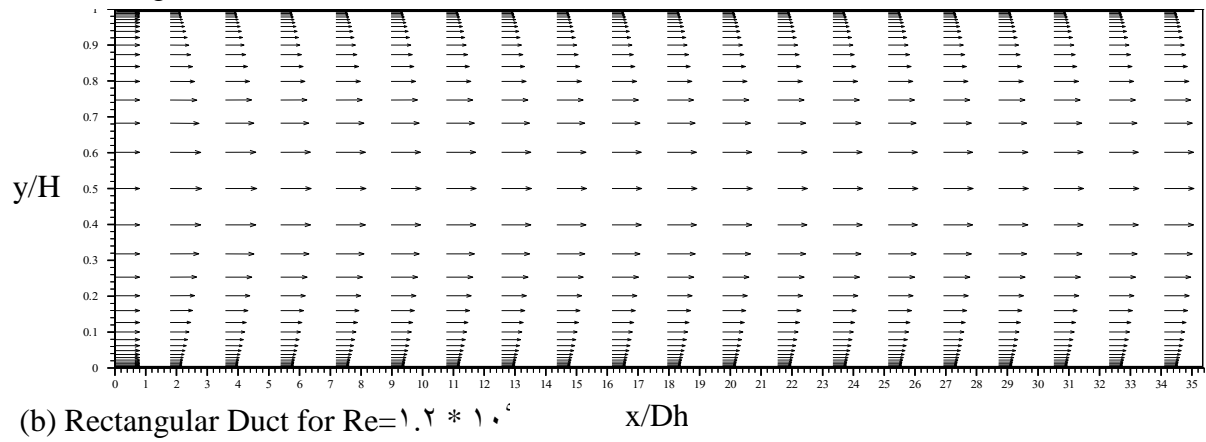
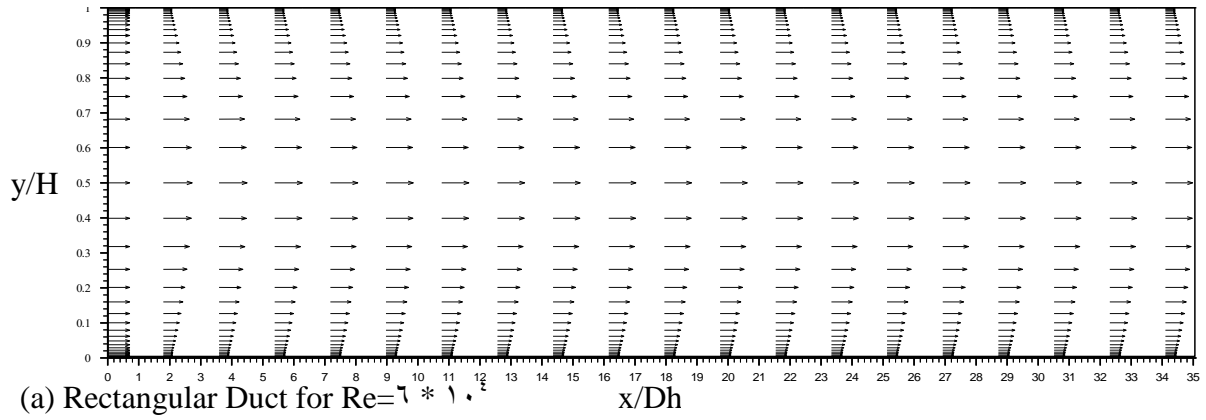


FIGURE (5.9): Developing of Turbulent Hydrodynamic Boundary layer of Rectangular and Circular Duct for  $Re=7 * 10^4$  and  $Re=1.2 * 10^4$  respectively with reducing Number of Nodal Points

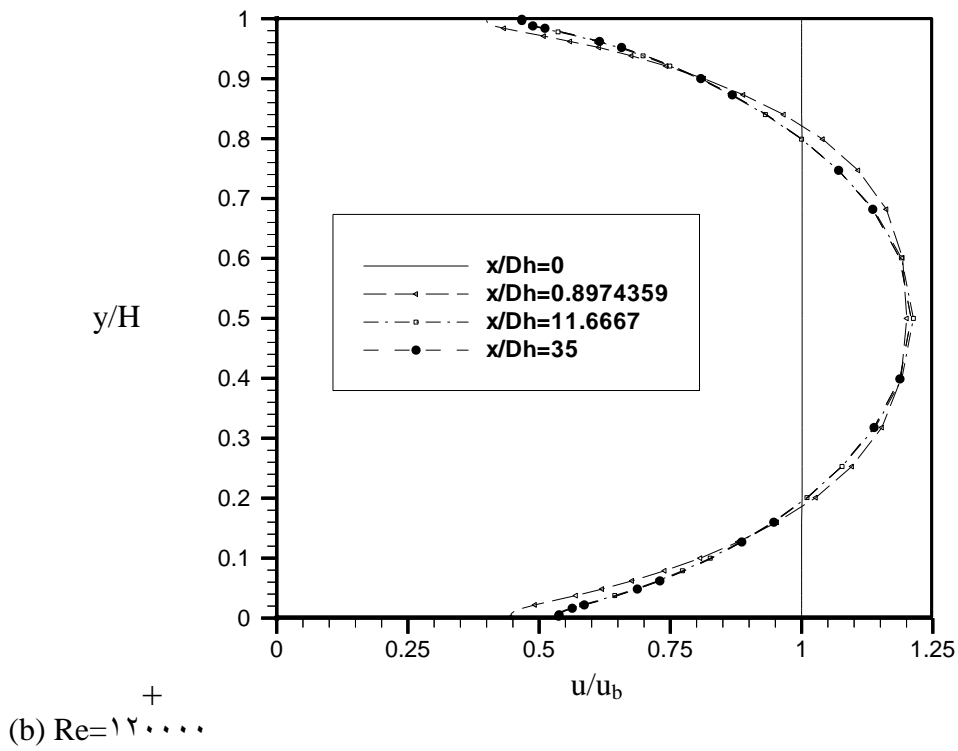
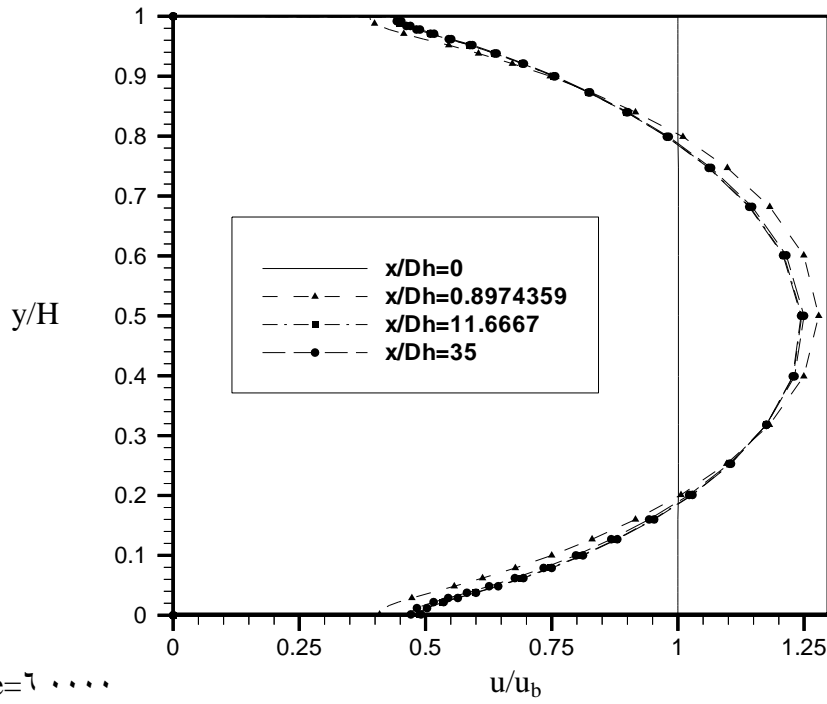
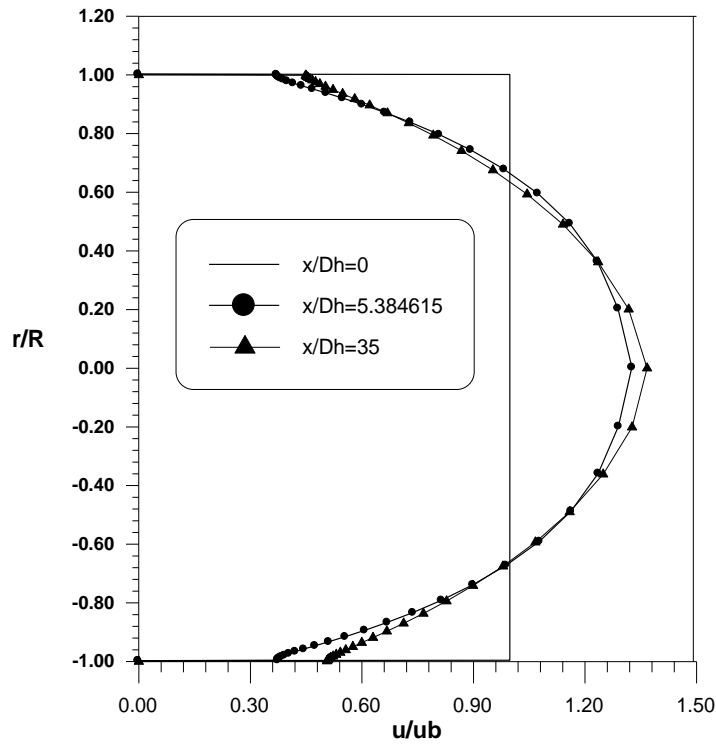
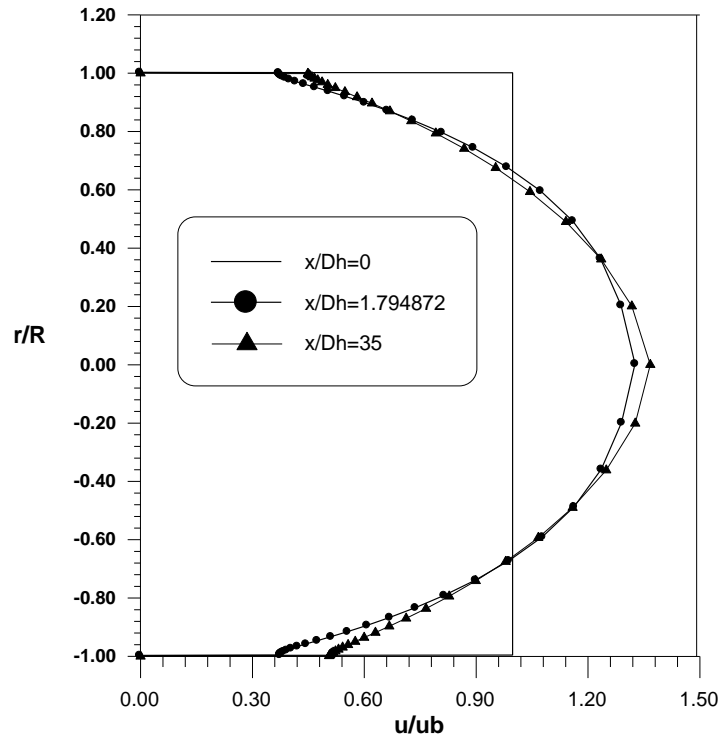


FIGURE (5.10): Axial Velocity Profiles of Rectangular Duct for Selected Values of  $x/Dh$

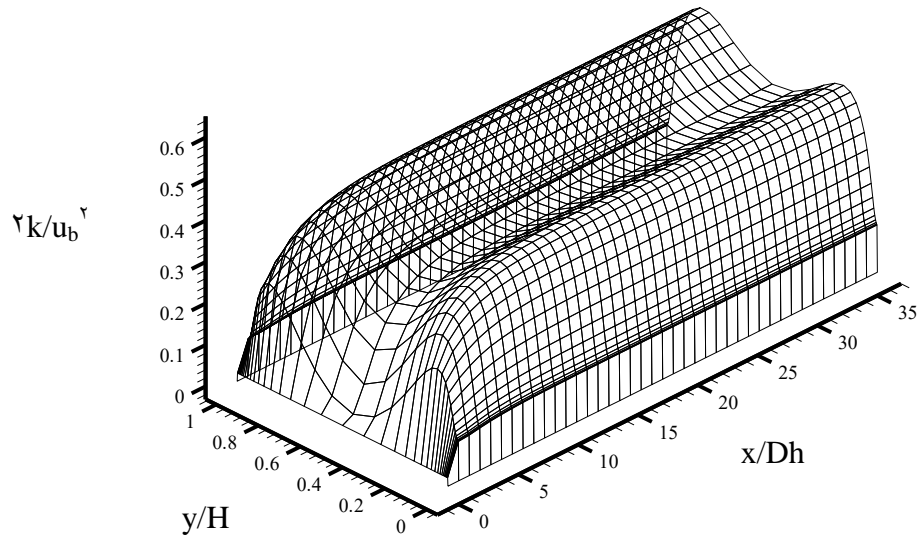


(a)  $Re=6000$

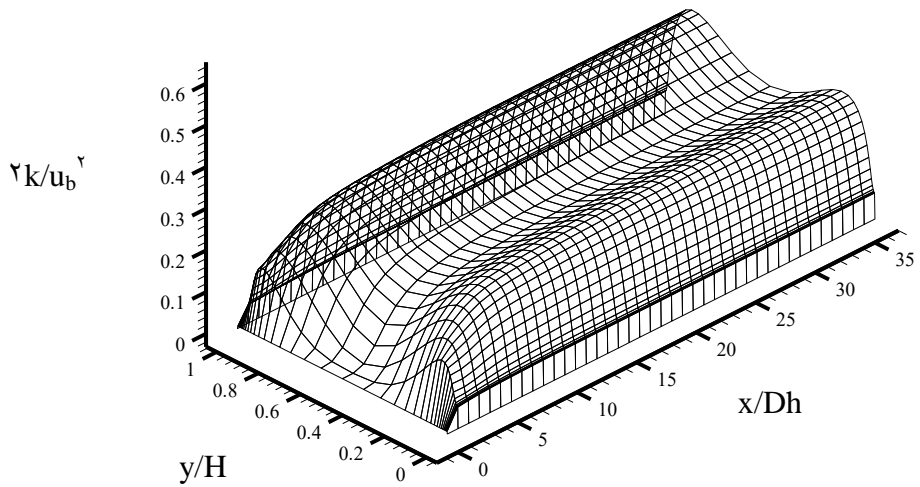


(b)  $Re=12000$

FIGURE (5.11): Axial Velocity Profiles of Circular Duct for Selected Values of  $x/D$

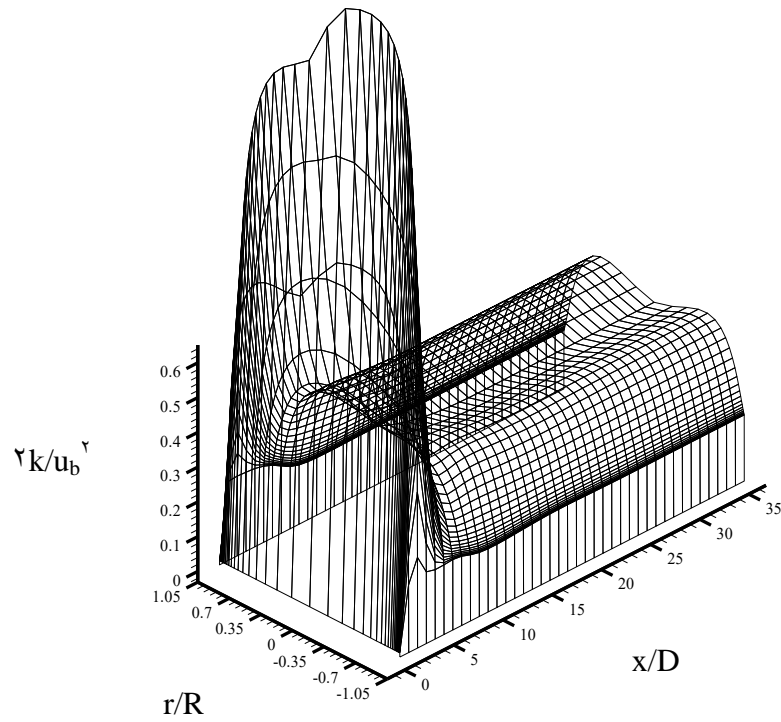


(a)  $Re=7000$

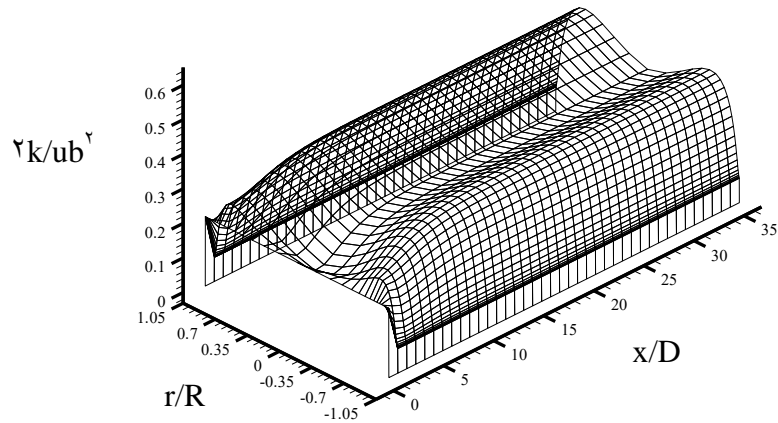


(b)  $Re=12000$

FIGURE (5.12): Development of Turbulent Kinetic Energy for Rectangular Duct



(a)  $Re=7000$



(b)  $Re=12000$

FIGURE (5.13): Development of Turbulent Kinetic Energy for Circular Duct

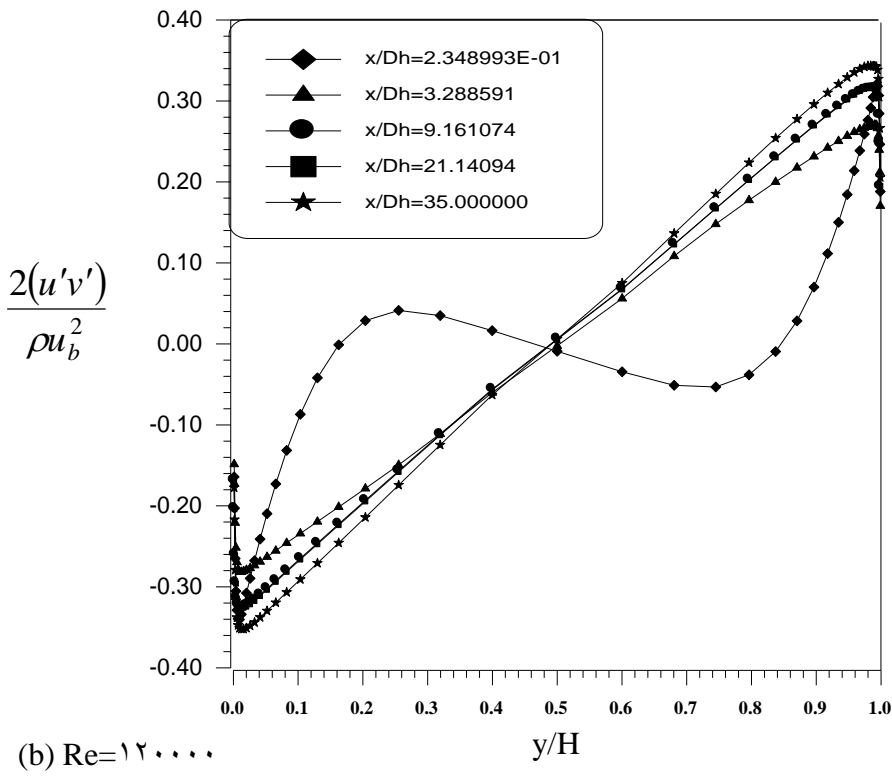
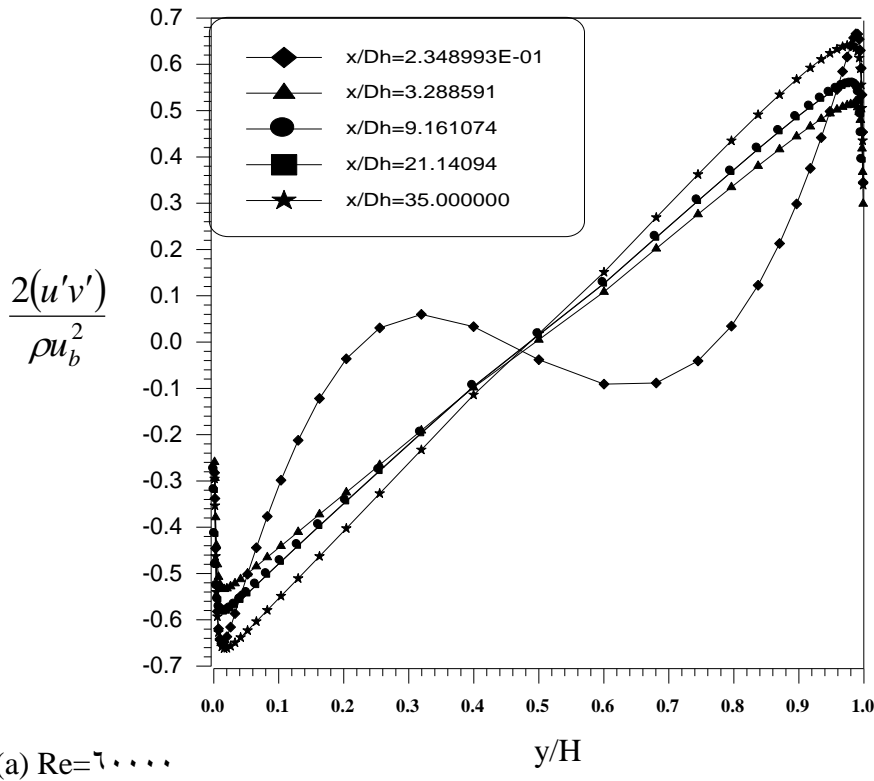


FIGURE (5.14): Development of axial Reynolds Stress for Rectangular Duct

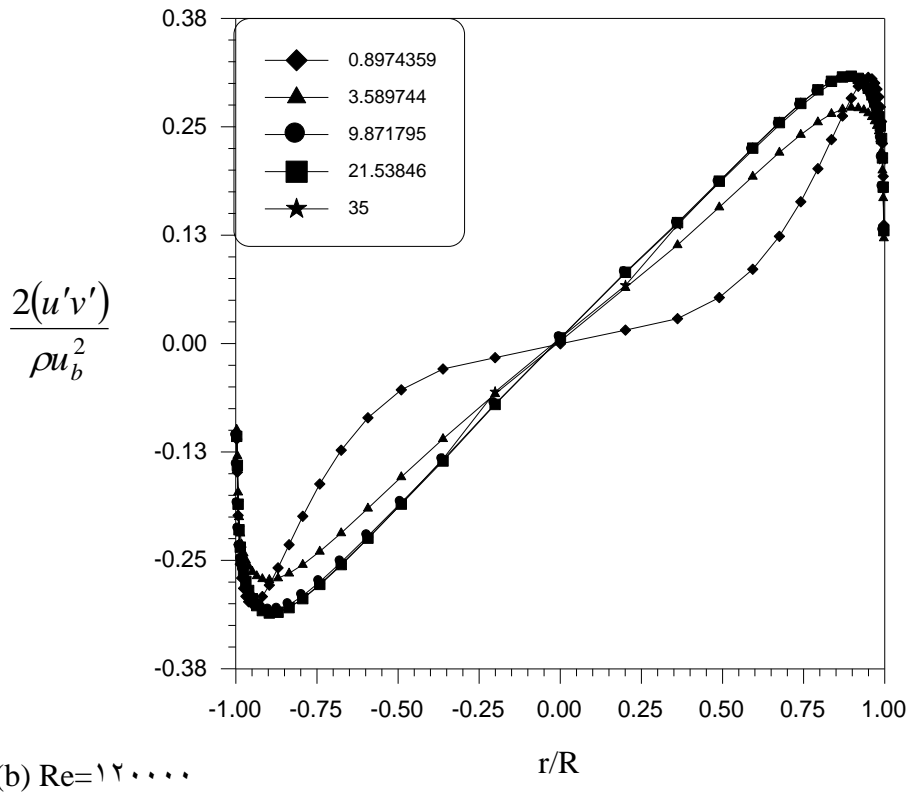
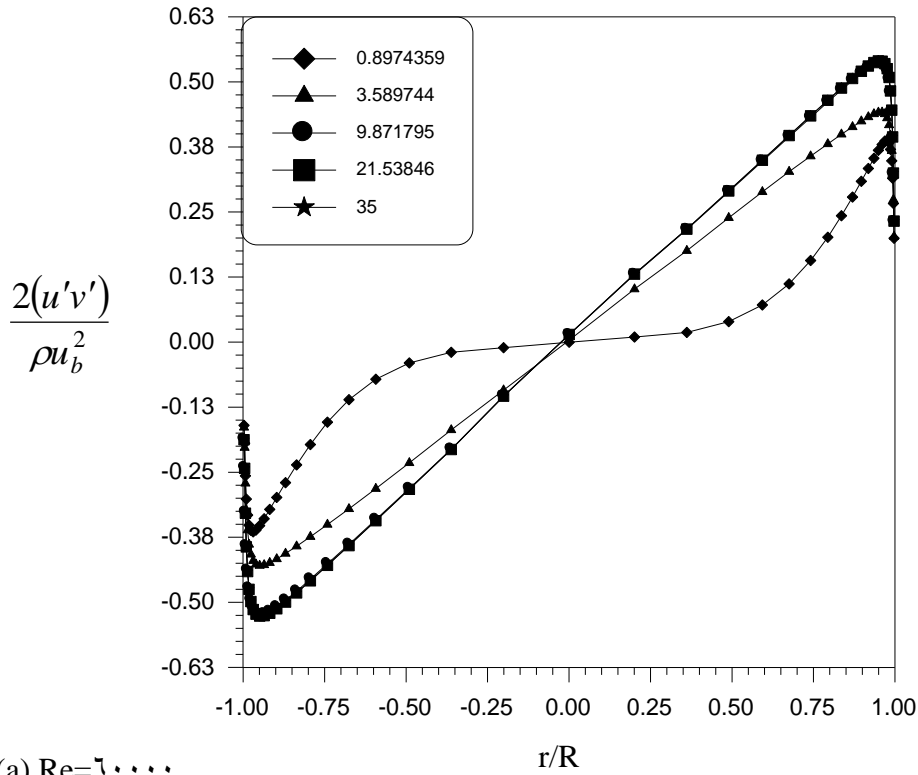


FIGURE (5.10): Development of axial Reynolds Stress for Circular Duct

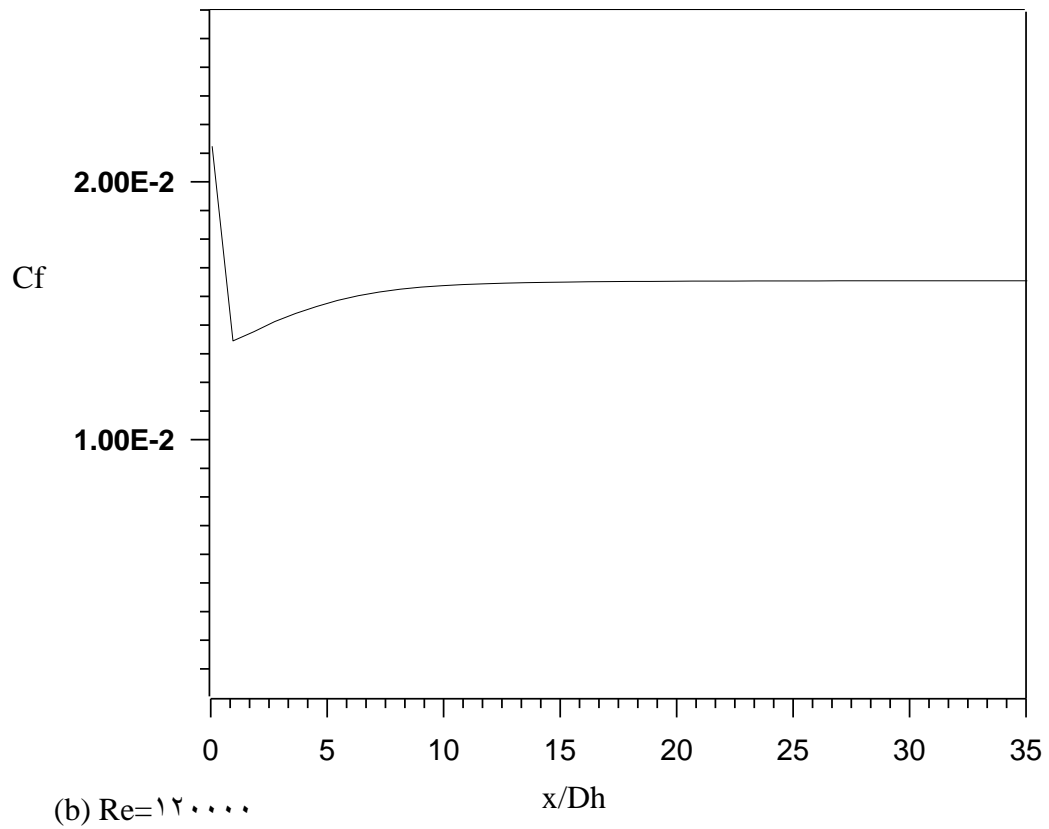
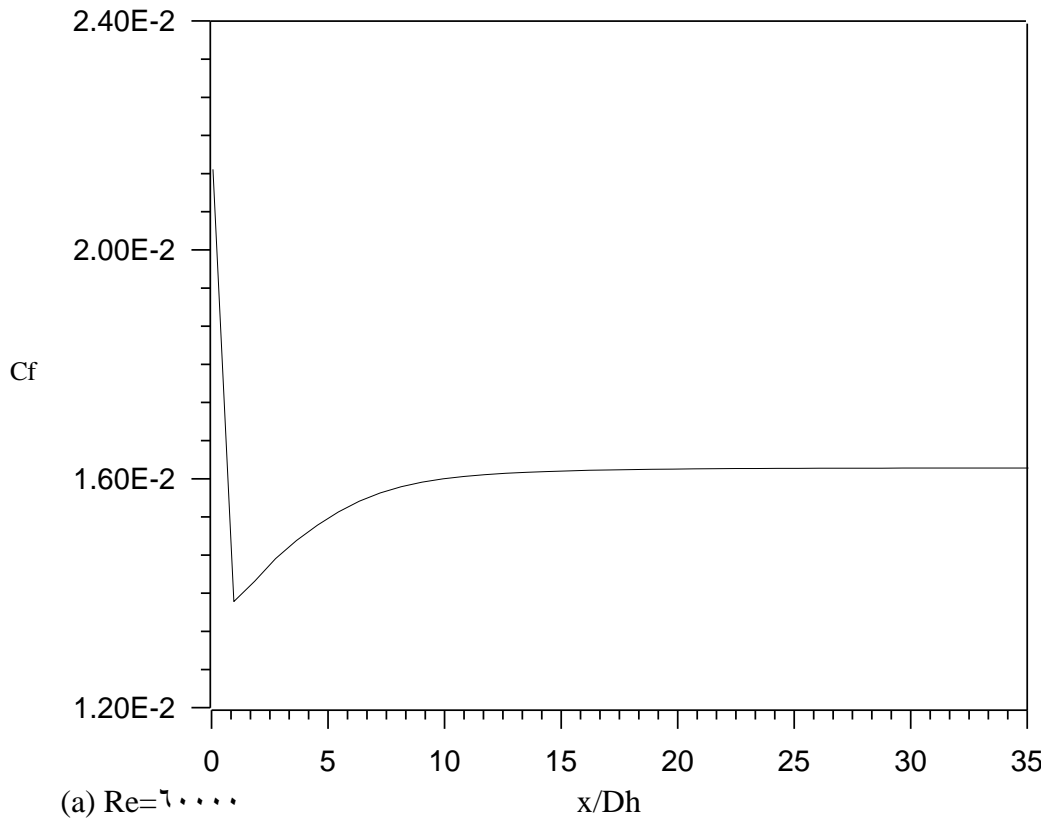


FIGURE (5.16): The Axial Distribution of Coefficient of Friction for Rectangular Duct

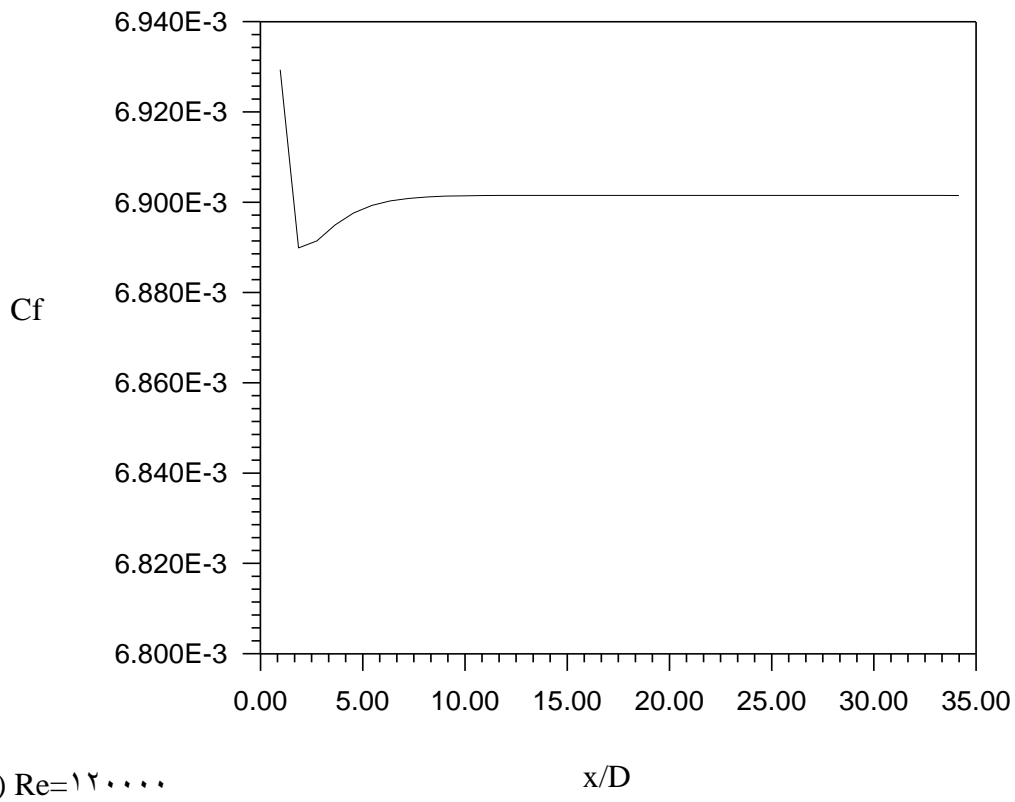
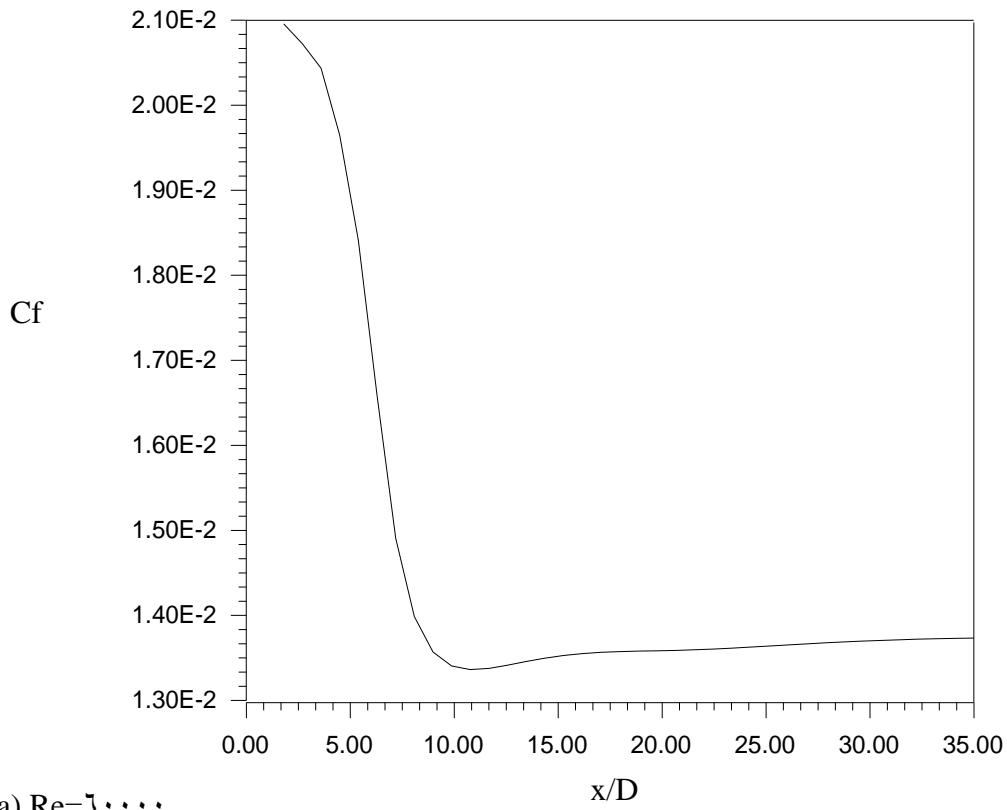
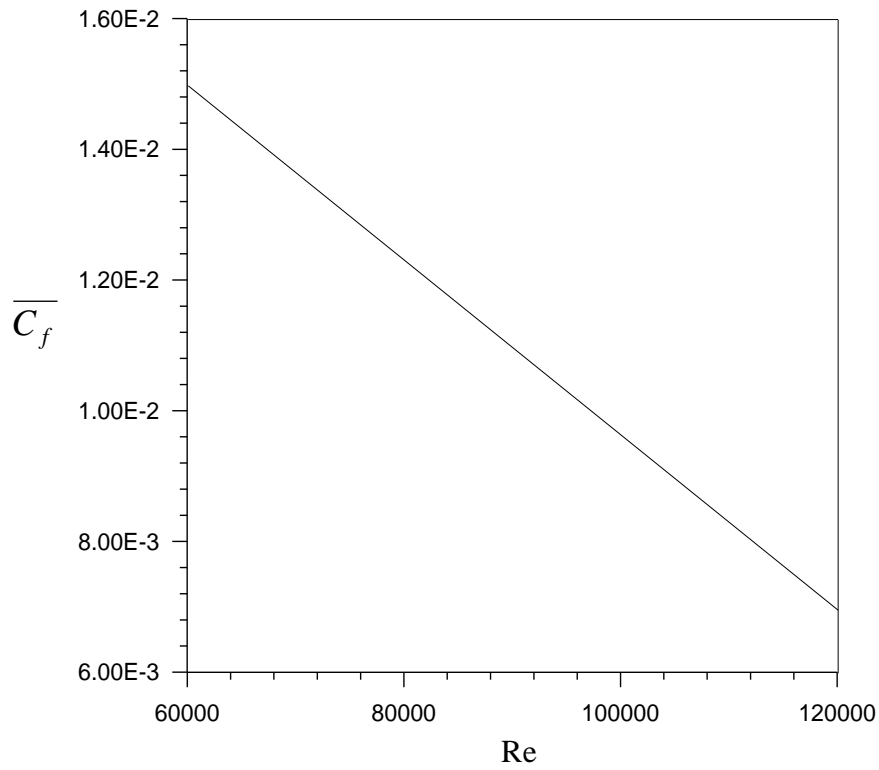
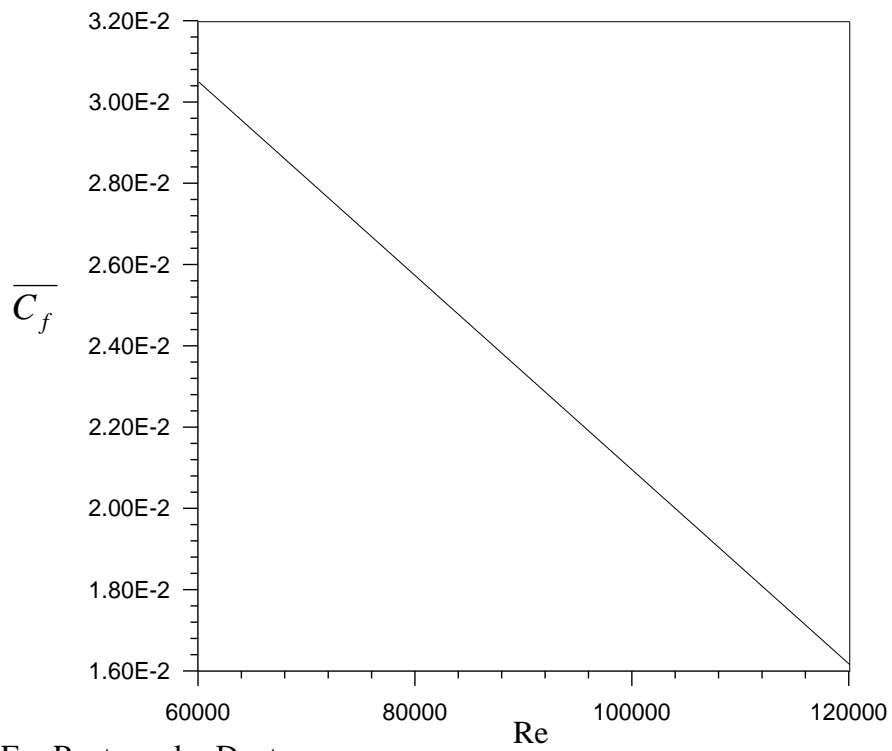


FIGURE (5.17): The Axial Distribution of Coefficient of Friction for Circular Duct



(a) For Circular Duct



(b) For Rectangular Duct

FIGURE (5.11): Effect of Reynolds Number upon an Average Coefficient of Friction for Circular and Rectangular Duct

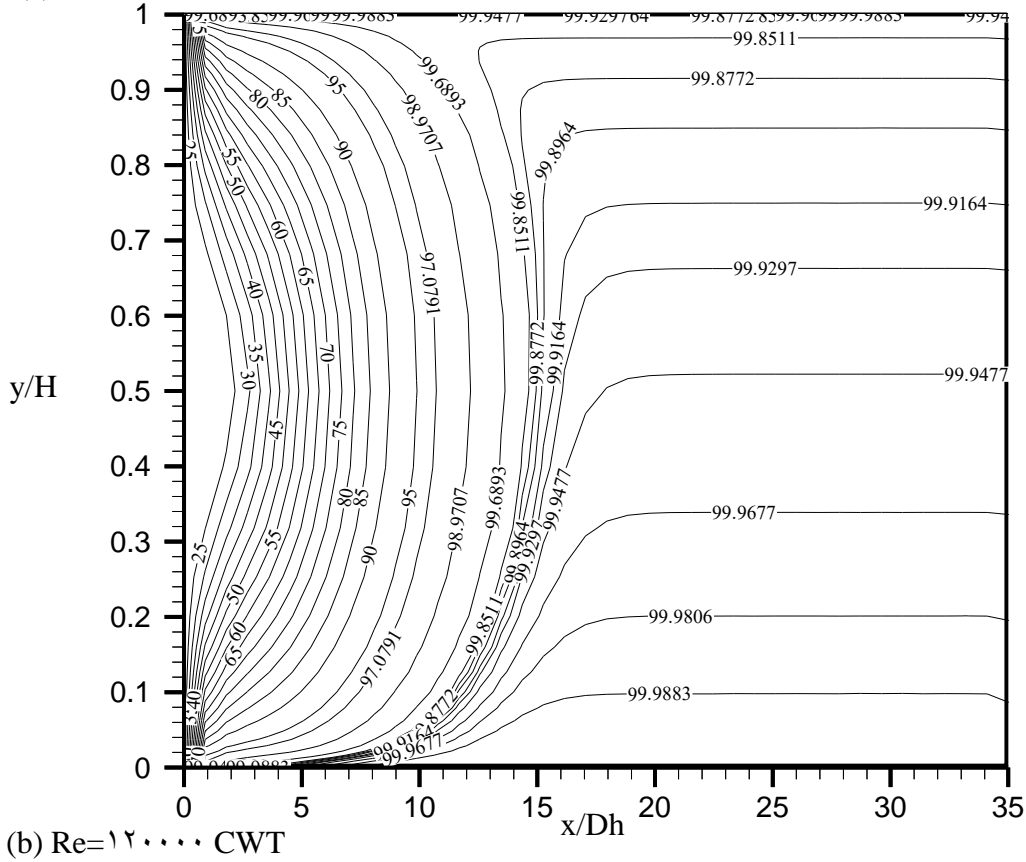
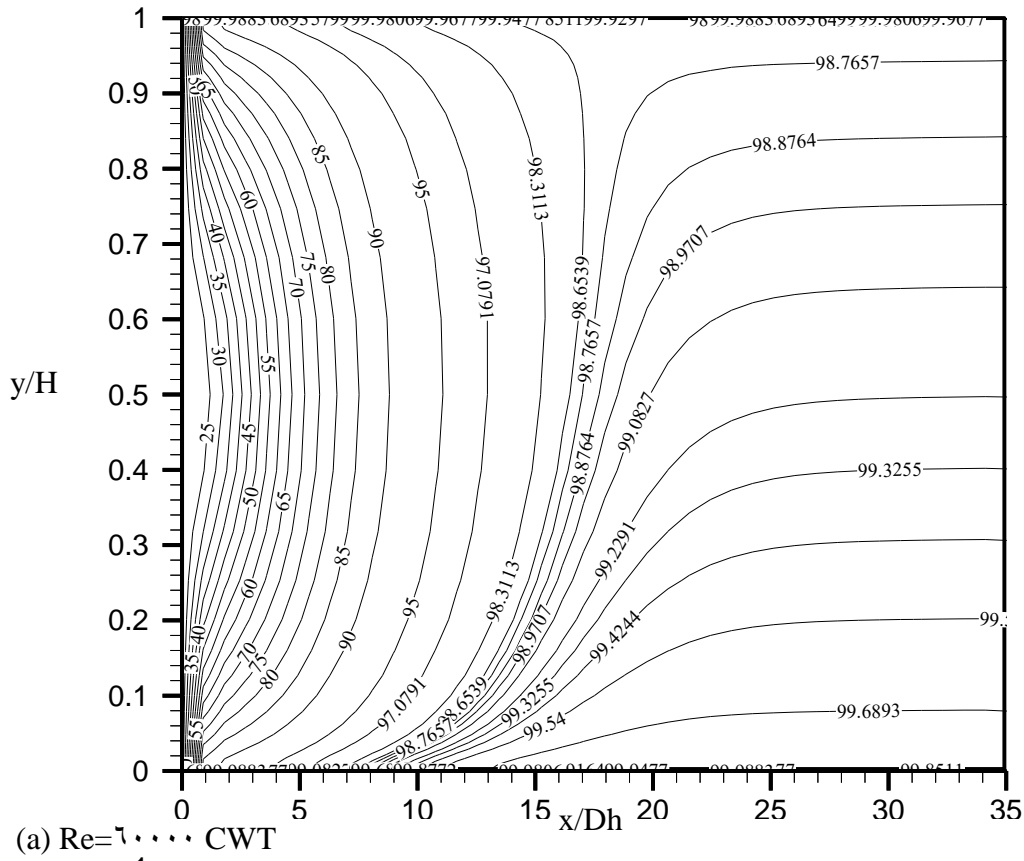
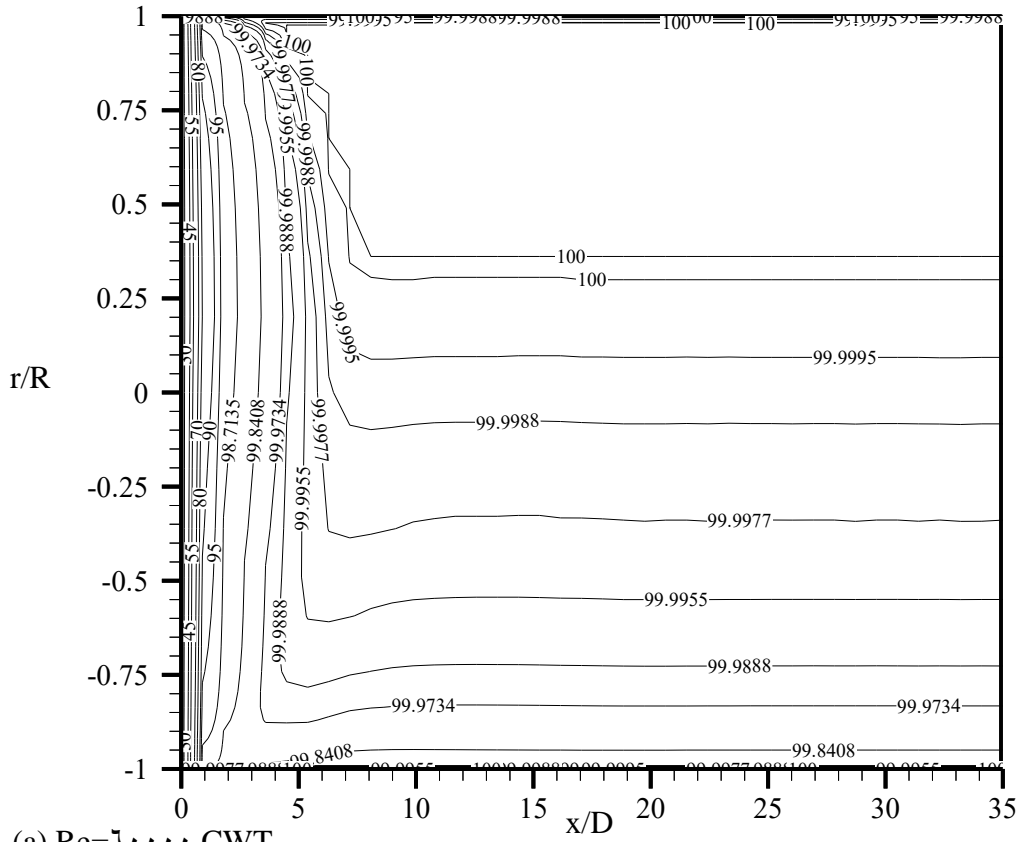
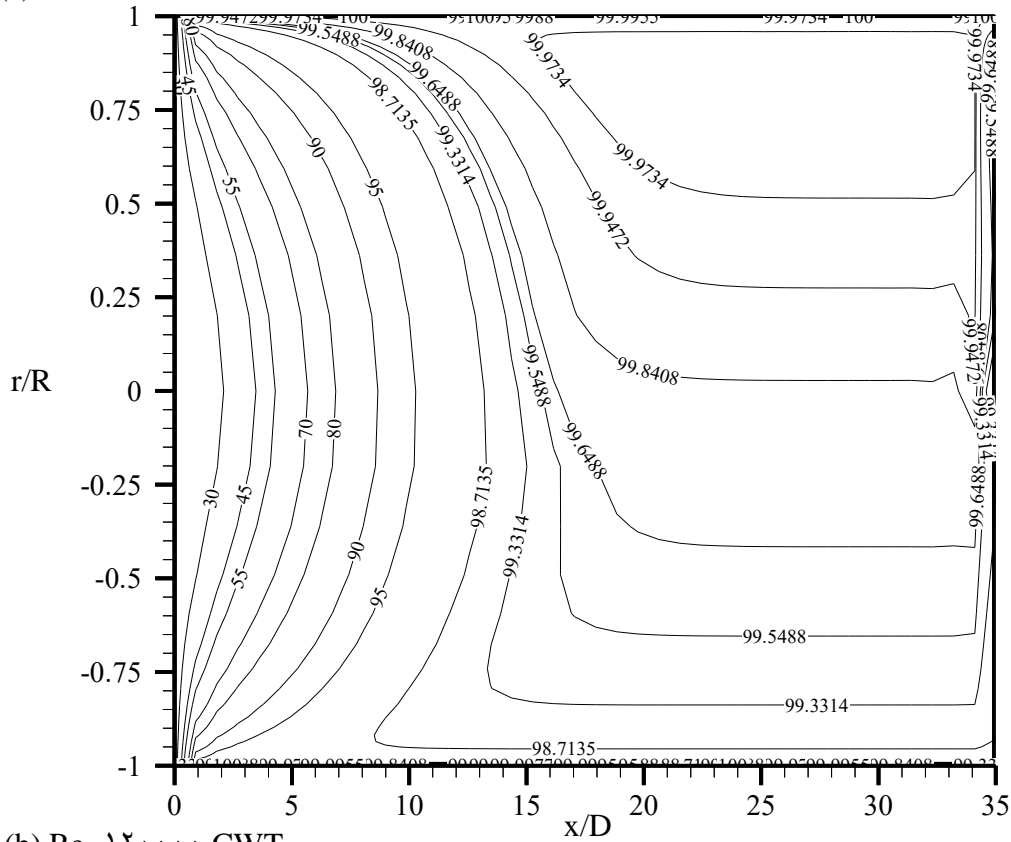


FIGURE (5.19): The Isothermal Contour Map of Temperature in the Rectangular Duct Exposed to Constant Wall Temperature for  $Re=6000$  and  $Re=12000$

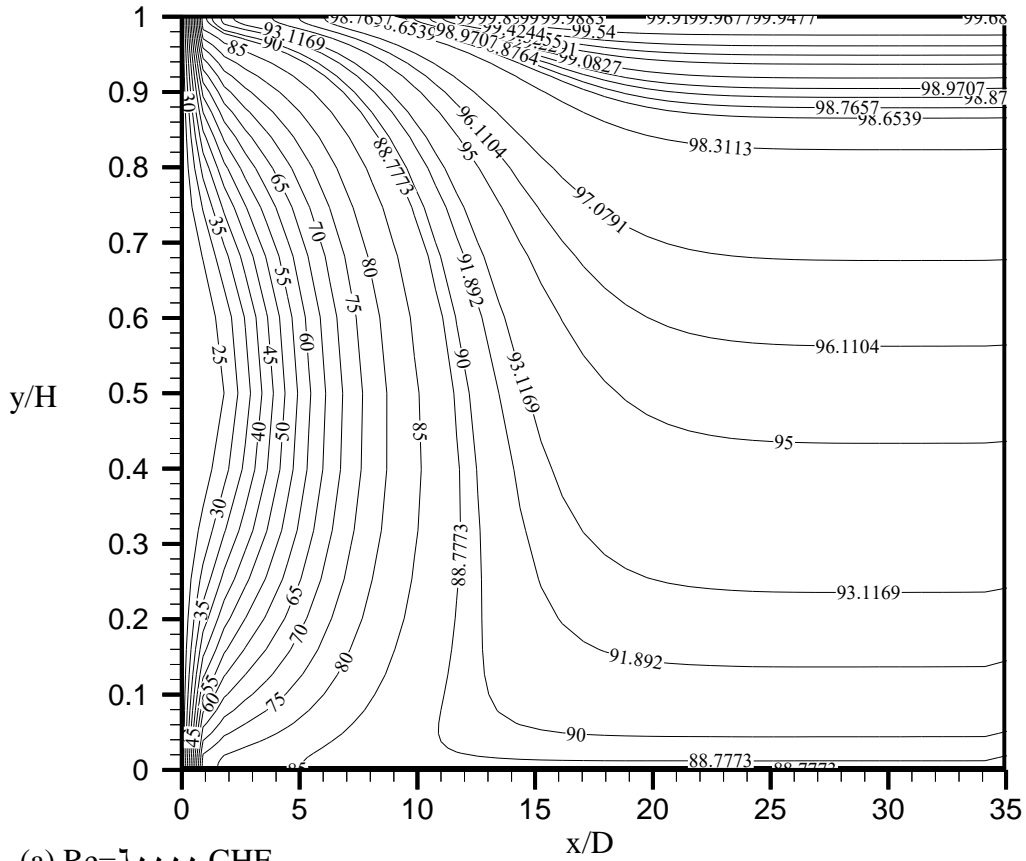


(a)  $Re=7000$  CWT

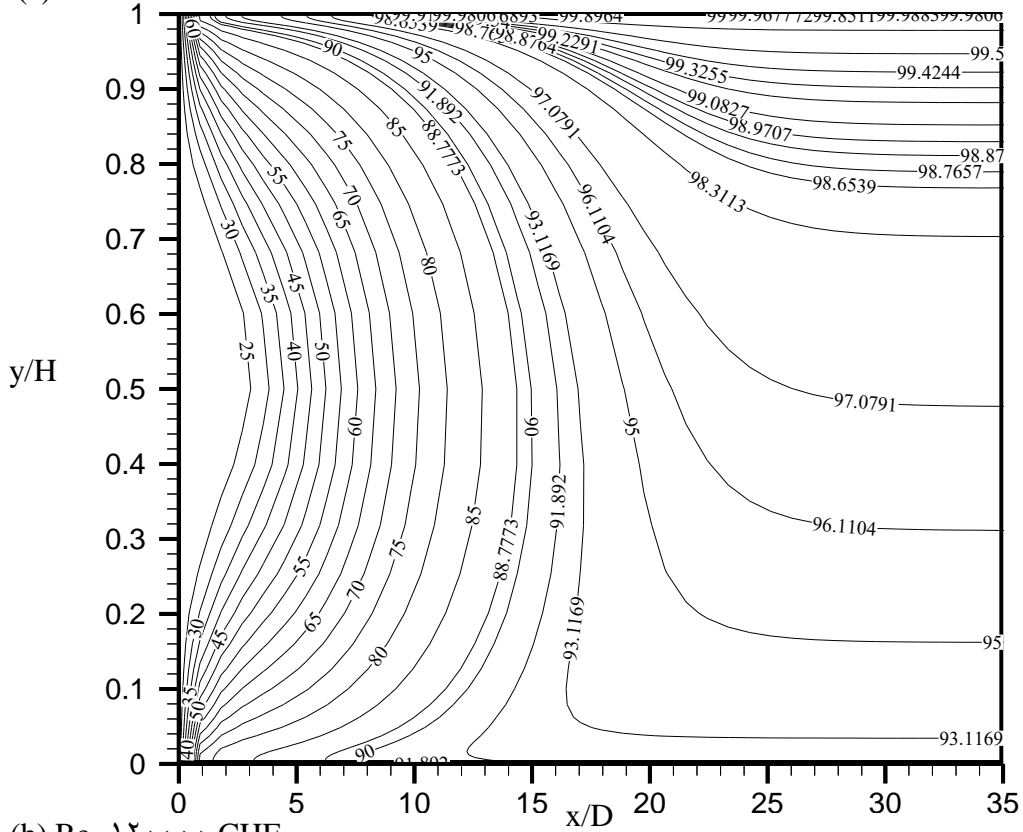


(b)  $Re=12000$  CWT

FIGURE (5.10): The Isothermal Contour Map of Temperature in the Circular Duct Exposed to Constant Wall Temperature for  $Re=7000$  and  $Re=12000$



(a)  $Re=7000$  CHF



(b)  $Re=12000$  CHF

FIGURE (5.1): The Isothermal Contour Map of Temperature in the Rectangular Duct Exposed to Constant Heat Flux for  $Re=7000$  and  $Re=12000$

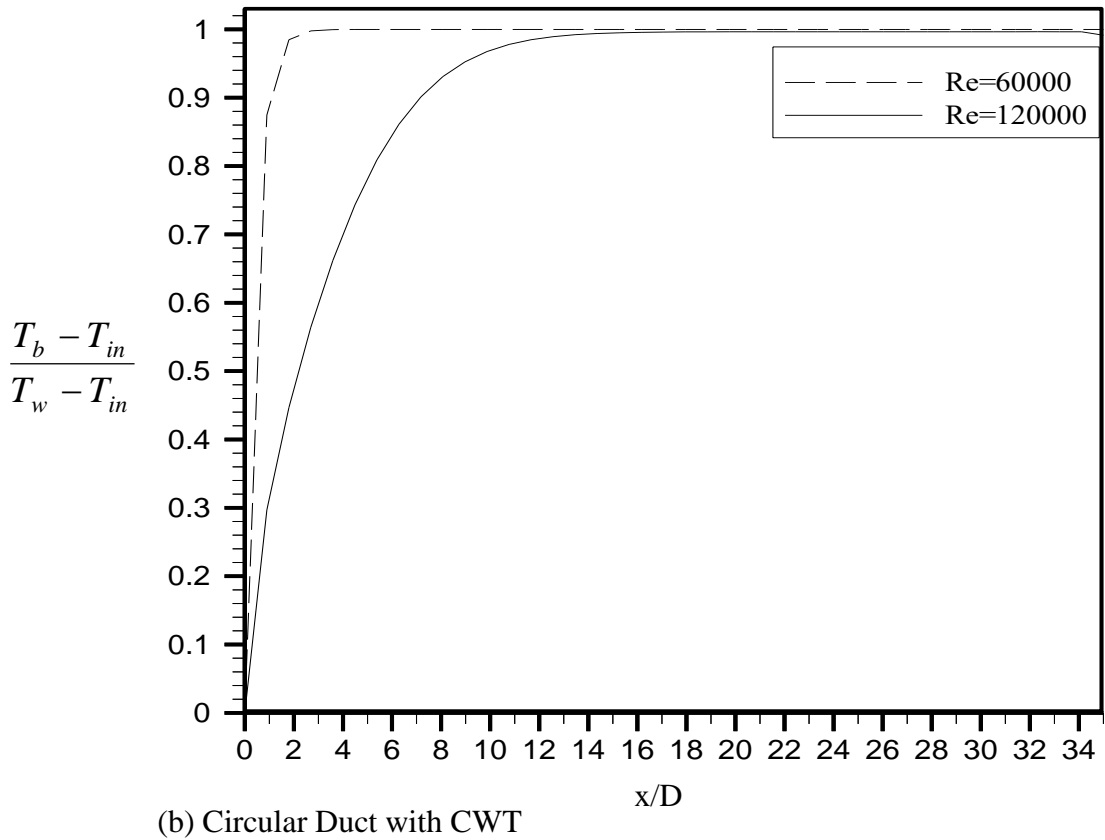
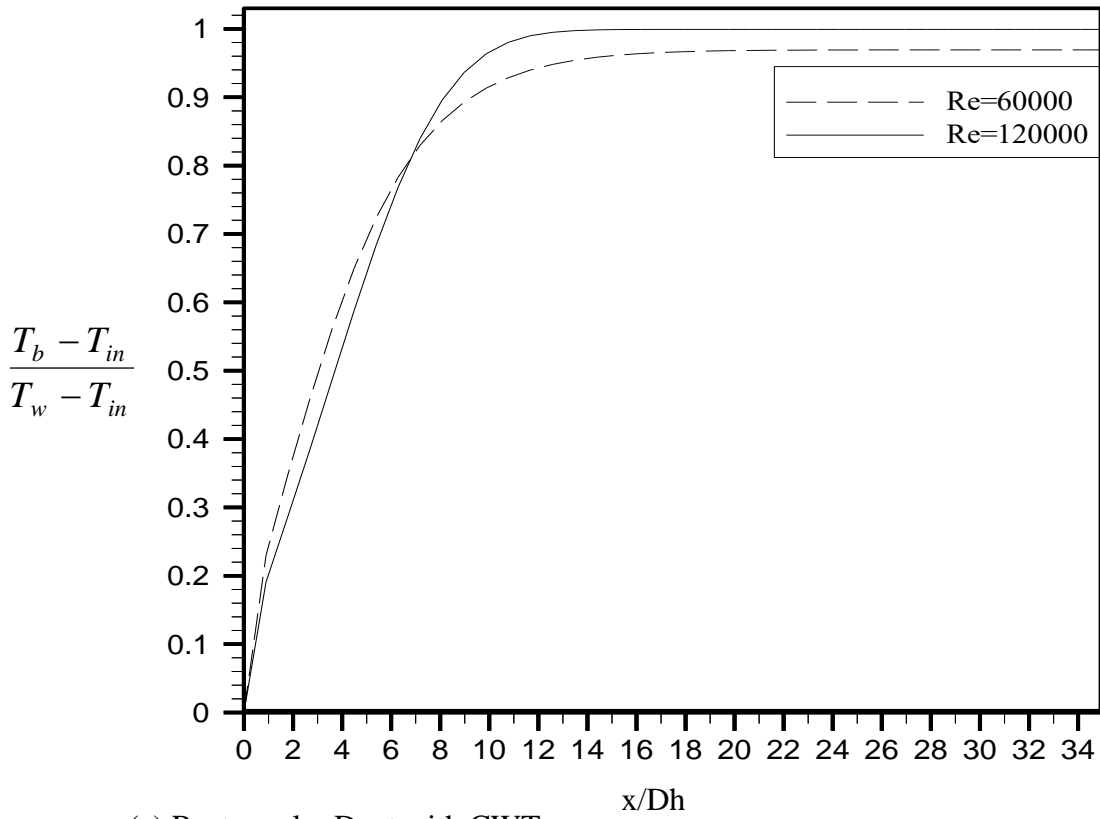


FIGURE (5.22): Axial Distribution of Overall Heating for Rectangular and Circular Duct with CWT

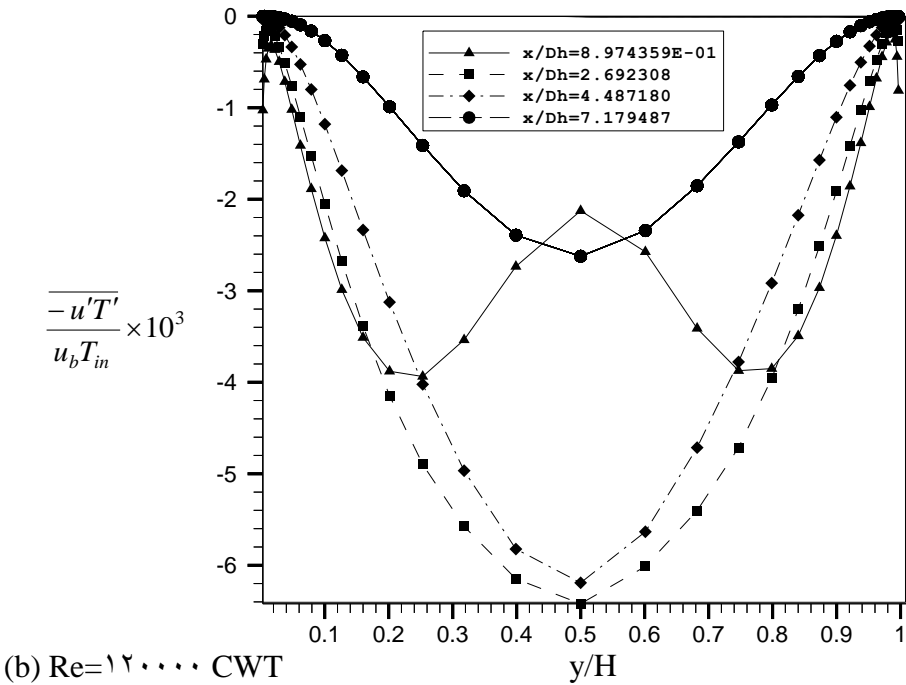
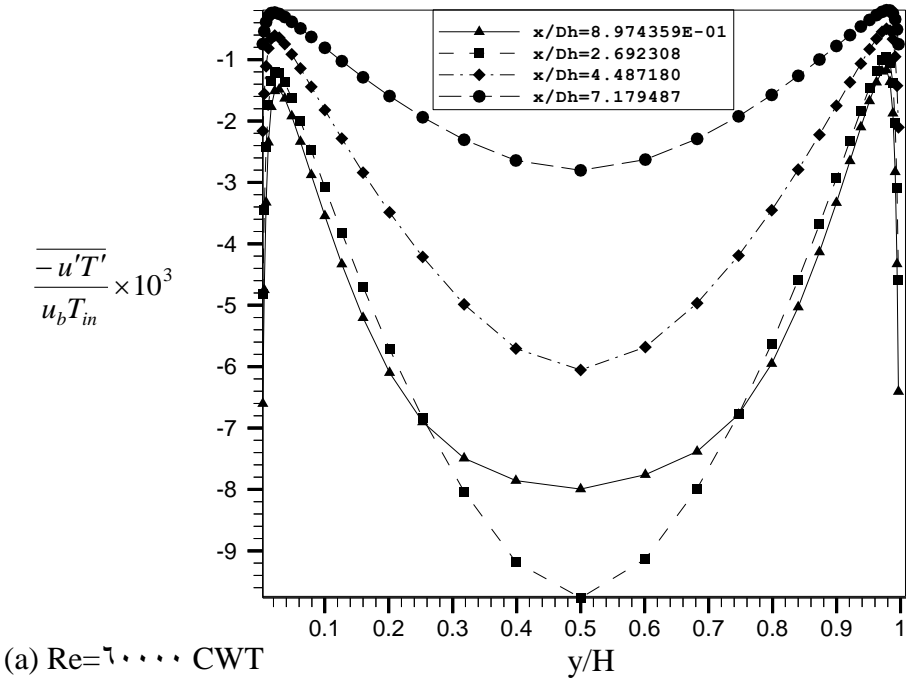
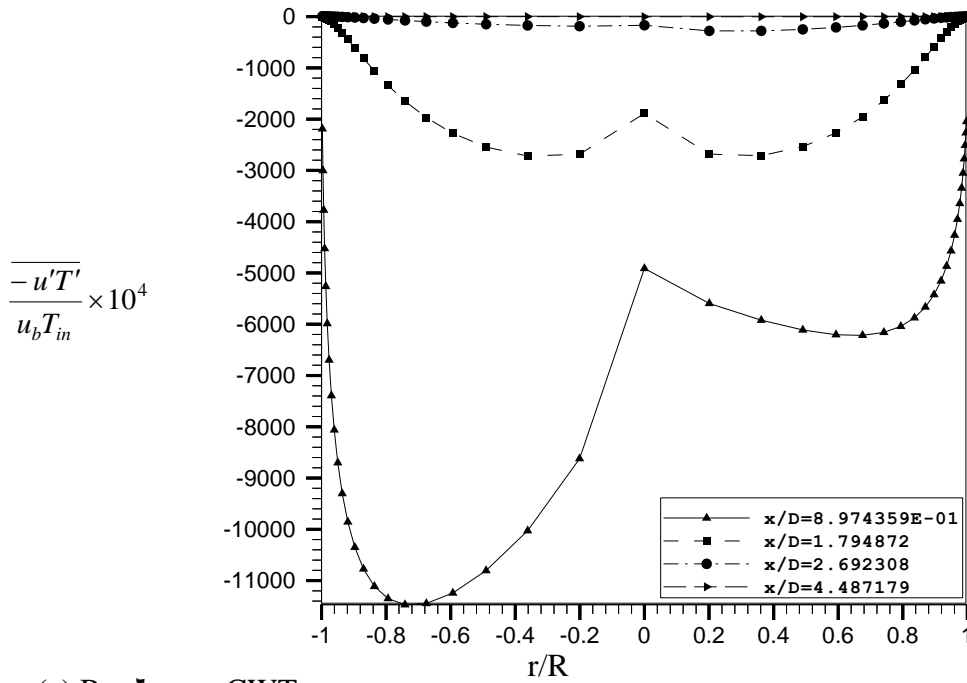
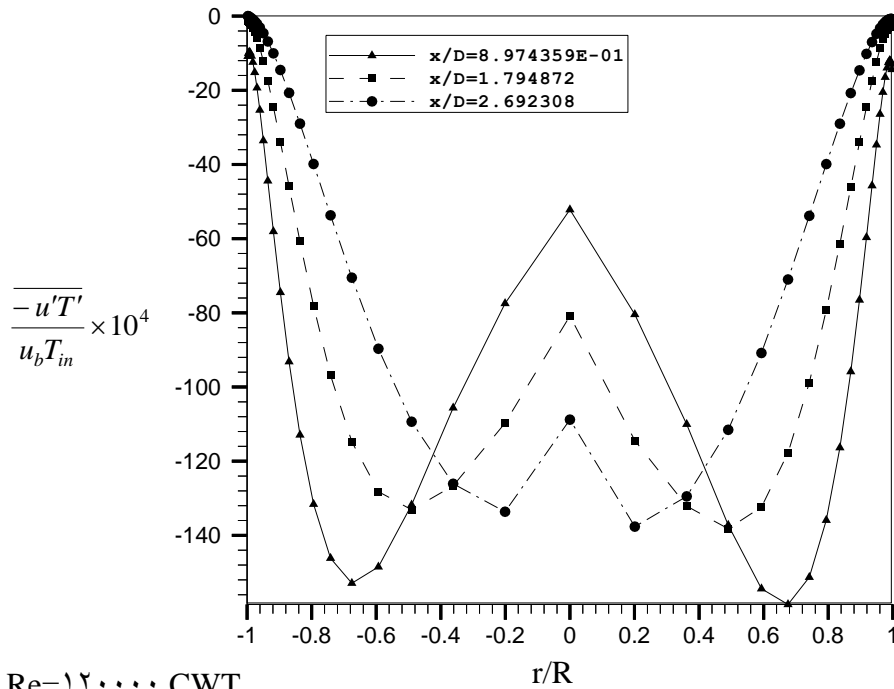


FIGURE (5.23): The Radial Distribution of Turbulent Heat Flux for Rectangular Duct with Reynolds Numbers ( $Re=6000$ ) and ( $Re=12000$ ) for CWT



(a)  $Re=6000$  CWT



(b)  $Re=12000$  CWT

FIGURE (5.25): The Radial Distribution of Turbulent Heat Flux for Circular Duct with Reynolds Numbers ( $Re=6000$ ) and ( $Re=12000$ ) for CWT

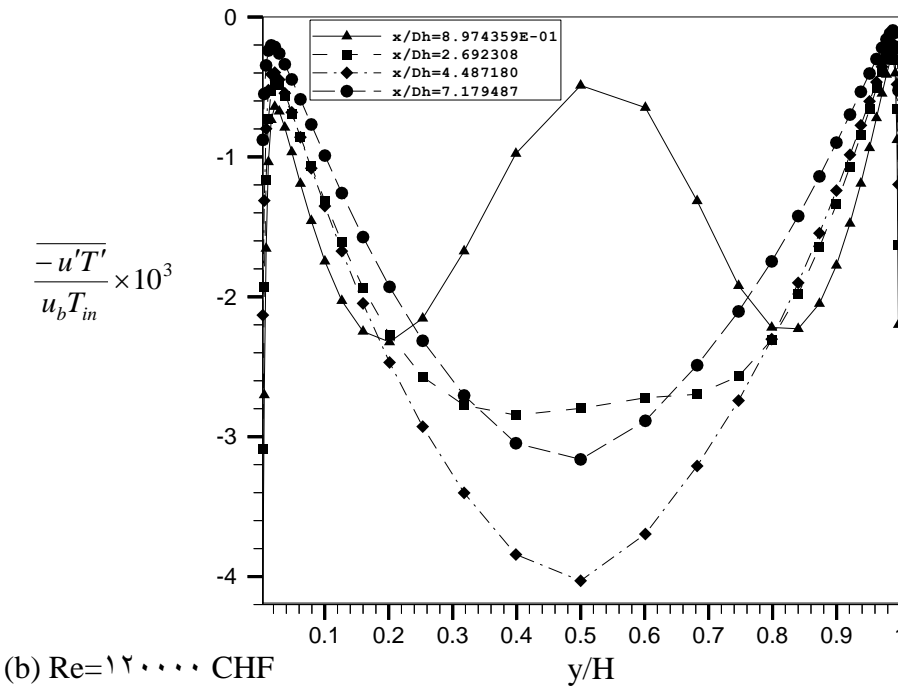
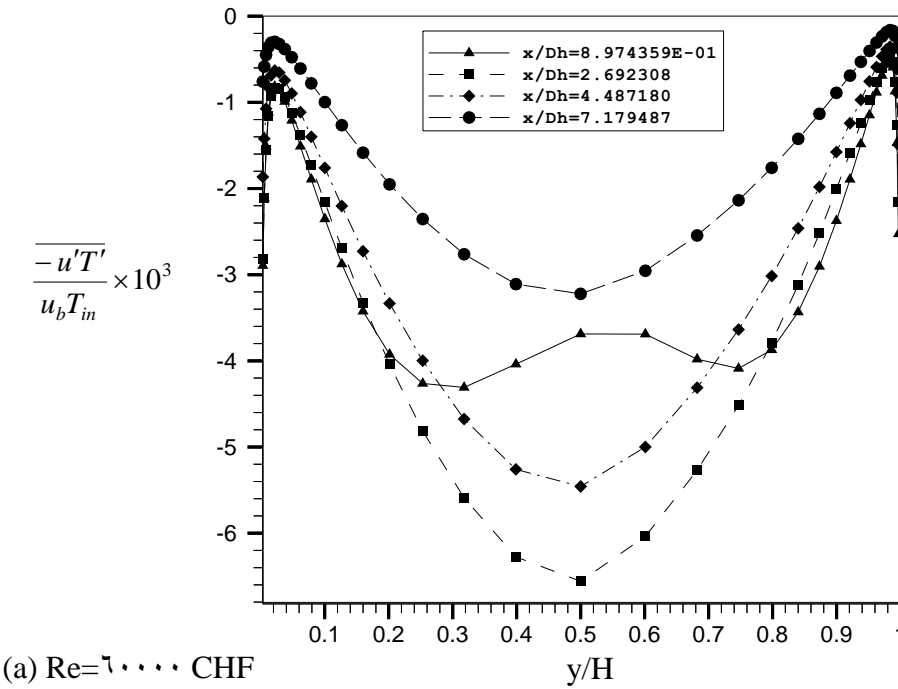
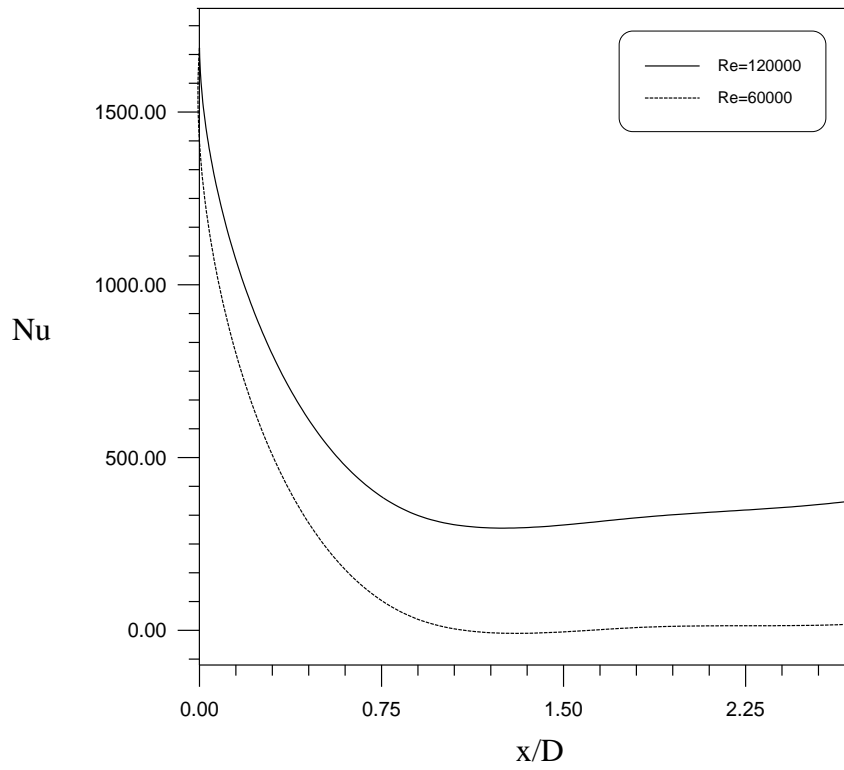
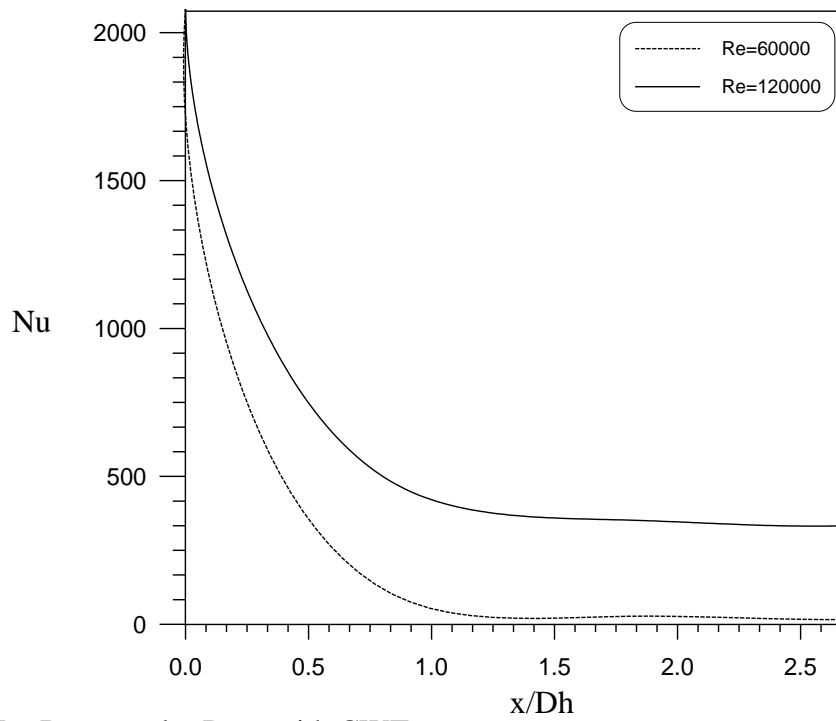


FIGURE (5.10): The Radial Distribution of Turbulent Heat Flux for Rectangular Duct with Reynolds Numbers ( $Re=6000$ ) and ( $Re=12000$ ) for CHF



(a) For Circular Duct with CWT



(b) For Rectangular Duct with CWT

FIGURE (5.26): The Nusselt Number for Circular and Rectangular Duct with  $Re=60000$  and  $Re=120000$  for CWT

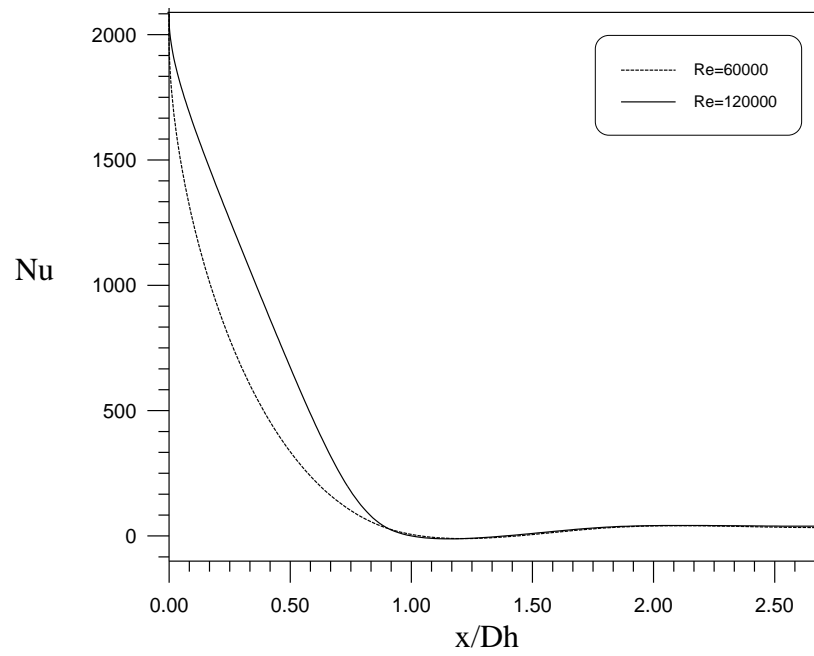


FIGURE (5.17): The Nusselt Number for Rectangular Duct with  $Re=60000$  and  $Re=120000$  for CHF

## References

1. Anderson, D.A., Tannehill, J.C., and Pletcher, R.H., "Computational Fluid Mechanics and Heat Transfer", 1984.
2. Young, D.F., Munson, B.R, and Okiishi, T.H., "A Brief Introduction to Fluid Mechanics", 1997
3. Hinze, J.O., "Turbulence", 1975.
4. Rapley, C.W., "Fluid and Heat Flow in Tubes of Arbitrary Cross-Section" Ph, D. thesis, Mechanical Engineering Department University of London, 1980.
5. Seban, R.A., Shimazaki, T. T., Berkeley, and Calif, "Heat Transfer to a Fluid Flowing Turbulently in a Smooth Pipe with Walls at Constant Temperature", Trans. ASME, PP. 803-809, 1951.
6. Peter, H.A. and Stuart W.C., "The Thermal Entrance Region in Fully Developed Turbulent Flow" A. I. Ch. E. Journal , Vol. 6, No. 2, pp.268-273, 1960.
7. Mills, A.F., "Experimental Investigation of Turbulent Heat Transfer in the Entrance Region of a Circular Conduit ", J. Mech. Eng. Science, Vol. 4, No. 1, pp. 63-77, 1962.
8. Yang, H.K. and Yu, C.P., "Combined Forced and Free Convection MHD Channel Flow in Entrance Region", Int. J. Heat Mass Transfer, Vol. 17, pp.681-691, 1974.
9. Stephenson , "A Theoretical Study of Heat transfer in Two-Dimensional Turbulent Flow in a Circular Pipe and Between Parallel and Diverging Plates", Int. J. Heat Mass Transfer, Vol. 19, pp.413-423, 1976.
10. Emery, A.F and Gessner, F.B., "The Numerical Prediction of Turbulent Flow and Heat transfer in The Entrance Region of a parallel plate Duct", ASME Journal of Heat Transfer, Vol. 98, No. 4, pp.594-600, 1976.
11. Emery, A.F., Neighbors, B.K., and Gessner, F.B., "The Numerical Prediction of Developing Turbulent Flow and Heat transfer in a Square Duct", ASME Journal of Heat Transfer, Vol. 102, pp.51-57, 1980.
12. Ching, J.C., and Jenq, S. C. , "Laminar and Turbulent Heat transfer in the Pipe Entrance region for Liquid Metals", Int. J. Heat Mass Transfer, Vol. 24, pp.1179-1189, 1981.

١٣. Emery, A.F, and Gessner, F.B., “The Numerical Prediction of Developing Turbulent Flow in Rectangular Ducts”, ASME Journal of Fluid Engineering, Vol. ١٠٣, pp. ٤٤٥-٤٥٥, ١٩٨١.
١٤. Jicha, M., and Ramik, Z., “Turbulent Boundary Layer Heat Transfer in the Entrance Region of a Pipe”, The Seventh INT. Heat Transfer Conf., pp. ٤٥-٤٩, ١٩٨٢.
١٥. Mousa, K.H “Prediction of Turbulent Flow and Heat Transfer in a Circular Air Duct”, M.Sc. thesis, Mechanical Engineering Department University of Mosul, ١٩٨٩.
١٦. SUGIYAMA, H., and WATANABE, C., “Numerical Analysis of Developing Turbulent Flow in a U-bend of Strong Curvature with Rib-Roughened Walls”, ٢٠٠٣, E-mail: sugiyama@cc.utsunomiya-u.ac.jp
١٧. Salman, A.M., “Turbulent Forced Convection Heat Transfer in The Developing Flow Through Concentric Annuli ” M.Sc. thesis, Mechanical Engineering Department University of Technology, ٢٠٠٣.
١٨. Majumdar, A. K., Partap, V. S., and Spalding, D. P., “Numerical computation of Flow in Rotating Ducts”, ASME Journal of Fluid Engineering, pp. ١٤٨-١٥٣, ١٩٧٧.
١٩. Launder, B.E., and Spalding, D.P., “The Numerical computation of Turbulent Flows”, Computer Methods in Applied Mechanics and Engineering, No.٣, pp. ٢٦٩-٢٨٩, ١٩٧٤.
٢٠. Hoffmann, K.A., “Computational Fluid Dynamics for Engineers” The University of Texas at Austin, a publication of engineering education system <sup>TM</sup>, Austin, Texas ٧٨٧١٣, USA, ١٩٨٩.
٢١. Rahmatalla, M.A, “Computation of Three-Dimensional Flow Through Turbomachines” Ph, D. thesis, Mechanical Engineering Department University of Manchester., ١٩٨٠.
٢٢. Poult, A., and Srivetsa, S.K., “CORA ٢- A Computer Code for Axi-symmetrical Combustion Chamber” CHAM Computer Code ٢٠١, London England, ١٩٧٧.
٢٣. Wang, Y., and Komori, S., “Predictions of Duct Flows With Pressure-Based Procedure” J. Numerical Heat transfer, part A, Vol. ٣٣, pp. ٢٦٩-٢٨٧, ١٩٩٨.
٢٤. Versteeg, H.K., and Malalasekera, W., “An Introduction to Computational Fluid Dynamics the Finite Volume Method” The Longman Group Ltd, ١٩٩٥.

- 
۲۵. Caretto, L.S., Curr, R.M., and Spalding, D.P., “The Numerical Methods for Three Boundary Layers”, Computer Methods in Applied Mechanics and Engineering, No. ۱, pp. ۳۹-۵۷, ۱۹۷۲.
۲۶. Arpaci, V.S., and Larsen, P.S., “Convection Heat Transfer” prentice-Hall, INC, ۱۹۸۴.
۲۷. Petrovic, Z. and Stuper, S., “Computational Fluid Dynamics One” Mechanical Engineering Faculty, University of Belgrade, ۱۹۹۶.
۲۸. Adams, J.A., and Rogers D.F., “Computer Aided Heat Transfer Analysis”, McGraw-Hill Book Company, ۱۹۷۳.
۲۹. Help of ANSYS version ۵.۴, (۱۹۹۷).
۳۰. Ozisik, M.N., “Basic Heat Transfer”, McGraw-Hill Book Company, ۱۹۷۷.